

INFORMATION TO USERS

This manuscript has been reproduced from the microfilm master. UMI films the text directly from the original or copy submitted. Thus, some thesis and dissertation copies are in typewriter face, while others may be from any type of computer printer.

The quality of this reproduction is dependent upon the quality of the copy submitted. Broken or indistinct print, colored or poor quality illustrations and photographs, print bleedthrough, substandard margins, and improper alignment can adversely affect reproduction.

In the unlikely event that the author did not send UMI a complete manuscript and there are missing pages, these will be noted. Also, if unauthorized copyright material had to be removed, a note will indicate the deletion.

Oversize materials (e.g., maps, drawings, charts) are reproduced by sectioning the original, beginning at the upper left-hand corner and continuing from left to right in equal sections with small overlaps. Each original is also photographed in one exposure and is included in reduced form at the back of the book.

Photographs included in the original manuscript have been reproduced xerographically in this copy. Higher quality 6" x 9" black and white photographic prints are available for any photographs or illustrations appearing in this copy for an additional charge. Contact UMI directly to order.

U·M·I

University Microfilms International
A Bell & Howell Information Company
300 North Zeeb Road, Ann Arbor, MI 48106-1346 USA
313/761-4700 800/521-0600

Order Number 9130326

**A surface-enhanced Raman scattering spectroscopic study of five
p-amino substituted tetraphenyl porphyrins and NAD**

Hosten, Charles M., Ph.D.

City University of New York, 1991

Copyright ©1991 by Hosten, Charles M. All rights reserved.

U·M·I
300 N. Zeeb Rd.
Ann Arbor, MI 48106

A

A SURFACE ENHANCED RAMAN SCATTERING SPECTROSCOPIC
STUDY OF FIVE P-AMINO SUBSTITUTED TETRAPHENYL
PORPHYRINS AND NAD

by

Charles M. Hosten

A dissertation submitted to the Graduate Faculty in Chemistry in
partial fulfillment of the requirements for the degree of Doctor of
Philosophy, The City University of New York.

1991

© 1991

Charles M Hosten

All Rights Reserved

This manuscript has been read and accepted for the Graduate Faculty in Chemistry in satisfaction of the dissertation requirement for the degree of Doctor of Philosophy.

4/29/91
date

Ronald L. Burke
Chairman of Examining Committee

4/30/91
date

Richard Page
Executive Officer

William E. L. Grossman

John R. Lohr

Supervisory Committee

Abstract**A SURFACE ENHANCED RAMAN SCATTERING SPECTROSCOPIC
STUDY OF FIVE P-AMINO SUBSTITUTED TETRAPHENYL
PORPHYRINS AND NAD
by****Charles M. Hosten****Advisors: Professors R. Birke and J. Lombardi**

The technique of surface enhanced Raman spectroscopy is applied to the study of the orientation, conformation and structural characterization of five p-amino substituted tetraphenyl porphyrins and NAD adsorbed on silver and gold electrodes

For a series of p-amino substituted tetraphenyl porphyrins dissolved in acetonitrile, the combination of SERS and cyclic voltammetry allowed for the identification of two types of adsorbates at -0.6V. The p-amino tetraphenyl porphyrin molecules were found to adsorb with their axes oriented parallel to the electrode surface resulting in maximum interaction between the amino nitrogens and the electrode surface. The SERS spectrum of meso-tetrakis(4-aminophenyl)porphine, (TAPP), obtained in the absence of solvent molecules indicates that rotation of the phenyl rings into near planarity with the porphyrin macrocycle occurs, resulting in an extension of the porphyrin aromatic system to include the phenyl groups.

TAPP was electropolymerized on a gold electrode from both non-aqueous and aqueous solutions. SERS was used to characterize the structural linkage between the monomers in the polymer. The linkage was identified as being identical to that found

in nitrilo-2,5-cyclohexadiene-1,4-diylidene-nitrilo-1,4-phenylene which has been identified as one of the structural units found in polyaniline.

The relative SERS intensities of five different p-amino substituted TPP compounds were studied as a function of the number of amino groups on the molecule. A linear relationship was observed with the exception of the cis-disubstituted compound whose SERS intensity was approximately five times that of the trans disubstituted compound. This difference in intensity was related to differences in the orientation of the two molecules on the electrode surface.

The electrocatalytic activity of electropolymerized TAPP towards a number of biologically significant molecules, e.g. N-methyl nicotinamide, NAD and NADH, was investigated by cyclic voltammetry.

Finally the effect of electrode potential, solvent polarity and pH on the orientation and conformation of NAD adsorbed on a silver electrode was studied by SERS. At physiological pH, NAD adsorbs on the electrode surface in the folded conformation with interaction between the adsorbate and the silver electrode occurring through the external amino group of the adenine ring. When NAD is adsorbed from a methanolic solution it adsorbs in the extended conformation with interaction occurring between the adenine, ribose and phosphate parts of the molecule. The nicotinamide group is oriented away from the surface. This conformation is similar to the conformation of NAD in biological systems.

Acknowledgements

I had never identified the influences which led to my wanting to be a scientist. I remember the day, I was about 12 years old, when a friend and I snuck into my high school's chemistry lab. We poured this deep purple solution, which we later learned was potassium permanganate, into a clear solution, sodium oxalate, and to our surprise the solution remained colorless. Overcome with curiosity we confronted a science teacher and informed him of our discovery. After patiently explaining the chemistry of the reaction to us we were escorted to the Dean of discipline, who rewarded our scientific curiosity with two weeks of detention.

This is the experience that started me dreaming of becoming a chemist and I have spent much of my life since then, pursuing this dream. My family provided me with a number of chemistry sets when I was growing up, and they encouraged me and provided me with the type of environment that is conducive to academic success. My high school teachers and my professors at the University of the West Indies provided me with a solid foundation in Chemistry which served me well in Graduate School.

I was especially motivated during my latter years in high school by the new political movements developing in the Caribbean. These movements especially the one in Grenada led by Maurice Bishop, with their emphasis on Caribbean identity and self determination inspired an entire generation to strive for academic success.

At City College I was exposed to a level of scholarship which I had never known existed. I still remember the first day Dr. Birke took me into his lab. I was so scared that I would destroy the apparatus I purposely kept both my hands in my pockets. I overcame my initial fears thanks to the patience of both Profs.

Birke and Lombardi. In different ways they both have shown me the attributes of true scientists. Prof. Lombardi whose ability to analyze a problem is so clear that answering one of his questions require three months of experimental work and Prof. Birke whose knowledge of the scientific literature and abundance of research ideas have afforded me excellent models. Dr. Sun and George, soon Dr. Sukenic, were also very helpful.

I would like to thank my family for all their support. My mother for all her sacrifices, my father who shared the dream but did not see it completed, my two sisters for their love, my brother who protected and counseled me and my nieces and nephews, Sonja and Ayana, Richard, Roger and Dave also to Rashida. To Shirley who was always there for me and Afiya for the love she brought me. All my friends especially Wayne, Clyde, Crisp and Ferro ; my adopted mothers in NY Merlin, Edna and Beryl and everyone else thanks for the assistance.

It would take many more pages to describe the joys, frustrations, disappointments and insecurities that I experienced while working on this thesis. Always there was some one, my brother, Shirley or a friend,Zena or Mars, who would encourage me and provide me with the strength to continue. However in the Fall of 1990, when I realized that writing this dissertation would take longer than I had planned and it's direction seemed hazy, that my money was exhausted and it appeared that this dream of mine would never materialize, I obtained comfort and solace in a song by two Brazilians.

Translated it goes:

Dream of mine

Go get someone who lives far off

Go and show them this longing in me

Take the liberty that you have

For in my heavens the guiding star is lost
And the cold dawn only brings me melancholy
Dream of mine

Thanks to all.

Table of Contents

Copyright	ii
Approval	iii
Abstract	iv
Acknowledgement	vi
Table of Contents	ix
List of Figures	xiii

Chapter one: An Introduction to Surface Enhanced Raman Spectroscopy

1.1 Introduction	2
1.2 Pretreatment	3
1.3 Types of substrates for SERS	5
1.4 Characteristics of SERS	6
1.5 Adsorbate surface interaction	7
1.6 Orientation studies using SERS	9
1.6a Orientation of phthalazine	
1.6b Orientation of pyridine	
1.7 The Electromagnetic Enhancement mechanism	13
1.7a Evidence for the Electromagnetic enhancement	
1.8 The Charge Transfer mechanism	15
1.8a Evidence for the Charge Transfer mechanism	
1.9 Raman Spectroscopy	16
1.9a A Classical explanation of Raman Spectroscopy	
1.10 Literature survey of the SERS of biomolecules	18
1.11 Motivation for this study	24

1.12 Adsorption spectra of porphyrins	25
---------------------------------------	----

Chapter two: A spectroelectrochemical study of TAPP in acetonitrile

2.1 Abstract	28
2.2 Introduction	28
2.3 Experimental	30
2.4 Results and discussion	31
2.4a Metal Incorporation	33
2.4b Spectroscopy and electrochemistry	34
2.4c Orientation of adsorbed porphyrin	38
2.4d SERS from a roughened dried electrode	40
2.5 Conclusion	44

Chapter three: SERS study of p-amino substituted TPP in aqueous solvent

3.1 Abstract	65
3.2 Introduction	65
3.3 Experimental	67
3.4 Results and discussion	68
4.4a Relative intensity measurements	68
4.4b Spectroscopy	73
4.4c 488 vs 514 nm excitation	75
4.4d Porphyrins adsorbed on Au and Ag	76
4.4e Porphyrin AAAA; A comparison on Ag and Au	76

Chapter four: Electropolymerized TAPP: structure and catalytic properties

4.1	Abstract	97
4.2	Introduction	97
4.3	Experimental	98
4.4	Discussion	100
	4.4a Electropolymerization	100
	4.4b Polymer characterization	102
	4.4c Catalysis	105
	4.4d Catalysis of NADH oxidation	106
	4.4e Catalysis of NMN reduction	107
4.5	Conclusion	108

Chapter five: The effect of pH, electrode potential and solvent polarity on the orientation of adsorbed NAD

5.1	Abstract	124
5.2	Introduction	124
5.3	Experimental	126
5.4	Results and discussion	127
	5.4a SERS of N-methyl nicotinamide	127
	5.4b SERS of NAD	128
	5.4c Conformation of NAD in solution	131
	5.4d Conformation of adsorbed NAD	132
	5.4e Effect of electrode potential on the orientation of NAD	
	5.4f SERS spectra of NAD in methanol	136
	5.4g Comparison of in situ vs ex situ SERS spectra	136

5.4h Orientation of adsorbed NAD	137
5.4i Adenine vibrations	137
5.4j Sugar vibrations	138
5.4k Effect of the number of ORC on the SERS of NAD	139
5.4l Conclusions	141
Bibilography	154

List of Figures

Chapter 2

Figure 2.1 a Structure of p-amino substituted TPP. Pg.46

Figure 2.1 b Structure of TAPP to show the labelling of the carbon atoms in the macrocycle. Pg.47

Figure 2.2 SERS spectra of TAPP in acetonitrile on a silver electrode at -0.6V with 488 nm laser excitation. (a) Por. AAAA (b) AAAO (c) AAOO and (d) AOAO. Pg.48

Figure 2.3 Visible absorption spectrum of TAPP in 0.05M HCl. (a) represents excitation frequency 514 and (b) 488 nm. Pg.49

Figure 2.4 SERS of TAPP in acetonitrile with 488nm laser excitation and a silver electrode. (a) 0.0V (b) -0.2V (c) -0.4V and (d) -0.6V. Pg.50

Figure 2.5 SERS spectra of TAPP in acetonitrile on a silver electrode with 488 nm laser excitation. (a) at -0.5V (b) at -0.6V and (c) at -0.7V. Pg.51

Figure 2.6 Cyclic Voltammogram of TAPP dissolved in acetonitrile with TBAP as the supporting electrolyte. Potential range from 0.0V to -1.2V./ Scan rate 100mV/sec. Ag electrode. Pg.53

Figure 2.7 CV of TAPP dissolved in acetonitrile with TBAP as the supporting electrolyte and a potential range from 0.0V to -1.2V on a polished Ag electrode and a scan rate of 500mV/sec. Pg.54

Figure 2.8 CV of TAPP in acetonitrile with TBAP as the supporting electrolyte on a polished gold electrode. Scan rate 100mV/sec. Pg.55

Figure 2.9 Plot of peak current vs the square root of the scan rate for the -1.0 peak of TAPP dissolved in acetonitrile on a silver electrode. Pg.56

Figure 2.10 Plot of peak current vs scan rate for the -0.6V peak of TAPP dissolved in acetonitrile on a silver electrode. Pg.57

Figure 2.11 Potential dependent absorption spectrum. Pg.58

Figure 2.12 Plot of absorbance against concentration for TAPP dissolved in acetonitrile. Pg.59

Figure 2.13 Normal Raman spectrum of TAPP in acetonitrile with 488 nm laser excitation. Pg.60

Figure 2.14 SERS from a silver electrode roughened in an acetonitrile solution of TAPP and left to dry. 488 nm laser excitation. Pg.61

Chapter 3

Figure 3.1 Structure of five p-amino substituted tetraphenyl porphyrins. Pg.79

Figure 3.2 Absorption spectrum of TAPP. Pg.80

Figure 3.3 Laser line intensity vs intensity of the SERS signal.

Pg.81

Figure 3.4 Plot of SERS intensity of the 1012 band vs the number of amino groups on the molecule, 514 nm laser excitation.

Pg.82

Figure 3.5 Plot of SERS intensity vs the number of amino groups on the molecule for the 1012 band, with 488 nm laser excitation. Pg.83

Figure 3.6 plot of the number of amino groups on the porphyrin against the SERS intensity for the 984 band. Laser excitation frequency was 480 nm. Pg.84

Figure 3.7 plot of the number of amino groups on the porphyrin against the SERS intensity for the 984 band. Laser excitation frequency was 514 nm. Pg.85

Figure 3.8 SERS spectra of 5 p-amino substituted TPP on a silver electrode at 488 nm laser excitation (a) Por. AAAA (b) AAOO (c) Por. AAAO (d) Por.AOAO and (e) Por. AOOO. Pg.86

Figure 3.9 SERS of 0.01M TAPP in 0.05M HCl on a silver electrode with 488 nm laser excitation (a) at 0.0V (b) at -0.2V (c) at -0.4V and (d) at -0.6V. Pg.87

Figure 3.10 SERS of TAPP in 2M HCl on a silver electrode with 488 nm laser excitation. Pg.88

Figure 3.11 Potential dependence SERS spectra of TAPP in 2M HCl on a silver electrode with 488 nm laser excitation. Pg.89

Figure 3.12 SERS spectra of Por.AAO in 0.05 M HCl (a) Ag electrode at 488 nm (b) Au electrode at 647 nm and (c) Ag electrode at 647 nm laser excitation. Pg.90

Figure 3.13 SERS spectra of Por.AOAO in 0.05 M HCl (a) Ag electrode at 488 nm (b) Au electrode at 647 nm and (c) Ag electrode at 647 nm laser excitation. Pg.91

Figure 3.14 SERS spectra of Por.AAAO in 0.05 M HCl solution (a) Ag electrode 488 nm (b) Au electrode 647 nm and (c) Ag electrode 647 nm laser excitation. Pg.92

Figure.3.15 SERS of TAPP a) on a silver electrode with 488 nm excitation b) on a gold electrode and c) on a silver electrode both with 647 nm laser excitation. Pg.93

Figure 3.16 SERS spectra of four TAPP in 0.05M HCl on Au at 647 nm (a) Por. AOAO (b) AAAO (c) Por. AAOO (d) Por.AAAA. Pg.94

Figure 3. 17 a) SERS spectrum of TAPP in 0.05 M HCl, 488 nm excitation on a silver electrode. b) normal Raman spectrum of TPP. Pg.95

chapter 4

Figure 4.1 Cyclic voltammogram for the electropolymerization of TAPP on a Au electrode. (a) scan2 (b) scan10 (c) scan 15 and (d) scan 20. The unlabelled line represents the first scan. Pg.110

Figure 4.2 Cyclic voltammograms for MnTAPP on a Pt electrode Pg.111

Figure 4.3 Cyclic voltammograms for Zn(Et₂N)TPP. Pg.112

Figure 4.4 Cyclic voltammograms for the electropolymerization of ZnEt₂NTAPP on a Pt electrode. Pg.113

Figure 4.5 Structure of emeraldine. Pg.114

Figure 4.6 Diagram of the constitutional unit structures of polyaniline. Pg.115

Figure 4.7 SERS spectra of four TAPP in 0.05M HCl on Au at 647 nm (a) Por. AAO (b) AAAO (c) Por. AAOO (d) Por.AAAA. Pg.116

Figure 4.8 SERS spectrum of TAPP electropolymerized on a roughened Au electrode with 488 nm laser excitation. Spectrum (a) was digitally smoothed whilst spectrum (b) was not. Pg.117

Figure 4.9 Diagram of the constitutional unit structure of electropolymerized TAPP. Pg.118

Figure 4.10 Attempts at catalysis of NADH by polymerized TAPP (A) shows the CV obtained during electropolymerization of TAPP (B) CV for polymer coated electrode in 0.1 M KCl solution (C) CV for polymer coated electrode in 1mM NADH solution . Pg.119

Figure 4.11 Cyclic Voltammograms of NMN from 0.0V to -1.6V (A) on a polished Ag electrode (B) on a roughened Ag electrode (C) on a Ag electrode roughened in TAPP and then washed and (D) on a AG electrode roughened in TAPP and left to dry.
Pg120

Chapter 5:

Figure 5.1 Diagram to show the structure of NAD (a) NAD (b) Nicotinamide part of the molecule and (c) Adenine part of the molecule. Ribose carbon contain hydrogen and hydroxy groups to satisfy valence requirements. Pg. 142

Figure 5.2 SERS of NMN on a silver electrode with 488 nm laser excitation at pH 11.3. Pg.143

Figure 5.3 Structure of NMN. Pg.144

Figure 5.4 SERS of NAD on a silver electrode with 488 nm laser excitation at pH 7.4 (a) -0.2 (b) -0.4 (c) -0.6 and (d) -0.8V. Pg.145

Figure 5.5 SERS of NAD adsorbed on a Ag electrode at pH 6.4 with 488 nm laser excitation (a) at 0.0V and (b) at -0.3V.

Pg.146

Figure 5.6 SERS of NAD on a silver electrode with 488 nm laser excitation at pH 5.3 (a) -0.2V (b) -0.4V (c) -0.6V and (d) -0.8V. Pg.147

Figure 5.7 SERS of NAD on a silver electrode with 488 nm laser excitation at pH 3.5 (a) at 0.0V (b) at -0.2V and (c) 0.4V.

Pg.148

Figure 5.8 Conformation of NAD (a) the extended conformation and (b) the folded conformation. Pg.149

Figure 5.9 SERS spectra of NAD in 80% methanol 20% water on a silver electrode with 488 nm laser excitation. (a) Obtained with ex situ roughening and (b) by in situ roughening. - 0.2V. Pg.150

Figure.5.10 SERS of NAD on a Ag electrode at pH 7.4 with 488 nm laser excitation. a) 2, 2 sec. pretreatment pulses, b) 4, 1 sec. pulses and c) 4, 2 sec. pulses. Pg.151

List of Tables

Chapter 2

- Table 2.1 Assignment of SERS bands for TAPP. Pg.52
- Table 2.2 Comparison of normal Raman bands vs SERS bands for TAPP. Pg.62
- Table 2.3 Comparison of RDE spectrum and in situ SERS spectrum for TAPP. Pg.63

Chapter 4

- Table 4.1 SERS of polymerized and unpolymerized TAPP. Pg.121
- Table 4.2 Characteristic frequencies for the unit structures of polyaniline. Pg.121

Chapter 5

- Table 5.1 Assignment of NAD vibrations (aqueous). Pg.152
- Table 5.2 Assignment of NAD vibrations (methanol). Pg.153

CHAPTER ONE

AN INTRODUCTION TO SURFACE ENHANCED RAMAN SCATTERING SPECTROSCOPY

1.1 INTRODUCTION

Numerous spectroscopic techniques have been developed to investigate surfaces and interfacial regions with the hope of obtaining information on the method of interaction between the adsorbate and the surface. Techniques commonly used are a) Low Energy Electron Diffraction¹ b) Secondary ion mass spectroscopy² c) Auger spectroscopy³ and d) High Resolution Electron Loss Spectroscopy⁴. These methods can give data regarding the surface structure and the spatial arrangement of atoms. High Resolution Energy Loss Spectroscopy and IR/FTIR⁵ provides vibronic information on the adsorbate. Internal Reflectance Spectroelectrochemistry and ellipsometry also allow for obtaining *in situ* spectral data.

Because of its inherent molecular specificity and the vast amount of structural information that it provides, surface scientists have for a long time recognized the vast potential that Raman spectroscopy offers if it could be applied to the *in situ* investigation of interfaces.

The main limitation was thought to be low intensity. Calculations, for example, those done by Van Dyne⁶, showed adsorbates would yield possible count rates of around 0.1 to 10 counts per second against a background of 100 to 1000 counts per second. This weak signal would be undetectable against such a large background.

A report published in 1973 by Fleischmann, Hendra and McQuillan⁷ indicating that *in situ* Raman spectra could be obtained from a thick layer of mercurous halides formed from mercury plated on platinum did not receive much attention. However a subsequent paper⁸ in 1974 by the same authors reporting the spectrum of pyridine on a roughened silver electrode in an

electrochemical system opened the field of Surface Enhanced Raman Spectroscopy (SERS). Two other groups of workers, Jeanmarie and Van Dyne⁹ along with Albrecht and Creighton¹⁰ quantified the enhancement to be about five to six orders of magnitude over what would be expected and they also established the pretreatment conditions necessary for obtaining SERS.

The significance of this new analytical technique was instantly recognized by electrochemists who predicted that SERS would allow for the acquisition of vibrational spectra of electrochemical intermediates and thus offered the possibility of completely identifying the nature of the electrode process.

Although SERS has been obtained on only a few solid substrates, Ag, Au and Cu, the range of molecules for which SERS spectra have been obtained is enormous. Molecules containing coordinating atoms e.g., nitrogen with lone pairs have been extensively studied by SERS. This has allowed for the study of the spectroelectrochemistry of a number of biologically significant compounds. When it was first discovered the original SERS enhancement was thought to be due to the increased surface concentration of the molecule resulting in an increase in the number of adsorbates and a corresponding increase in the Raman signal. Subsequent work has shown this theory to be incorrect and the large SERS enhancement is explained using two roughness based models. One is the electromagnetic effect and the other is the charge transfer effect.

1.2 PRETREATMENT

It is generally accepted that some form of surface roughness is necessary to obtain a SERS signal. A number of methods for obtaining this surface roughness have been used.

The most commonly used method involves electrochemical roughening of the surface. To the silver electrode in 0.1M KCl solution is applied a potential step from 0.0V to + 0.3 V and back to - 0.1V, all potentials are relative to the saturated calomel electrode. The potential is held at the positive potential for a period of time ranging 1 to 5 seconds. One cycle usually produces a roughened silver surface which give intense spectra. It has been shown that when a charge of more than 50 mC cm^{-2} is passed the resulting roughened silver electrode does not produce an intense SERS spectrum.

During the oxidation part of the ORC when the oxidized silver is produced in the presence of the halide ion, insoluble silver halide is formed on the electrode surface. On the reverse potential scan, the cathodic scan, this silver halide is reduced back to silver. The potassium salts of chlorine, bromine and iodine have also been used to roughen the silver electrode.

While intense reproducible SERS have been obtained on silver using the pretreatment described above, when the electrode is switched from silver to gold, the pretreatment condition necessary for producing intense SERS is not as simple or reproducible.

Weaver ¹¹ has shown that stable SERS on gold can be obtained by using 100 to 500 mV sec^{-1} potential sweeps between -300 and 1200 mV vs the SCE. Twenty five successive oxidation reduction cycles resulted in the most intense and most reproducible SERS. It was found that holding the potential at the positive limit for $1 - 1.5$ seconds was also conducive to increased SERS spectra. After pretreatment the electrode was rinsed and transferred to a solution containing the adsorbate.

Another method for producing SERS active gold electrodes was developed by Busby¹² and involved electroplating from a solution of KAuCl_4 . Using plating currents of 0.4 mA cm^{-2} and a solution of $5 \times 10^{-3} \text{ M KAuCl}_4$ in

the absence of supporting electrolyte a pale brown surface was observed. This surface gave intense SERS spectra. Scanning electron microscopy showed the surface to be made up of spheres having a diameter of about 70 nm. This electroplated surface could have its adsorbates washed off with 0.1 M H₂SO₄ and can adsorb different adsorbates upon subsequent immersion in a suitable solution.

Experiments¹³ measuring the intensity of the SERS signal of pyridine as a function of charge passed during electroplating shows a maxima for the pyridine signal at 80 cm⁻² plating charge. This charge corresponds roughly to the formation from AuCl₄ of a single layer of 70 nm diameter gold spheres. The spheres are in contact with an average of three neighbors.

1.3 TYPES OF SUBSTRATES FOR SERS

Since SERS was first observed on a silver electrode a number of other substrates in addition to Au and Cu have been investigated in an attempt to expand the range of usable materials to catalytically more interesting electrodes. Moderate success has been reported on hydrogenated Pd¹⁴ electrodes but no success has been reported for Pt electrodes. Small SERS enhancements along with catalytic activity have been reported^{15,16} on Pt colloids. SERS has also been reported on Li, Na, K¹⁶ in matrix form and aluminium. Although SERS has been reported for substrates like Fe, Cd, Hg, Pb, In, Sn and TiO, these reports are unconfirmed and unreliable.

SERS has also been reported in a number of environments. While most published work is in either an electrochemical environment or ultra high vacuum, a number of other morphologies have been used to obtain SERS. The

surfaces range from powders, thin films coated on smooth and rough substrates, thin films, sols and catalysts supported on insulator granules. The range of substrates and environment all indicate that surface roughness is a necessary requirement for SERS. It is not however the only or sufficient requirement.

1.4 CHARACTERISTICS OF SERS SPECTRA

- 1) The intensity of a single scatterer is enhanced by a factor of 10^4 to 10^6 .
- 2) The degree of enhancement depends on the substrate material, e.g.,
Ag \gg Cu, Au \gg Pt.
- 3) Roughness of the metal surface plays an important role in generating the strong enhancement.
- 4) The excitation energy dependence of the Raman intensity does not obey the ω^4 rule, where ω is the frequency of the excitation light.
- 5) The depolarization ratios are all in the range of 0.6 to 0.75 even for totally symmetric vibrations.
- 6) There is an angular dependence of the intensity with respect to the direction of the incoming light.

- 7) An intense continuum background is observed.
- 8) There is a potential dependence of the intensity in an electrochemical system.

1.5 ADSORBATE SURFACE INTERACTION

Because SERS is a surface phenomenon the interaction between the adsorbate and the surface has been of concern to investigators. It is believed that when certain molecules become adsorbed on to the silver surface, a very weak chemical bond may develop between the metal and the molecule. For unsaturated systems some type of π bond interaction may also be involved. SERS spectra of benzene and monosubstituted benzenes¹⁷ adsorbed on a gold electrode indicate a flat adsorbate orientation with interaction occurring through the π system of the adsorbate and the surface. Evidence for this is the significant downshift, of about 20 - 30 cm^{-1} , in the symmetric ring breathing mode and the absence of other ring modes in the spectra. Along with this observation is the fact that in the SERS of the nitrile and nitro derivatives of benzene, the frequencies of the ring breathing modes were unaltered whilst the appearance of the vibrations of the substituents indicate that interaction between the molecule and the surface is no longer through the π system but rather through the substituents on the benzene ring. Further evidence for π interaction was produced by Moscovits¹⁸ who obtained the spectra of ethylene

and acetylene adsorbed on colloidal silver particles formed by gas aggregation and isolated at low temperature in solid adsorbate/argon matrices. No SERS spectra were obtained for ethane under similar experimental conditions. These results confirmed the hypothesis that SERS is visible only for the first layer of adsorbed molecules which can chemically bind to the surface and that the absence of a SERS signal for ethane indicates that the molecule was not chemically bound to the surface.

Another type of interaction involves that of the lone pair of the adsorbed molecule and the metal surface. An examination of the literature reveals that a sizeable percentage of the molecules studied by SERS fall into this category, such as those containing either a nitrogen heterocycle e.g. pyridine, cyanide or a carboxylate group.

The importance of the lone pair was investigated when the SERS spectra of isonicotinic acid ¹⁹ was compared with that of benzoic acid. Isonicotinic acid contains a nitrogen atom possessing a lone pair of electrons whilst benzoic acid does not. It was observed that isonicotinic acid, which has two coordination sites, the carboxylate group and the pyridine nitrogen, was more effective in giving a SERS signal compared to benzoic acid. This difference must be related to the pyridine nitrogen possessing a lone pair and being capable of interacting with the surface.

The observation of SERS from molecules which do not possess a lone pair of electrons such as ions leads to the theory of ion pair adsorption. Examples of these ions are pyridinium and its analogues, e.g. methyl pyridinium. Sun et. al.²⁰ has shown that the adsorption of pyridinium is closely related to the adsorption of halide. If the SERS active sites involve Ag^4+ clusters, then it is not possible for the positively charged pyridinium ion to be attracted to the surface, instead it should be repelled. If however a halide ion

is adsorbed on to the Ag^{4+} cluster then it is possible for the pyridinium ion to interact with the adsorbed halide ion through the conjugated π orbital or through some sort of electrostatic interaction.

1.6 ORIENTATION STUDIES USING SERS

A comparison of the SERS spectrum and the normal Raman spectrum of most molecules indicate that the relative intensities of the SERS bands are different from those of the molecule in solution²¹. Initial research suggested that this difference might be due to the orientation effect of the adsorbed molecule on to the surface²². This inspired investigation of SERS spectra to obtain information on adsorbate orientation.

Moskovits²³ produced calculations which resulted in surface selection rules for SERS. These surface selection rules attempt to explain the variation in the intensities of the SERS bands as due to the variation in the normal and tangential enhancement of the local field of a molecule near a small spherical metal surface.

Before the discovery of SERS, surface selection rules had already been obtained for molecules adsorbed on to metal surfaces using surface Infrared spectroscopy^{24,25,26}. In IR the intensity of a vibrational mode is proportional to the square of the component of the vibrational dipole matrix element perpendicular to the surface. Similarly simple rules do not apply to SERS for two reasons; 1) the molecular polarizability response for Raman scattering is a tensor not a vector and 2) the electromagnetic field component parallel to the surface for real metals is not zero for illumination at optical frequencies. Greenler²⁵ has shown that the adsorption intensities of IR modes of molecules

adsorbed on flat metal surfaces are modified due to the presence of the surface so that the only vibrations which are seen are those having a non vanishing component of the transition dipole moment normal to the surface.

1.6(a) Orientation of Phthalazine.

Moskovits²⁷ developed three equations which he used to determine the orientation of phthalazine adsorbed on silver sols. He predicted that the three classes of vibrational modes would show the following SERS enhancement :

$$\alpha_{zz} : (\overline{E_n^2}) \quad (\overline{E_n'^2}) \propto |1 + 2g|^2 |1 + 2g'|^2$$

$$\alpha_{xz}, \alpha_{yz} :$$

$$\frac{1}{2} [\overline{E_n^2} \overline{E_t'^2} + \overline{E_t^2} \overline{E_n'^2}] \propto \{ |1 + 2g|^2 |1 - g'|^2 + |1 - g|^2 |1 + 2g'|^2 \}$$

$$\alpha_{xx}, \alpha_{yy}, \alpha_{xy} : \overline{E_t^2} \overline{E_t'^2} \propto 4 |1 - g|^2 |1 - g'|^2$$

$$g = (\varepsilon - \varepsilon_0) / (\varepsilon + 2\varepsilon_0)$$

ε = dielectric function of the small sphere

ε_0 = dielectric function of liquid

' indicates properties calculated at Raman shifted frequencies whilst unprimed are calculated at the incident frequencies.

E represents the field strength of the radiation

α represents the polarizability tensor.

These sets of equations assume that the source of the SERS enhancement is primarily electromagnetic in origin. Assuming a small sphere the problem was reduced to one of electrostatics.

For a molecule of C_{2v} symmetry if the molecule was lying down then b_1 would span α_{xz} while b_2 would span α_{xy} . From the above equations the ratio

of intensities of bands belonging to the former and latter should depend on exciting frequency roughly as the ratio $\frac{E_n^2}{E_i^2}$ does. If the molecule were standing up then b_1 and b_2 would span α_{xz} and α_{xy} . Bands belonging to these representations would depend on frequency in the same way. The result is that their intensities should be independent of frequency.

Using phthalazine to exemplify the calculations the SERS spectra of phthalazine were obtained at 488, 514 and 602 nm. laser excitation. A comparison of the spectra shows that the spectrum obtained at 602 nm is greatly simplified compared to that at 488 and 514 nm. Phthalazine is C_{2v} symmetry and its vibrations belong to the representations a_1 , a_2 , b_1 , and b_2 . The spectrum at 488 nm is dominated by bands due to b_1 and b_2 whilst at 602 nm these vibrations are virtually absent being replaced by a_1 modes. The ratio of the intensities of two bands at 805 (a_1) and 754 (b_2) cm^{-1} were compared to the calculated $\frac{E_n^2}{E_i^2}$ ratio. The calculated ratio of $\frac{E_n^2}{E_i^2}$ was scaled by a factor of 16. This factor represents the ratio of the two bands in solution. When this scaling factor was used good agreement was obtained for the two ratios. Bands at 1384 (a_1) and 487 (b_2) cm^{-1} were also compared and satisfactory results were obtained when a scaling factor of 19 was used.

When the phthalazine molecule is lying down then b_1 spans α_{xz} whilst b_2 spans α_{xy} . The ratio of the band intensities should depend on the excitation frequency roughly as $\frac{E_n^2}{E_i^2}$ does. If the molecule is standing up then b_1 and b_2 should span α_{xz} and α_{xy} . Bands would depend on the excitation frequency in the same way and their intensities should be independent of frequency. The second case is observed, therefore the molecule is standing up.

1.6(b) Orientation of pyridine.

Pyridine also belongs to the symmetry group C_{2v} as does phthalazine. The axis is defined so that the molecule is in the yz plane and the C_2 axis is along the z plane. The symmetry classes of the pyridine vibrations and the effect of orientation of the molecule on the Raman polarizability tensor have been determined²⁸. From calculations using the small sphere enhancement factor, if pyridine is adsorbed edge on the a_2 vibrations should be the least enhanced whilst if it is adsorbed face on it is the b_2 vibrations that should show the least enhancement. A comparison of the SERS spectra with the normal Raman spectra show that it is the b_2 modes which are the least enhanced. The conclusion is that on silver colloids pyridine adsorbs face on. This analysis provides a qualitative application using the electromagnetic effect.

Birke and Lombardi³² expanded on the surface selection rules developed by Moskovits and Suh²⁷ and came up with a set of equations which they applied to pyridine and correctly determined the orientation of the molecule as a function of electrode potential.

Using a molecule having C_{2v} symmetry, they developed a relationship for the relative intensities of the b_2 , b_1 , a_2 and a_1 modes when the molecule is excited by radiation in the blue and in the red.

The result is that the intensity ratio $(a_2 / b_1)_{\text{blue}} / (a_2 / b_1)_{\text{red}}$ is greater than one when the molecule is standing up and equal to one when the molecule is lying down.

Also $(b_2 / b_1)_{\text{blue}} / (b_2 / b_1)_{\text{red}}$ is equal to one when the molecule is standing up and greater than one when the molecule is lying down.

Birke and Lombardi³² applied these calculations to the case of pyridine adsorbed on a silver electrode. Using $a_1 = 388 \text{ cm}^{-1}$ $b_1 = 414 \text{ cm}^{-1}$ $b_2 =$

1155 cm^{-1} and $b_1 = 944 \text{ cm}^{-1}$ they found that the ratio $(a_2 / b_1) 488 \text{ nm} / (a_2 / b_1) 647 \text{ nm}$ was equal to 0.98 and $(b_2 / b_1) 488 \text{ nm} / (b_2 / b_1) 647 \text{ nm}$ was equal to 1.6 at an electrode potential of - 0.6 V . From this they concluded that the molecule was lying flat on the surface. When the potential was changed to - 0.9 V the first ratio increased to 2.8 and the second was 1.3 . This indicates that at the potential of -0.9 V the molecule had changed orientation from flat to perpendicular relative to the electrode surface.

1.7 THE ELECTROMAGNETIC ENHANCEMENT MECHANISM

The electromagnetic theory has its groundings in the realization that some form of surface roughness is necessary for the observation of SERS. The enhancement originates from the interaction between the metallic particle and the incident radiation. The theoretical considerations have as their genesis a single isolated sphere or spheroid model. The incident field polarizes the metal spheroid and there develops surface charges of opposite signs on opposite sides of the metal particle. These charges alternate with the frequency of the incident radiation producing a localized dipolar surface plasmon, DSP. Calculations which assume a spherical metal particle show that the DSP enhancement using a spherical metal particle predicts an enhancement of about 50 at 500 nm excitation, which is much less than the observed enhancement in SERS . When however the particle is considered as a prolate metal spheroid, a much larger enhancement is predicted from the calculations. These calculations also predict that the electromagnetic enhancement decays relatively slowly with distance from the metal sphere. An accompanying electromagnetic enhancement effect is due to the oscillating molecular dipole

inducing a dipole in the metal particle. The metal particle therefore acts as an antenna for the near field of the oscillating molecular dipole and the emitted Raman radiation from the molecule is then enhanced by the presence of the metal particle.

1.7a Evidence for the Electromagnetic enhancement.

A number of experiments have been performed to establish the Electromagnetic enhancement.

- 1) Long distance enhancement effects have been established by inserting a spacer layer between the Raman active molecule and the roughened metal surface ²⁹.
- 2) By measuring the excitation profile of Raman molecules on lithographically produced silver and gold microstructures immersed in several surrounding media of different refractive indices, the importance of the electrodynamic enhancement was demonstrated³⁰.
- 3) The existence of the Electromagnetic effects were confirmed when general agreement was found between the excitation profiles of adsorbates on non aggregated silver colloids and the extinction profiles of the colloids ³¹.

1.8 THE CHARGE TRANSFER THEORY

In the charge transfer process an incident photon causes an intraband transition, where an electron from the metal is transferred to the excited electronic level of the adsorbate or vice-versa. This process can occur through tunnelling for physisorbed species and by hybridization for chemisorbed adsorbates. An electron can then be transferred back from the excited adsorbate level to the metal resulting in the adsorbate being left in a higher vibrational level. Photon emission occurs. This process is charge transfer from metal to molecule, the reverse process is also possible. The charge transfer theory explains the resonance excitation and the resonance potential dependence.

1.8a Evidence for the Charge Transfer Mechanism

Some of the experimental evidence for the existence of the charge transfer mechanism is;

1) The fact that the first adsorbed layer shows a much greater enhancement than does the subsequent layers³⁴. This suggests enhancement of the first layer by short term charge transfer process since the Electromagnetic enhancement has a fall off dependence of the form $(a + b)^{-6}$ where;

a = cluster size

b = separate distance measured for the cluster surface

2) observation of the potential of the maximum SERS intensity shows that it shifts linearly with the incident photon energy³⁵ and that the direction of the

shift depends on whether the process is molecule to metal or metal to molecule charge transfer³³.

1.9 RAMAN SPECTROSCOPY

The Raman effect was predicted by A. Smekal³⁶ and observed by C. V. Raman³⁷. Raman scattering results from the energy transfer between the scattering system and the incident radiation. The wavenumber of the shift in scattered Raman radiation lies principally in the range associated with transitions between vibrational energy levels.

1.9(a) A Classical Explanation Of Raman Scattering^{38,39}

When a molecule interacts with light the electric field will induce oppositely directed forces on the electron and on the nuclei. This results in an induced dipole moment.

$$\mathbf{P} = \alpha \mathbf{E} \quad (1)$$

Where:

\mathbf{P} = The induced dipole moment

α = Polarizability (a property of the molecule)

\mathbf{E} = The electric field

$$\mathbf{E} = \mathbf{E}_0 \cos 2\pi\nu_0 t \quad (2)$$

ν = the frequency of light

Substituting equation (2) into equation (1) results in

$$\mathbf{P} = \alpha \mathbf{E}_0 \cos 2\pi\nu_0 t \quad (3)$$

α depends on the position of the nuclei in the molecule.

For a molecule containing N atoms there are 3N degrees of freedom.

3N-6 results in vibrations of the molecule and 3N-5 if the molecule is linear.

Group theory allows for this complicated vibrational motion to be a set of normal mode vibrations.

The position of the nuclei at any instant can be expressed relative to their equilibrium position in terms of normal coordinates Q_i where $i = 1, 2, \dots, N - 6$.

For a diatomic molecule the dependence of α on Q_1 is

$$\alpha = \alpha_0 + (\partial\alpha / \partial Q_1)Q_1 + \dots \quad (4)$$

α_0 is the equilibrium value of the polarizability

The position of the nuclei is time dependent because the molecule is vibrating.

This motion is expressed by

$$Q = Q_1^0 \cos 2\pi\nu_1 t \quad (5)$$

where

ν_1 = the frequency of vibration

t = time

Q_1^0 = the maximum vibrational amplitude

Therefore α also oscillates with a frequency ν_1 .

Substituting Equation (4) and (5) into (1) results in

$$P = \left[\alpha_0 + (\partial\alpha / \partial Q_1)_0 Q_1 \right] E_0 \cos 2\pi\nu_0 t$$

$$P = \left[\alpha_0 + (\partial\alpha / \partial Q_1)(Q_1^0 \cos 2\pi\nu_1 t) \right] E_0 \cos 2\pi\nu_0 t$$

$$\text{From } P = [\alpha_0 + (\partial\alpha / \partial Q_1)(Q_1^0 \cos 2\pi\nu_1 t)] E_0 \cos 2\pi\nu_0 t$$

$$P = \alpha_0 E_0 \cos 2\pi\nu_0 t + E_0 Q_1^0 (\partial\alpha / \partial Q_1) X [\cos 2\pi t(\nu_0 + \nu_1) + \cos 2\pi t(\nu_0 - \nu_1)]$$

This classical equation for a diatomic molecule predicts three types of light scattering ;

α_0 produces scattered light of unshifted frequency , Rayleigh Scattering

If $\partial\alpha / \partial Q \neq 0$ Raman scattering occurs and incident light of frequency ν_0 is shifted to scattered light with higher frequency $\nu_0 + \nu_1$ (anti Stokes) and $\nu_0 - \nu_1$ lower frequency (Stokes).

1.10 LITERATURE SURVEY OF THE SERS OF BIOMOLECULES

Once the large enhancement and selectivity of SERS was established by Van Dyne⁴⁴ and it was recognized that SERS spectra could be obtained from very dilute solutions, as low as 10^{-8} M, the technique was expanded to the study of biomolecules. Prior to this the technique was restricted to the investigation of a few organic substances, mainly pyridine and its derivatives and a few simple inorganic adsorbates. The first report of the SERS technique applied to an adsorbed biomolecule was by Koglin⁴⁵ who presented the SERS spectra for adsorbed biopolymers and nucleic acids.

SERS studies of bases e.g. adenine⁴⁶ , were performed as precursors to the study of more complex biomolecules such as DNA. Early SERS studies of DNA⁴⁷ examined the effect of adsorption on the conformational changes of the molecule. Later the effect of gamma radiation on DNA was studied by SERS⁴⁸. Information on the direct interaction of surface active protein sites with a

charged surface was obtained by studying the SERS of proteins⁴⁹. SERS of citric acid⁵⁰⁻⁵³, which is an important compound in the Krebs's cycle, and anabolic steroids⁵⁴ have also been reported. Flavins^{55,56} and retinal chromophore⁵⁷ have recently been used as adsorbates for SERS studies.

The realization that Resonance enhancement could further increase the intensity of the SERS signal lead to surface enhanced resonance Raman scattering, SERRS. Porphyrins were perfect candidates for SERRS studies because they possess an intense adsorption band in the visible which allows for them being easily excited by the radiation from conventional CW and dye lasers.

SERS studies of porphyrins have been concerned mainly with metal incorporation reactions, aggregation-dissociation processes and redox processes. The earliest studies of the SERS of porphyrins were performed independently by Cotton⁵⁸ and Itoh's group⁵⁹. Both investigated meso-tetrakis(4sulfanato)phenyl)porphine,(TSPP). Cotton used Na_2SO_4 as the electrolyte whilst Itoh used 0.05 M H_2SO_4 . Cotton observed peaks at 1346 cm^{-1} , 425 cm^{-1} and 355 cm^{-1} which are characteristic of the metallated porphyrin. She concluded that metallation of the porphyrin occurred during the anodization process of the ORC. Itoh⁵⁹ also observed metal incorporation but he concluded that metallation occurred at - 0.5 V. He also showed that the porphyrin was adsorbed onto the electrode in the aggregated form and at a potential of -0.3 V dissociation of the adsorbed TSPP aggregate into the monomer occurs. Cotton⁵⁸ observed no such aggregation. Nor did she observe a metal incorporation process at - 0.4 V. Comparing the adsorption behavior of the tetrasulfanato and tetracarboxy phenyl porphyrins(TCPP), Cotton found that the spectra of the carboxy compound could be obtained at more negative potentials than that of the sulfanato porphyrin. This is explained as being due to

a coulombic repulsion between the sulfanato groups and the negatively charged electrode. For TCPP, neutralization of the carboxylate group by complexation with Ag^+ during the activation procedure would limit the electrostatic factors which would result in the desorption behavior that is observed.

Cotton⁵⁸ and Itoh⁵⁹ in their early study suggested that interaction between the porphyrin and the silver electrode was through the substituents (sulfanato and carboxy) on the phenyl ring and not through the 4 nitrogens which are part of the heterocyclic ring. Holze⁶⁰ obtained the SERS spectra of the μ -oxo-iron meso tetramethoxyphenyl porphyrin. He identified the aromatic C-O stretching mode of the methoxy group and observed that it was downshifted by 67 cm^{-1} relative to the solution spectra. From this he concluded that adsorption was through the two methoxy phenyl groups i.e. the orientation was edge on. In an attempt to understand oxygen catalysis Holze⁶⁰ examined the SERS spectra of μ -oxo dimer in the presence of a solution saturated with oxygen. The spectrum showed a band characteristic of the stretching mode of the peroxide ion. His result agreed with those obtained from other experiments which show that hydrogen peroxide is the reduction product of oxygen catalysis. No Fe - O stretching vibration was identified because of the abundance of bands in the region where the Fe - O stretch should be observed.

McMahon⁶¹ obtained the SERS spectra of Iron Protoporphyrin IX . The lack of any perturbation of the porphyrin ring vibration lead him to the conclusion that Fe PP (IX) had an edge on orientation through the carboxylate groups. He investigated the SERS spectra for evidence of the oxidation state of the central Fe atom and observed bands at 1370 cm^{-1} , the oxidation state marker band as well as structure sensitive bands at 1491 , 1570 and 1628 cm^{-1} at an electrode potential of -0.1V . At more negative potentials, -0.6 V , these

bands were replaced by bands at higher frequencies. This was interpreted to represent a change from the high spin 5 coordinated Fe (III) to the intermediate spin Fe(II). These results also showed that the products formed from reduction of hemin are different depending on whether the hemin is in solution or adsorbed on the electrode surface. Spiro and Sanchez⁶² studied the SERS of hemin, Iron (II) protoporphyrinIX chloride, dissolved in aqueous base and the dimethyl ester dissolved in acetonitrile. Like McMahon they concluded that interaction between the porphyrin and the surface was through the peripheral vinyl groups for the dimethyl ester, and the propionate groups for the aqueous hemin. Spiro observed the spectra of surface bound Fe(III) and noted changes in the SERS spectra at - 0.65 V which he attributed as due to a change to the high spin Fe(II). The non Nernstian behavior of the ratio of the RR band intensities along with the irreversibility of the cyclic voltammetric redox process reflects differences in the rates of adsorption and desorption of the oxidized species.

T. Koyama⁶³ identified the Fe(III) to Fe(II) transition for Fe (III)tetrakis N methyl 4 pyridinium porphine at both pH 1.0 and 10.05. The transition from ferric to ferrous occurs at - 0.35 V. When the electrode potential was swept to + 0.135 V the central metal of the porphyrin macrocycle was eliminated.

SERS of cytochrome c⁶⁴ on silver colloids at low temperature have shown that on adsorption onto the colloidal silver surface cytochrome c is partly converted from the low spin state to the high spin state. Room temperature SERS of cytochrome c indicate that it is adsorbed in both the high spin and low spin states. Temperature dependent SERS with temperatures ranging from room temperature to - 196⁰ C reveal that at low temperature the low spin state predominates. This work by Hilderbrandt⁶⁴ was significant because it provides

detailed information on the apparatus necessary for obtaining low temperature SERS of porphyrins.

Cotton⁶⁵ also reported the SERS of cytochrome c, but on a solid Ag electrode. She obtained SERS spectra at - 0.2 and - 0.6 V with 514 nm laser excitation. From her results she concluded that the spectra at - 0.6 V is representative of heme Fe in the low spin reduced state. No denaturing of cytochrome c was observed at the electrode surface. This conclusion was based on the excellent agreement between the surface and solution spectra. SERS studies of cytochrome c₃⁶⁶ by Nikki et.al. examined the conformation of adsorbed cytochrome c₃. The bulk redox properties of cytochrome c₃ as measured by voltammetry were retained when the molecule is adsorbed onto the electrode surface. Redox potentials of the adsorbed species monitored by SERS corresponds to the most positive redox site among the four hemes in the molecule. This is related to the mode of adsorption of cytochrome c₃ unto the silver electrode.

By selectively choosing the wavelength of the excitation source Cotton⁶⁷ discriminated the chlorophyll pigment from the other pigments in the photoreaction center. The combination of the potential dependence of SERS, the excitation of a specific chromophore by using the appropriate excitation wavelength along with the quenching of fluorescence by the surface allows for the investigation of individual chromophores in a complex biological matrix.

Bile pigments which are produced in the liver of mammals and which are related to the phytochromes found in plants have also been studied by SERS. These pigments consists of four pyrrole molecules which are not closed as in porphyrins. Lippitsch⁶⁸ first studied these pigments. Normal Raman spectra of these compounds were impossible to obtain because of their intense fluorescence. Using 2×10^{-7} M solutions of actiobiliverdine and dimethyl

pyrrromethone^{69,70}, intense spectra were obtained on sols. This experiment was the first to demonstrate the quenching of the fluorescence by the surface.

Itoh in a series of experiments⁷¹⁻⁷⁴ developed a novel surface for obtaining SERS of porphyrins. The surface was prepared by depositing a layer, 150 nm thick, of CaF_2 by thermal evaporation on to a microscope glass plate. On top of this, a monolayer of porphyrin was deposited by evaporating off the solvent from two drops of the porphyrin in CH_2Cl_2 . A thin layer of Ag was then vacuum deposited on top of the porphyrin and the SERS spectra obtained from this surface (surface I). A variation of this surface had a CaF_2 /silver/porphyrin structure. Spectra from surface 1 gave information regarding the chemical interactions taking place between the silver atoms and the porphine whilst (surface II) provided information on how adsorption affects the structure of the sample. Using this surface Itoh obtained the SERS spectra of Fe (III) TPPP Cl, MnTPP Cl and Cr (III) TPP Cl. His results show that on incorporation into the layered structure Fe(III) is partially converted to the μ -oxo dimer as evidence by the 366 cm^{-1} Fe - O - Fe stretching vibration of the dimer⁷². There is also evidence of adsorbed monomer present on the surface by the appearance of the 400 cm^{-1} band. To further investigate this μ -oxo dimer formation the rate of Ag deposition was varied from very quick, 4 \AA/sec , to the slow rate of 0.4 \AA/sec . When Ag is quickly deposited no Fe - O - Fe vibration is observed in the spectra but it is observed at slower deposition rates. This suggests that the μ -oxo dimer formation is the result of either a kinetically controlled interaction between Fe(III) and Ag vapor or that the formation depends on the interaction between the complex and the Ag layer and is affected by the method of surface preparation and surface morphology.

Although the number of papers published on the SERS of porphyrins is small, they have provided valuable insight into porphyrin metal interaction as

well as the identification of electrochemical intermediates. SERS studies of porphyrins would continue to be an area of active research because of the biological importance of the porphyrins and the increasing use of adsorbed porphyrins and metalloporphyrins as catalyst or sensitizers in photochemical cells.

1.11 MOTIVATION FOR THIS STUDY

Porphyrins consist of 4 pyrrole rings linked together by methine bridges. In metal free porphyrins such as those used in this study, there is an inner 16 member conjugation pathway containing 18 electrons. Iron porphyrins are prosthetic groups of heme and a number of macrocyclic complexes such as chlorophyll and vitamin B₁₂ are closely related to porphyrins. Because of their occurrence in biological systems porphyrins have been the subject of considerable scientific investigation^{40,41}.

The initial Raman spectroscopic studies of porphyrins^{42,43} were intended to assist in the understanding of the biological properties of the compounds. It was soon discovered that the vibrational spectra of porphyrins provided information regarding changes in porphyrin geometry, and that configuration interaction and vibronic mixing can produce a variety of Resonance Raman effects which proved interesting to theorists.

The results presented in this thesis are part of a broad study of the properties of amino and nitro substituted tetra phenyl porphyrins. The study includes novel methods for the synthesis of the porphyrins, fluorescence life time decay measurements, hole burning spectroscopy and time dependent

Raman studies. The overall objective of the study is the understanding of the structural basis for the primary photochemical events in photosynthesis.

The initial experiments in this thesis centered on the investigation of the effect of molecular symmetry on the SERS spectra of a number of p-amino substituted tetraphenyl porphyrins. These p-amino substituted tetraphenyl porphyrins are very soluble in acetonitrile, one of the few porphyrins soluble in this solvent. Furthermore, because of the lack of many SERS studies of porphyrins in non aqueous media and the inherent simplicity of electrochemical processes in non aqueous media, the SERS study of TAPP was extended to a non aqueous medium, acetonitrile. The use of water as the solvent for SERS experiments severely limits the range of compounds which can be studied by the technique. As a result the expansion of the technique to include non aqueous media allows for an increase in the adsorbates which can be studied by the technique and thus increases its applicability.

1.12 ABSORPTION SPECTRA OF PORPHYRINS

Goutterman's⁷⁵ four orbital model has been used to explain the characteristics of the absorption spectra of porphyrins. Assuming idealized D_{4h} symmetry for the porphyrin ring system, then the lowest lying unoccupied π orbitals are degenerate possessing e.g. symmetry. The highest filled π orbitals are of the a_{1u} and a_{2u} symmetries. There exist a large interaction between the two filled orbitals because they possess nearly the same energy; the transition dipoles add up for an intense B transition and almost cancel out for the weaker Q_0 transition. Some intensity is regained for the Q transition through vibronic mixing with the B transition. This leads to the Q_v side band. If there is extensive

interaction between the π electrons of the porphyrin macrocycle and the electrons of a central metal substituent, then interpretation of the absorption spectra involves more than the four orbital model.

CHAPTER TWO

A SPECTROELECTROCHEMICAL STUDY OF TAPP IN ACETONITRILE

2.1 ABSTRACT

The surface enhanced Raman scattering (SERS) spectra of five p-amino substituted tetraphenyl porphyrins were investigated at a silver electrode in the aprotic solvent, acetonitrile. Good quality spectra were obtained for both the neutral porphyrin and for its first reduction product the radical anion. Fluorescence interference from the porphyrin was completely quenched by the surface. SERS spectra allowed for the identification of two geometries of the adsorbate. Cyclic Voltammetry and UV Visible Thin layer spectro-electrochemistry were used to confirm information obtained by SERS. The utility of SERS as a technique for identifying electrochemical products in a non-aqueous environment, where elucidation of electrode mechanism is simpler and radical anions are more stable, is demonstrated.

2.2 INTRODUCTION

The redox properties of porphyrins play an important role in their biological activity¹. In an attempt to better understand their biological properties, extensive studies of the electrochemistry of porphyrins have been performed². Because of the relative simplicity of redox processes and the increased stability of electrochemically generated intermediates in non-aqueous solvents, many of the electrochemical studies of porphyrins have been performed in non aqueous media². In order to obtain information regarding the molecular structure of electrochemically produced porphyrin intermediates, cyclic voltammetry has been coupled with ESR and NMR spectroscopy^{3,4}. These two spectroscopic techniques, although providing information on molecular structure which could not be obtained electrochemically, do not offer the degree

of specificity which is necessary for the complete characterization of electrochemically generated porphyrin intermediates.

Since its discovery by Fleischmann et al⁵ surface enhanced Raman spectroscopy has been used^{6,7} to characterize the structure and orientation of electrochemically generated species on roughened Ag, Au and Cu electrodes. The large enhancement of the SERS spectra along with the high degree of specificity offered by Raman spectroscopy makes SERS an ideal tool for the characterization of electrochemically generated porphyrin species.

SERS has not been coupled with electrochemical techniques in the study of porphyrin electrochemistry in non-aqueous media because of the difficulties in preparing SERS active electrodes in non-aqueous solvents. There have been, however, some SERS studies of compounds in non-aqueous solvents e.g. pyridine in dimethylformamide⁸ and tris(2,2'-bipyridine)ruthenium (II)⁹ and one study of a porphyrin compound¹⁰. Spiro¹⁰ studied the transition from low spin Fe(II) to high spin Fe(III) in the dimethyl ester of hemin.

A number of acetonitrile soluble p-amino substituted TPP compounds were synthesized and their electrochemical and spectroscopic properties in acetonitrile studied using SERS spectroscopy. The results presented in this chapter show that at -0.6V an adsorption change occurs resulting in a more firmly bound adsorbate. The orientation of the adsorbate is established and spectroscopic evidence is presented to show that expansion of the porphyrin ring aromatic system occurs to include the phenyl substituents .

2.3 EXPERIMENTAL SECTION

The derivatives of tetraphenyl porphyrin used in this study incorporated p-amino substitution at one or more of the phenyl groups, Fig. 1a. Fig. 1b shows the labelling of specific carbon atoms on the macrocycle. The porphyrins were a gift from Prof. C. Guo and were synthesized¹¹ by condensation of pyrrole, benzaldehyde and p substituted benzaldehyde at different molar ratio in organic solvents. The aminoporphyrin with the desired substitution was isolated from the product mixture by chromatographic separation and recrystallization from solution¹¹. Porphyrin composition and structure were confirmed by elemental analysis, mass spectrometry, IR and NMR methods¹².

Dilute solutions, approximately 1×10^{-5} M, of the porphyrin in acetonitrile were used. Optima grade Acetonitrile, (Fisher products), was dried over 4 Å molecular sieves prior to use. Tetrabutyl ammonium perchlorate (TBAP) was recrystallized from pentane/ethyl alcohol, dried under vacuum and stored in a desiccator prior to use. Solutions of the porphyrin were degassed using nitrogen which was first passed through a drying agent and then acetonitrile before passing through the porphyrin solution.

The SERS experimental set up has been described elsewhere¹³. A Spectra Physics Model 164 Argon ion laser was used for 488 nm excitation. A Cary Model 11 spectrometer was used for the Visible spectroelectrochemistry. Cyclic voltammograms were recorded using a model 175 Universal Programmer and a Model 173 Potentiostat/Galvanostat, both EG+G Princeton Applied Research. SERS and Raman spectra were recorded with a Spex Model 1401 double monochromator with a wavenumber resolution of about 4 cm^{-1} . Photon counting detection was used and the intensities were recorded digitally and are presented here unsmoothed.

The sample cell for SERS consisted of a 99.999 % pure silver working electrode, a platinum counter electrode and a saturated calomel electrode(SCE) as the reference. All potentials are reported relative to the SCE. A bridge was used to separate the reference electrode from the rest of the electrochemical system. The oxidation reduction cycle (ORC) pretreatment was performed using a 2 second pulse from 0 V to +0.5 V and then returning the electrode to 0.0V.

2.4 RESULTS AND DISCUSSION

Fig.2 shows the SERS spectra for four of the five p-amino substituted porphyrins adsorbed on a roughened silver electrode at an electrode potential of -0.6V. The laser excitation was at 488 nm. The solutions were approximately 1×10^{-5} M porphyrin and 0.1 M tetrabutyl ammonium perchlorate(TBAP). The intensity of the laser radiation at the electrode surface was between 50-70 mW. The solvent bands occur at 380 cm^{-1} and 922 cm^{-1} and are labelled.

Because of the absence of SERS studies of porphyrins in acetonitrile as the solvent, it was necessary to determine whether the spectra obtained in this study were surface enhanced Raman spectra or solution spectra. Two experiments were performed. In the first experiment the electrode was roughened in a solution of the porphyrin in acetonitrile. This roughened electrode was then transferred to an acetonitrile solution without dissolved porphyrin and the spectra recorded (*in situ* roughening). In the second experiment the electrode was roughened in a porphyrin free acetonitrile solution. This roughened electrode was then placed in a 1×10^{-5} M porphyrin solution and the spectrum recorded (*ex situ* roughening).

In both cases good quality spectra were obtained with intensities far greater than those of corresponding solution spectra. The most intense spectra

were obtained from the *in situ* roughened electrode. The band frequencies were nearly identical for the spectra obtained from the *in situ* and *ex situ* roughened electrodes. The exception was two bands at 418 cm⁻¹ and 1340 cm⁻¹ which were observed in the spectra from the *in situ* roughened electrode but were absent from the spectra obtained from the *ex situ* roughened electrode. This difference is explained in the following section.

The significant increase in intensity of the spectra over the solution spectra, the improved peak separation along with the absence of a fluorescence background in the spectra indicates that the spectra obtained in this study are from the surface bound species and not solution species and that they are surface enhanced Raman spectra. It has been shown¹⁴ that in SERS, the electrode surface acts as a fluorescence quencher and, therefore, allows for the observation of spectra from surface bound species which if in solution would have had their signal masked by the intense fluorescence background. Significant changes in the intensity and frequency of the spectra were observed for ORC pretreated and unpretreated silver surfaces, reinforcing the view that the spectra observed here were of the surface bound porphyrin.

Fig.3 is the visible absorption spectrum of one of the p-amino substituted TPP compounds, porphyrin AAAA(TAPP) with arrow(b) indicating the position of laser excitation used in this chapter. TAPP shows an intense absorption at 422 nm., the Soret band. The laser excitation frequency used in this study was at 488 nm and was approximately 60 nm. away from the Soret band. It was, however, only 32 nm away from the weaker 520 nm absorption band. The spectra were therefore also resonance enhanced. The strong resonance enhancement coupled with the large enhancement due to SERS, on the order of 10⁶, make porphyrins ideal candidates for SERS studies. It also allowed for

very low concentration of TAPP, on the order of 10^{-6} to 10^{-7} M, to be used in the study.

The potential dependence SERS spectra of the five p-amino substituted TPP compounds used in this study show that for four of the compounds AAAA, AAAO, AAOO and AOA O spectra were obtained at potentials as negative as -1.4V. For compound AOOO spectra were obtained only up to a potential of -0.5V. At more negative potentials no spectra are obtained suggesting that the molecule is desorbed from the electrode surface. This facile desorption is a reflection of the the strength of the interaction between the porphyrin molecule and the electrode surface.

The four porphyrins AAAA, AAAO, AAOO, and AOA O all showed similar spectroscopic and electrochemical behavior. The results which are presented in this chapter are for compound AAAA, meso(tetrakis4-aminophenyl)porphyrin (TAPP). Its behavior is characteristic of that of the other three porphyrins studied.

2.4a METAL INCORPORATION

Cotton¹⁵ in her study of the water soluble porphyrin tetrasodium *meso*-tetrakis(4 sulfanatophenyl) porphine (TSPP) identified bands at 1346 cm^{-1} , 425 cm^{-1} and 355 cm^{-1} as being characteristic of metal incorporation into the porphyrin ring. An examination of the potential dependent spectra of TAPP, Fig.4, shows peaks at 418 and 1340 cm^{-1} . These peaks are equivalent to those found by Cotton and their absence from the spectra when the ORC was performed *ex situ* is further indication that they are due to metal incorporation.

The potential dependence spectra of TAPP shows that the intensities of the 418 and 1340 cm^{-1} bands greatly increase at -0.6 V . This could be due to a

closer interaction between the incorporated metal and the electrode surface. It is clear however that metal incorporation does occur for TAPP and that this incorporation occurs during the anodization step when the potential of the electrode is pulsed to +500 mV .

The 355 cm^{-1} band observed by Cotton in the SERS of TSPP was not observed in our study. Cotton in examining the spectrum of AgTSPP also failed to observe this band . Itabashi ¹⁶ also studied TSPP and his work again failed to show this 355 cm^{-1} band. Because the 355 cm^{-1} vibration was observed only for AgTSPP in H_2O , Cotton assigned this band as being due to a ligand mode involving water or the sulfanato group of another TSPP molecule. Itabashi also observed metal incorporation at -0.4 V for TSPP in 0.05 M sulfuric acid solution. No such incorporation was observed at -0.4V in our study.

2.4 b SPECTROSCOPY AND ELECTROCHEMISTRY

Fig.4 shows that at -0.6V(Fig.4d) there is a significant increase in the intensity of the spectrum. Fig.5 shows portions of the potential dependent SERS spectra in the region around 100 to 1500 cm^{-1} of porphyrin AAAA (see Fig.1a for structure) on a roughened Ag electrode at potentials of -0.5V, -0.6V and -0.7V. At -0.5V a singlet peak is observed at 1002 cm^{-1} . When the potential is changed to - 0.6 V two peaks are observed, one at 1002 and the other at 1010 cm^{-1} . Similarly at -0.5V one peak is observed at 1548 cm^{-1} while at -0.6V two peaks are observed one at 1534 cm^{-1} and one at 1548 cm^{-1} . As the potential is made more negative both the 1002 cm^{-1} and the 1548 cm^{-1} bands decrease in intensity while the 1010 cm^{-1} and the 1534 cm^{-1} increase in intensity

Table 1 lists the assignments of the Raman bands for TAPP. The 1010 cm^{-1} peak is assigned as a $\nu(\text{C}_\alpha - \text{C}_\beta)$ and the 1534 cm^{-1} band is assigned as a $(\text{C}_\alpha - \text{C}_m)$ vibration. See Fig.1b for atom labels.

To assist in characterizing the process observed spectroscopically at -0.6V, cyclic voltammetry (CV) was performed on TAPP in acetonitrile. The CV curves were obtained at scan rates ranging from 50 to 500 mV per second. Fig.6 and 7 for silver, and Fig.8 for gold electrode surfaces shows representative CV curves at either 100 or 500 mV/s.

An early study of the polarographic reduction of porphyrins in non aqueous media ¹⁸ showed that for H₂TPP and for a number of its metallated analogues, the first reduction peak occurred at - 1.05V for H₂TPP and potentials as negative as - 1.35V for Mg TPP. All of these derivatives of TPP showed a prewave having a peak potential of - 0.7 V for TPP and - 0.67 V for MgTPP. No discussion as to the reason for this prewave was given in the report¹⁸ except to say that the prewave was not due to an impurity and its peak height did not increase linearly with porphyrin concentration.

An examination of the cyclic voltammogram of TAPP at a scan rate of 200 mV per second (Fig.6) shows two cathodic peaks at - 0.6 and - 1.0 V. On the anodic scan two peaks are observed at - 0.3 and - 0.4 V. The CV scans do not show well defined oxidation peaks. Other studies of porphyrins in non aqueous media have shown a similar lack of reversibility which is believed to be due to the reaction of the electrochemically generated products with small traces of water from the solvent. The small anodic peak observed in the CV at - 0.4V is probably due to the reoxidation of the product formed at - 1.0 V.

The cyclic voltammogram peak currents for the processes occurring at - 0.6 and -1.0 V behave differently with changing scan rate. A plot of i_p vs the square root of the scan rate, Fig.9, for the -1.0 peak is linear whilst no such linearity is obtained for a similar plot of i_p for the -0.6V peak. A plot of peak current vs scan rate (Fig.10) is more linear for this peak. This indicates that the process that is occurring at -0.6V is an adsorption controlled process. Similar

results were obtained when the working electrode was switched from Ag to Au, with the only difference being that the position of the peak potentials were shifted to more positive values by approximately 200mV on the gold electrode, Fig.8.

Further confirmation of the non-Faradaic nature of the process occurring at -0.6V on Ag was obtained by performing thin layer visible spectroelectrochemistry of TAPP in an acetonitrile solution. A three electrode electrochemical system was used. This consisted of a gold minigrid working electrode having a transmission of 60 %, a platinum counter electrode and a saturated calomel electrode. Fig.11 shows the potential dependent spectra obtained for the 400-500 nm region of TAPP. At 0.00 V (Fig.11a) the spectrum of TAPP showed a peak at 422 nm. The potential of the system was changed in steps of - 0.2 V. No changes were observed in the spectra until -0.8V (Fig.11b). At this potential two Soret bands were observed, one at 422 nm and the other at 450 nm. As the time at - 0.8 V was increased (Fig.11c) the 422 band decreased in intensity whilst the 450 nm band increased in intensity.

Wilson and coworkers¹⁹ using TPP in dimethyl formamide (DMF) have shown that a 418 nm band is due to TPP whilst a 448 nm band is due to the radical anion. From this it can be concluded that the spectrum obtained at -0.8V on gold, equivalent to the -1.0V on silver is that of the radical anion. No change in the UV visible spectra was observed at - 0.4 V which corresponds to the - 0.6 V peak on the silver electrode. This confirms that the process occurring at - 0.6 V is not the first reduction of the porphyrin. The UV Visible spectra conclusively shows that first reduction product of TAPP occurs at -0.8 V on Au which is equivalent to the -1.0 V on silver.

V. Kadish and workers²⁰ studying meso tetrakis (1 methylpyridinium-4 yl) porphanato nickel in DMF observed two peaks in the Soret region of the UV

visible spectrum of the porphyrin. One peak was observed at 440 and the other at 420 nm. They assigned one of the peaks to the monomer and the other to the dimer. In an attempt to establish whether TAPP aggregates in solution and therefore whether the process occurring at - 0.6 V was the separation of the aggregate into the monomer, UV visible spectra were observed over a range of concentrations. All showed one Soret band at 422nm and a Beer's Law plot, Fig.12, was linear indicating that there was no aggregation of TAPP in acetonitrile solution and that the process occurring at - 0.6 V was not a dissociation of the aggregate into the monomer.

The shape of the -0.6V peak in the CV along with the results presented before suggests that the process occurring at -0.6V is an adsorption process. Weaver²¹ studied the SERS of benzene adsorbed on gold electrode and observed a single peak at 973 cm^{-1} at an electrode potential of - 0.5 V. He assigned this as the ring breathing mode. When the potential was shifted to more positive values this peak was split into two. Since there was no Faradic electrochemical process occurring at this potential, he explained this split as being due to the presence of two adsorbate geometries at the electrode surface.

The appearance in this study of two resolvable pairs of peaks, 1002 - 1010 and 1534 - 1548 cm^{-1} at - 0.6 V, suggests two binding geometries. The peaks at 1010 and 1534 cm^{-1} are associated with a more tightly bound surface species and those at 1002 and 1548 cm^{-1} with a more weakly bound species. The increase in the intensity of the SERS spectra is also evidence for a more tightly bound adsorbate.

The spectral and electrochemical results allow for the conclusion that the process occurring at -0.6V is an adsorption process resulting in an adsorbate which is more tightly bound to the electrode. Also the spectrum obtained at - 1.0V is established as being that of TAPP radical anion. The spectrum of the

radical anion is characterized by the absence of the 1024 and the 1042 cm^{-1} bands, a band at 1532 cm^{-1} which is the 1526 cm^{-1} band shifted by 6 cm^{-1} , and a 1594 cm^{-1} band which is the 1584 cm^{-1} band shifted by 10 cm^{-1} .

2.4 c ORIENTATION OF THE ADSORBED PORPHYRIN

Fig. 13 is the solution Raman spectra of TAPP. Because TAPP is highly colored it absorbs strongly at the wavelengths used in this study. It also fluoresces at longer wavelengths, in the red. No solution Raman spectra could be obtained by conventional methods. The spectrum shown here, Fig.13, was obtained by passing the 488 nm laser line through the sample and reflecting it from a polished silver electrode to the entrance slits of the monochromator. Fig.13 shows the 900 cm^{-1} to 1600 cm^{-1} region of the spectrum. Table 2 shows a comparison of the solution Raman and the SERS spectra. The intense peak at 922 cm^{-1} in the solution Raman is due to the solvent and it is found at about 920 cm^{-1} in the SERS spectra. A comparison of the intensity of the solvent peak in both the solution Raman and the SERS spectra show that it is greatly reduced in the SERS spectra. This shows that the SERS of the adsorbate is enhanced to a greater extent than the solvent. The 974 cm^{-1} band in the solution Raman is the 962 cm^{-1} band in the SERS down shifted by 12 cm^{-1} . The 1060 cm^{-1} solution Raman band is observed at 1002 cm^{-1} in SERS down shifted by 58 cm^{-1} whilst the 1130 cm^{-1} solution Raman band is the 1078 cm^{-1} SERS band down shifted by 52 cm^{-1} . A comparison of the intensities of the 974 and 1064 cm^{-1} solution Raman bands with their SERS counterparts shows that in the solution Raman the 974 cm^{-1} band is more intense than the 1064 cm^{-1} , whilst in the SERS the reverse is true. Other bands at higher frequencies show smaller shifts of 6 cm^{-1} or less and these shifts are

considered insignificant. The 1274 cm^{-1} band is unchanged for both the normal Raman and the SERS, whilst the 1550 cm^{-1} solution Raman band is virtually the same in the SERS and the 1598 cm^{-1} solution Raman band is down shifted by 6 cm^{-1} . The strongly downshifted bands in the SERS spectrum are at 962 , 1002 and the 1078 cm^{-1} . The 962 cm^{-1} band is a phenyl vibration, the 1002 cm^{-1} band is assigned as a ($C_{\alpha} - C_m$) and the 1078 cm^{-1} is a ($C_{\beta} - H$). A down shift of a stretching mode strongly indicates adsorptive interaction of one of the atomic participants involved in the stretching mode to a coordinating metal. These downshifts suggest a flat orientation of the molecule.

TAPP can assume two orientations on the surface, with the molecular plane either parallel or perpendicular to the electrode surface. A perpendicular orientation of the molecule would result in a strong interaction between the amino group and the surface. This would manifest itself by a downshift in the amino vibration. Examination of the $1600 - 4500\text{ cm}^{-1}$ region failed to detect the amino vibration. A number of porphyrin studies^{15,16} of sulfanato and carboxyl TPP have also failed to observe the vibrations due to the substituents on the phenyl ring. A perpendicular orientation should also affect the aromatic carbon to nitrogen vibration and a downshift of this vibration should be expected²². In the assignment of the Raman spectra of aniline the aromatic ($C - N$) stretch is listed as occurring at 1278 cm^{-1} . Examination of the solution Raman spectrum shows a moderate band at 1274 cm^{-1} whilst the SERS spectra shows a weak band at 1274 cm^{-1} which increases in intensity and becomes well defined at -0.6V . This band we assign as the aromatic $C - N$ vibration and the absence of any appreciable downshift (only 2 cm^{-1} is observed) suggests that bonding between the electrode and the porphyrin does not involve this vibration. This rules out the possibility that the molecule is oriented perpendicular to the electrode surface.

The above evidence is consistent with other results²³ regarding the geometry of the porphyrin molecule. The π conjugated system of the porphyrin is considered to consist of the 16 atom 18 π electron ring that excludes the β carbons²⁴. The ($C_\beta - C_\beta$) bond has been shown to have approximate double bond character²⁴. In the 16 atom 18 π electron ring system there is a flat bonding about the interior carbon atoms. The pyrrole ring is tilted about 6.6 degrees²⁵ resulting in the ($C_\beta - C_\beta$) not being coplanar with the rest of the molecule. The shifts observed in the SERS spectra for the ($C_\alpha - C_m$) and the ($C_\beta - H$) vibrations are consistent with this molecular geometry. Also because the aniline group is at an angle of between 40 - 60 degrees to the rest of the molecule the ($C_m - Ph$) and the aromatic ($C-N$) vibrations should not be in close contact with the surface and it is expected that no downshift in these vibrations should be observed if the porphyrin molecule is adsorbed flat. The absence of any shift in the 1274 cm^{-1} band further supports this assumption.

2.4 d SERS FROM A ROUGHENED DRIED ELECTRODE

In an attempt to obtain information regarding the role of the solvent in the orientation of the TAPP molecules on a silver electrode, spectra were obtained from a roughened dried electrode (RDE). The electrode was first roughened *in situ*. It was then removed from the solution and left to dry in air.

Intense well resolved spectra were obtained from this roughened dried electrode and the spectrum is presented in Fig14. An examination of the $900 - 1600\text{ cm}^{-1}$ region of the spectrum shows that the 922 cm^{-1} band which is present in the solution spectrum is absent in the spectrum from the dried electrode. This band is the solvent peak and its absence indicates that all the solvent has evaporated from the electrode. Therefore, the spectrum observed from the roughened dried electrode represents interactions between the

electrode and the TAPP molecules without solvent interference. A comparison of the spectra from the RDE with the *in situ* potential dependent SERS spectra of TAPP, Table3, indicates that the spectrum from the RDE is similar to that of the *in situ* SERS spectrum at - 0.6 V. The band at 1016 cm^{-1} on the RDE is equivalent to the 1010 cm^{-1} *in situ* band. The 1184 cm^{-1} band which is weak in the *in situ* spectra at potentials more positive than -0.6V increases in intensity when the potential is made more negative. This vibration is intense in the RDE spectrum. Also the 1536 cm^{-1} band from the RDE is equivalent to the 1534 cm^{-1} band which is found at - 0.6 V in the *in situ* spectra. The excellent agreement between the two sets of spectra is further evidence that the process occurring at - 0.6 V is a reorientation of the molecule and that the spectra obtained at - 0.6 V is that of the more strongly adsorbed porphyrin molecule with solvent molecules displaced.

There are also some differences between the RDE spectrum and the *in situ* SERS spectra. The 962 cm^{-1} band in the *in situ* SERS spectra is observed at 982 cm^{-1} on the RDE and the band found at 1274 cm^{-1} in the *in situ* SERS spectra is absent from the RDE spectrum. Also the 1174 cm^{-1} band of the *in situ* SERS spectrum is upshifted by 10 cm^{-1} to 1184 cm^{-1} on the RDE.

The 982 cm^{-1} band has been assigned as a phenyl vibration. The 1274 is an aromatic ($C-N$) stretch which is observed at 1278 cm^{-1} in aniline whilst the 1174 cm^{-1} peak is assigned as a C_m-Ph vibration. Shindo²² studying the SERS of aniline, observed a band 1278 cm^{-1} which he assigned as a C - N stretching vibration. This band was observed in the solution spectra of aniline but when the molecule was adsorbed flat onto the electrode surface this band disappeared. Shindo used this to characterize the orientation of the molecule on the electrode surface. The presence of the 1274 cm^{-1} band in the *in situ*

SERS spectra indicates that the aniline portion of the molecule is not adsorbed flat on the electrode surface.

X ray analysis²⁶ of triclinic TPP shows that the phenyl groups are rotated by about 60-63 degrees for free base TPP and are nearly perpendicular to the porphyrin ring in Ru(CO)TPP. For TAPP adsorbed parallel to the electrode surface, assuming no molecular distortion the phenyl groups would not be parallel to the surface but would be at an angle, the size of which would depend on the value of the dihedral angle between the phenyl substituent and the porphyrin ring. Calculations of the phenyl ring rotation angle in tetra phenyl porphyrins show that the minimum energy configuration occurs when the angle between the porphyrin plane and the phenyl ring is 44 degrees²⁷. There is, therefore, a wide range of values for the dihedral angle when the molecule is in solution.

The absence of the 1274 cm⁻¹ band in the RDE spectra indicates that the aniline portion of the molecule has become more coplanar with the porphyrin ring and has changed its orientation. The estimated activation energies for this rotation, ranges from 15.6 Kcal/mol for TiO(p-iPrTPP) to 18.6 Kcal/mol for Ru(CO)(p-i-PrTPP)(4,5-dimethylpyridazine)²⁸. Phenyl rotation requires some distortion of the porphyrin ring and the ease with which coplanarity is achieved for different porphyrins is a reflection of the differences in the ease of distortion of the complex.

Rotation of the phenyl groups into coplanarity with the porphyrin ring should result in some form of resonance interaction between the conjugated ring system of the porphyrin and the phenyl substituent. This effect has received some investigation²⁹. However, the extent and importance of this π delocalization is still unresolved. Molecular orbital calculations³⁰ focus on the 16 atom 18 π electron ring system and ignore any contribution due to

delocalisation of the π electron ring system over the phenyl substituents. There is experimental evidence which has been interpreted as indicating delocalisation of the π electron system into the phenyl substituents. An example^{31,32} is work done on linear force energy correlations. However, other explanations³³ which ignore π delocalization have been presented to explain the experimental data.

Because of its specificity, resonance Raman spectroscopy has been used to identify π delocalisation. Early studies on protoporphyrin and its derivatives could not unequivocally identify the $\text{C}=\text{C}$ stretching frequency and so could not demonstrate whether the vinyl group was part of the delocalised π system. W. H. Fuchsman³⁴ studied the resonance Raman spectroscopy of three Tetra(p-halophenyl) porphines and their derivatives. He observed halogen sensitive bands, of medium intensity, in the 1050 to 1100 cm^{-1} region the spectra. These bands were assigned as phenyl ring modes containing significant C - X stretching character. They are strong in the IR but very weak in the RR of the solid porphyrin dication, solid neutral porphyrin and the solid Cu II porphyrin. The authors attribute the presence of these bands and their increase in intensity in solution as an indication of delocalisation of the π electron system. Fuchsman³⁴ has suggested that even a dihedral angle of over 60 degrees would not preclude π overlap between the phenyl groups and the porphyrin aromatic system. These conclusions are strongly denounced by theoreticians³⁵.

To further investigate the effect of phenyl rotation and the possible extension of the π system to include the phenyl rings we identified the $\text{C}_m\text{-Ph}$ vibration. This vibration is found at 1174 cm^{-1} in the *in situ* SERS spectra. Rotation of the phenyl ring into coplanarity with the sixteen atom eighteen π electron aromatic system should result in electron donation to this bond

resulting in an increase in its bond order which should express itself by a shift to higher frequency of the $C_m - Ph$ vibration. Cotton³⁶ observed a similar effect in the study of 4,4 bipyridine and C. Takahashi³⁷ observed a similar upshift in the study of the biphenyl negative ion.

Examination of our spectra show that the $C_m - Ph$ vibration is observed at 1174 cm^{-1} in the *in situ* SERS spectra and at 1184 cm^{-1} for the RDE spectra. Although the upshift of 10 cm^{-1} is relatively small it is still significant and along with the upshift of 20 cm^{-1} for the phenyl vibration is additional proof of rotation of the phenyl ring and an indication of some degree of increased overlap between the π electron system of the porphyrin aromatic system and the phenyl groups.

It appears that when TAPP is adsorbed onto the electrode in the presence of solvent molecules the solvent molecules are coadsorbed with the porphyrin. When the electrode is dried, the solvent molecules evaporate and the TAPP molecules are left directly adsorbed onto the electrode surface without the interaction of solvent molecules. This results in a more tightly bound TAPP which forces rotation of the phenyl groups so that the phenyl substituent and the 16 atom 18 π electron porphyrin core either become coplanar or closer to coplanarity.

2.5 CONCLUSION

The results presented in this study have illustrated the application of SERS to the study of five acetonitrile soluble porphyrins at a silver electrode. The results indicate how vibrational spectra can be used to determine the orientation and the mode of interaction between the adsorbed porphyrin molecules and the electrode surface. The SERS spectra indicate that the

process which is observed at - 0.6 V in the cyclic voltammetry is due to a change in the geometry of the adsorbed porphyrin. The spectra also indicate that in the absence of coadsorbed solvent, adsorption of the porphyrin results in a rotation of the phenyl rings into coplanarity or near coplanarity with the 16 atom 18 π electron porphyrin skeleton resulting in an extension of the porphyrin π conjugation system to include the phenyl substituents. Thus SERS is utilized to obtain information regarding adsorbate/surface interaction that would be hard to obtain by other analytical methods.

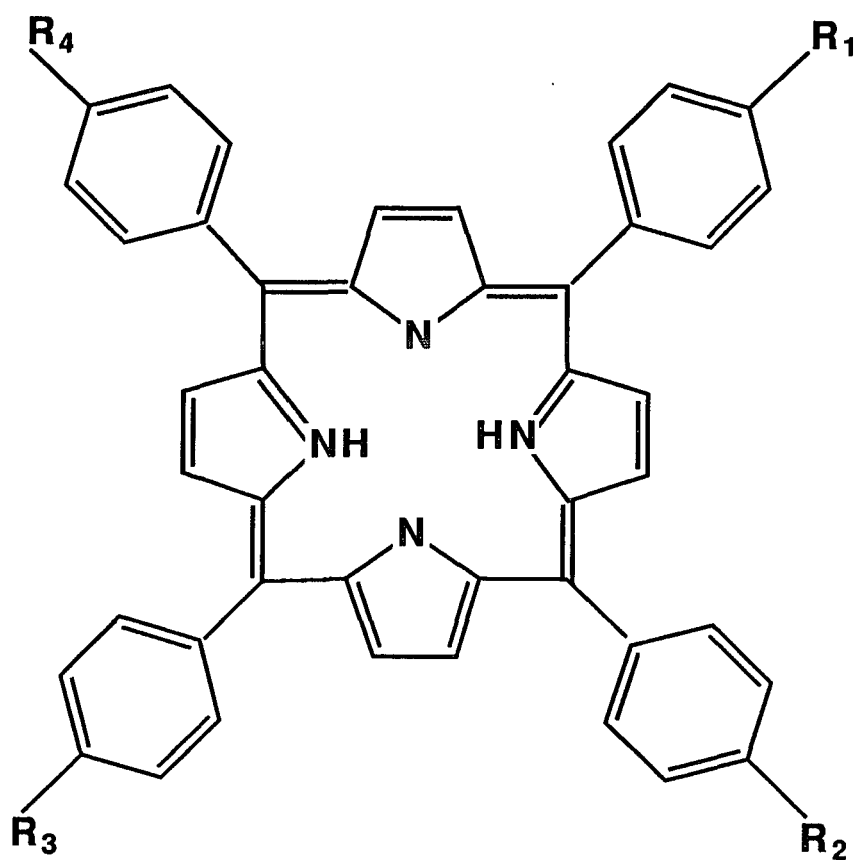


Fig. 1(a) Structure of p-amino substituted TPP

TPP	R_1, R_2, R_3 and R_4 are equal to H
AOOO	$R_1 = \text{NH}_2$, R_2, R_3 and R_4 are equal to H
AAOO	R_1 and $R_2 = \text{NH}_2$, R_3 and R_4 are equal to H
AOAO	R_1 and $R_3 = \text{NH}_2$, R_2 and R_4 are equal to H
AAAO	R_1, R_2 and $R_3 = \text{NH}_2$, R_4 is equal to H
AAAA	R_1, R_2, R_3 and R_4 equal to NH_2

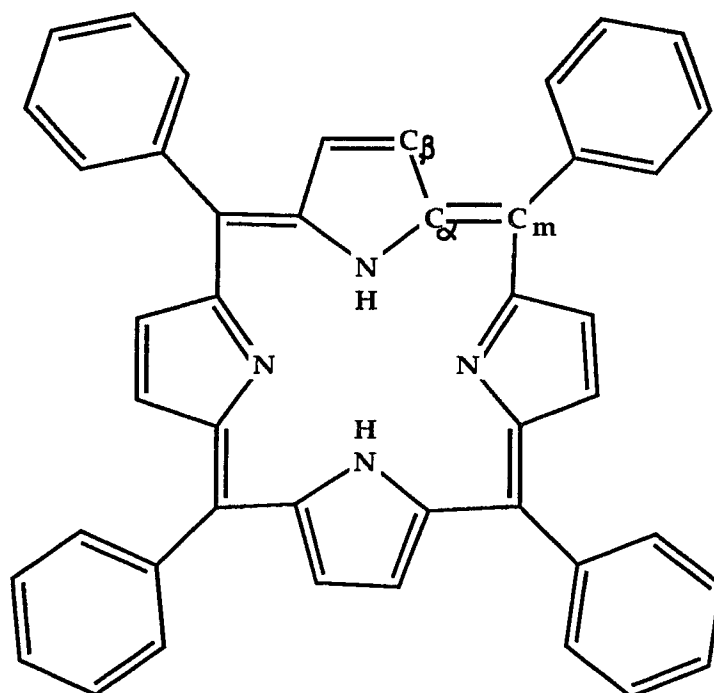


Figure 1b. Structure of TPP to show the labelling of the carbon atoms.

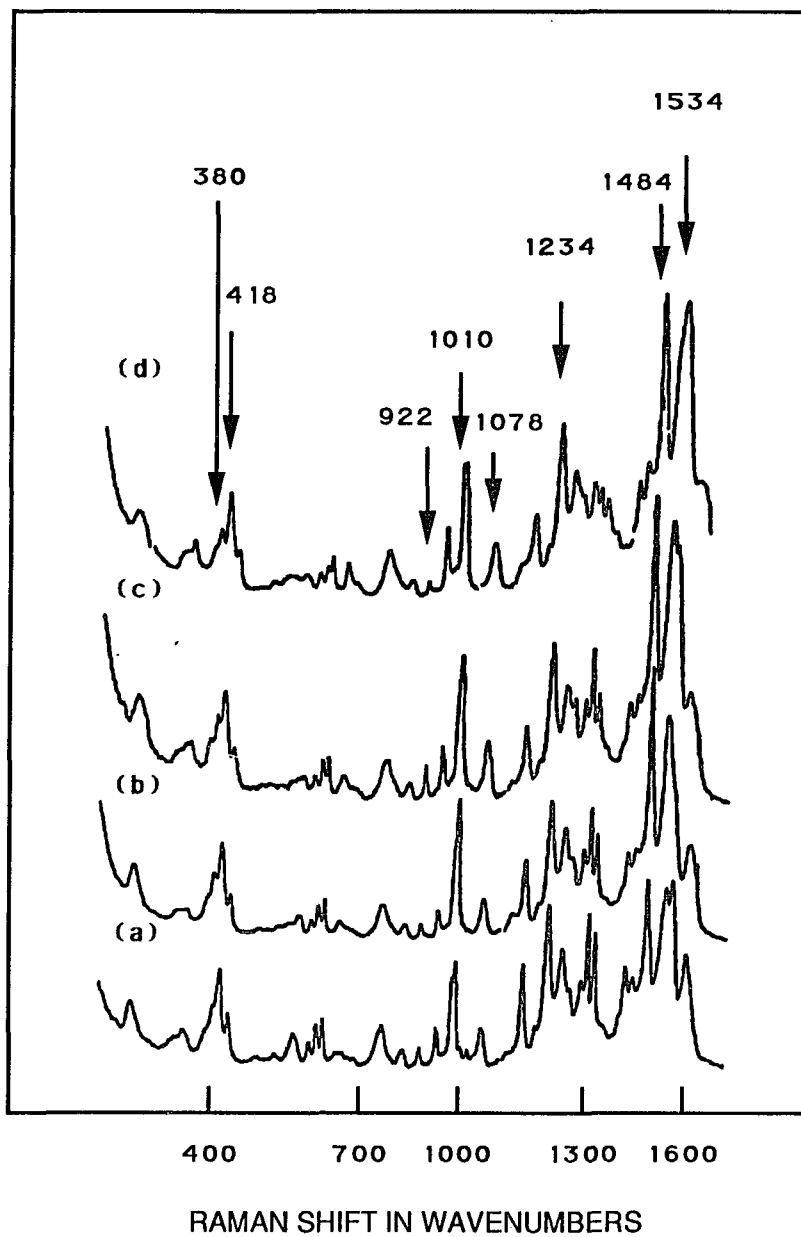


Fig.2 SERS spectra of four p-amino substituted TPP compounds in acetonitrile on a roughened silver electrode at 488nm excitation. (a) AAAA (b) AAAO (c) AAOO and (d) AAOO

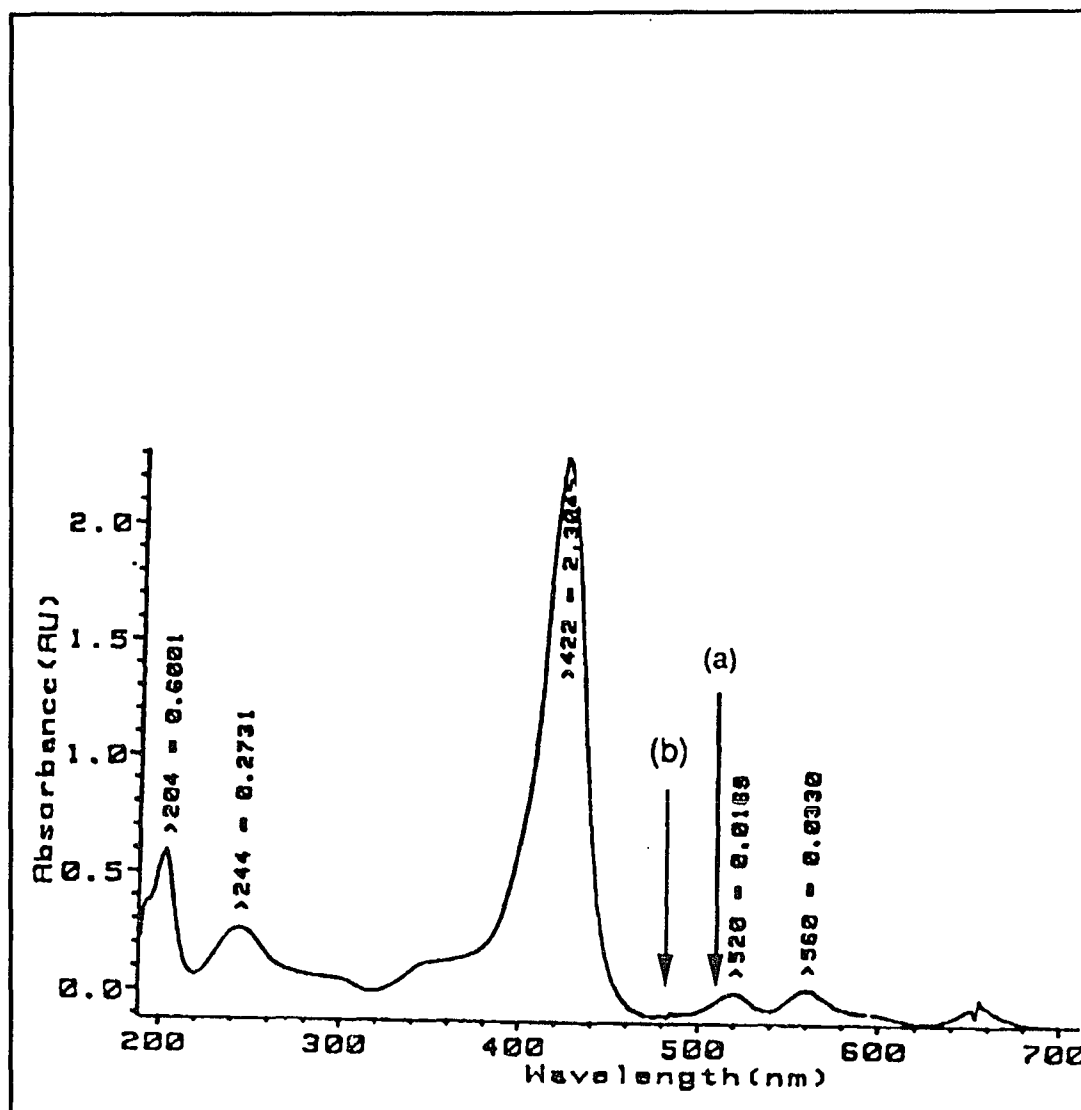


Fig.3 Visible absorption spectrum of TAPP in 0.05M HCl
(a) Represents laser excitation frequency 514 nm and (b) 488 nm

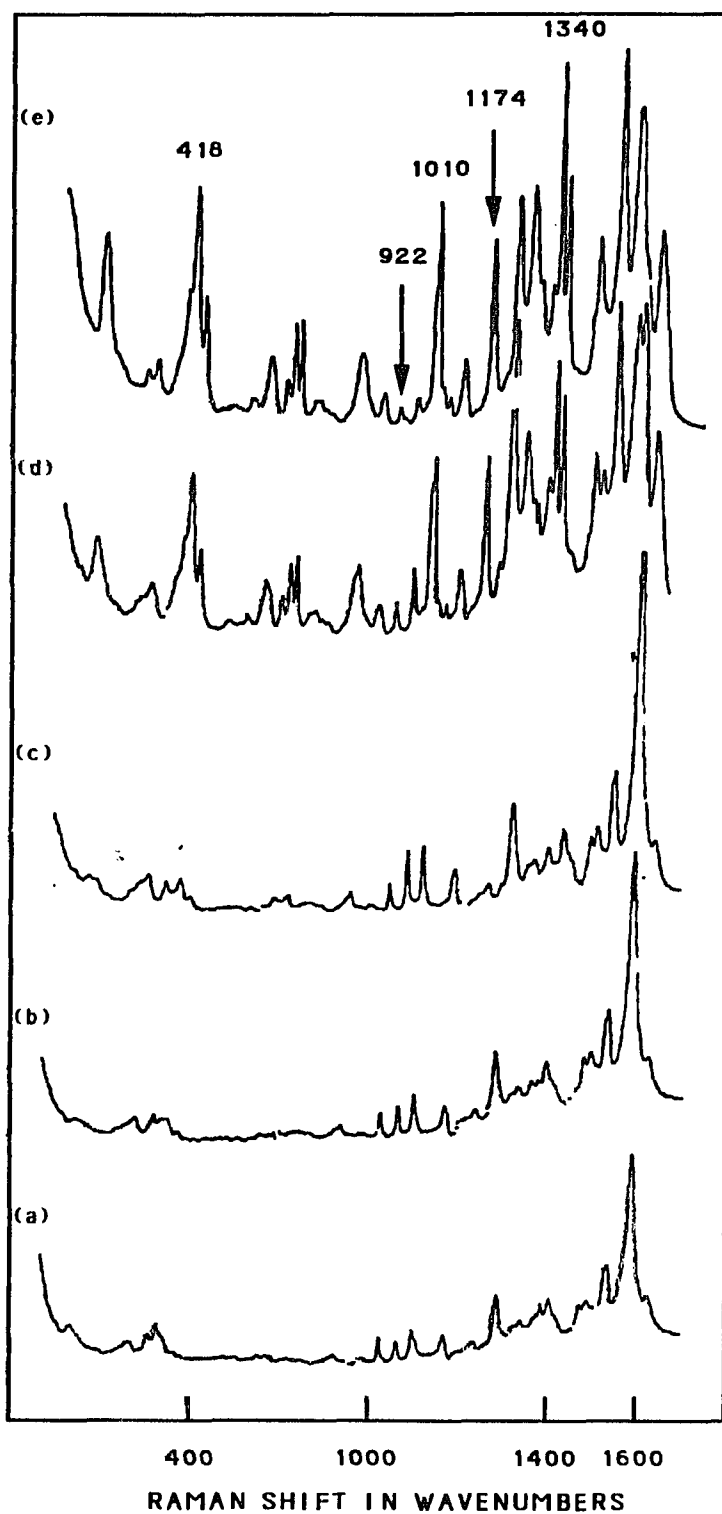


Fig.4 SERS of TAPP in acetonitrile with 488 nm laser excitation and a silver electrode . (a) 0.0 V (b) -0.2 V (c) - 0.4 V and (d) - 0.6 V (e)-0.7V

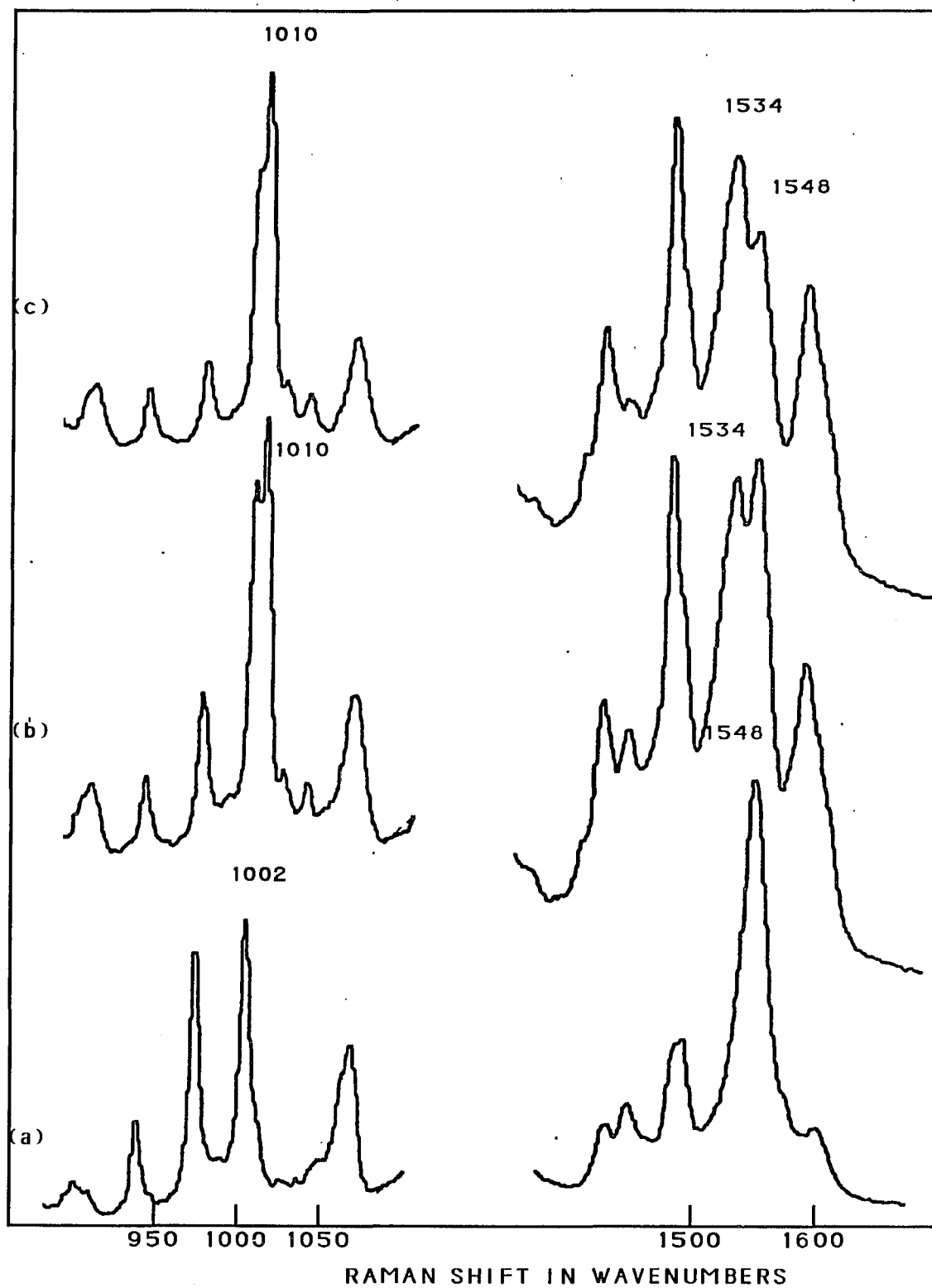


Fig.5 SERS spectra of TAPP in acetonitrile on a silver electrode with 488 nm laser excitation .a) at - 0.5 V b) at - 0.6 V and c) at - 0.7 V

Band in wavenumbers	Assignment.
418	metal sensitive
670	porphyrin deformation
920	solvent
962	phenyl
1002 -1010	$C\alpha-C_m$
1078	$C\beta-H$
1174	$C_m-Ph.$
1236	$C\alpha-N$
1274	aromatic C - N
1340	metal sensitive
1356	$C\alpha-N$
1364	solvent
1484	unassigned
1548 -1534	
1598	$C\alpha-C_m$ phenyl

T. M. Cotton J. Am. Chem. Soc. 104 6528 (1982)
T. G. Spiro and X. Y. Li "Biol. Appl. of Raman Spec.
J. M. Burke J. R. Kincaid and T. G. Spiro
J. Am. Chem. Soc. 100 6077 (1978)

Table 1 Assignment of the SERS bands
for TAPP

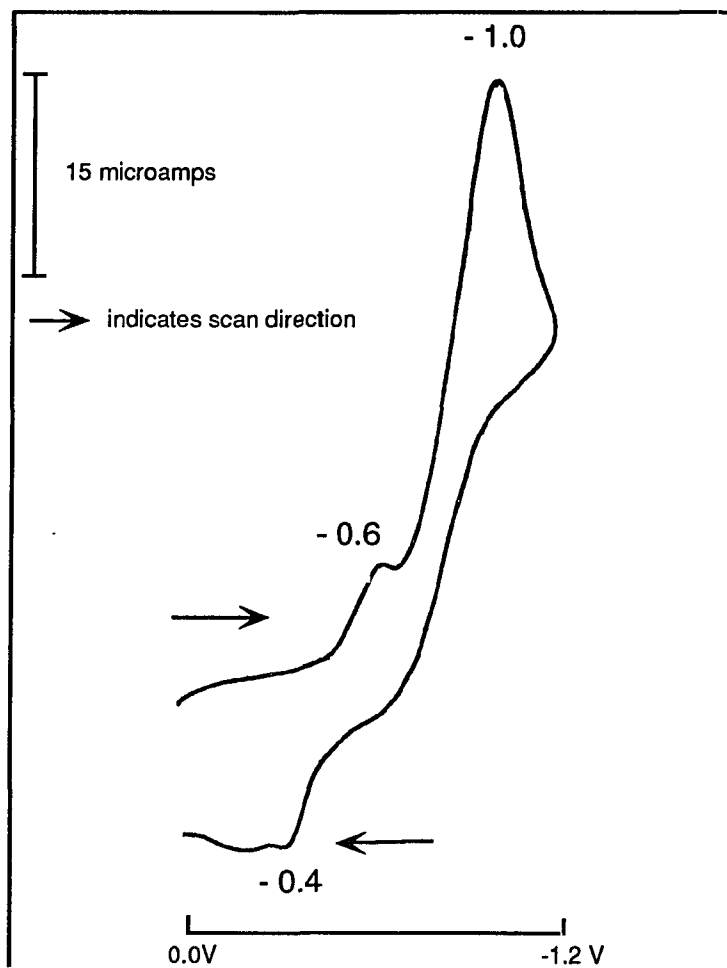


Fig.6 Cyclic Voltammogram of TAPP dissolved in acetonitrile with TBAP as the supporting electrolyte. Potential range from 0.0 V to - 1.2 V . Scan rate 100 Mv/sec. Ag electrode has an area of 1.6 square mm.

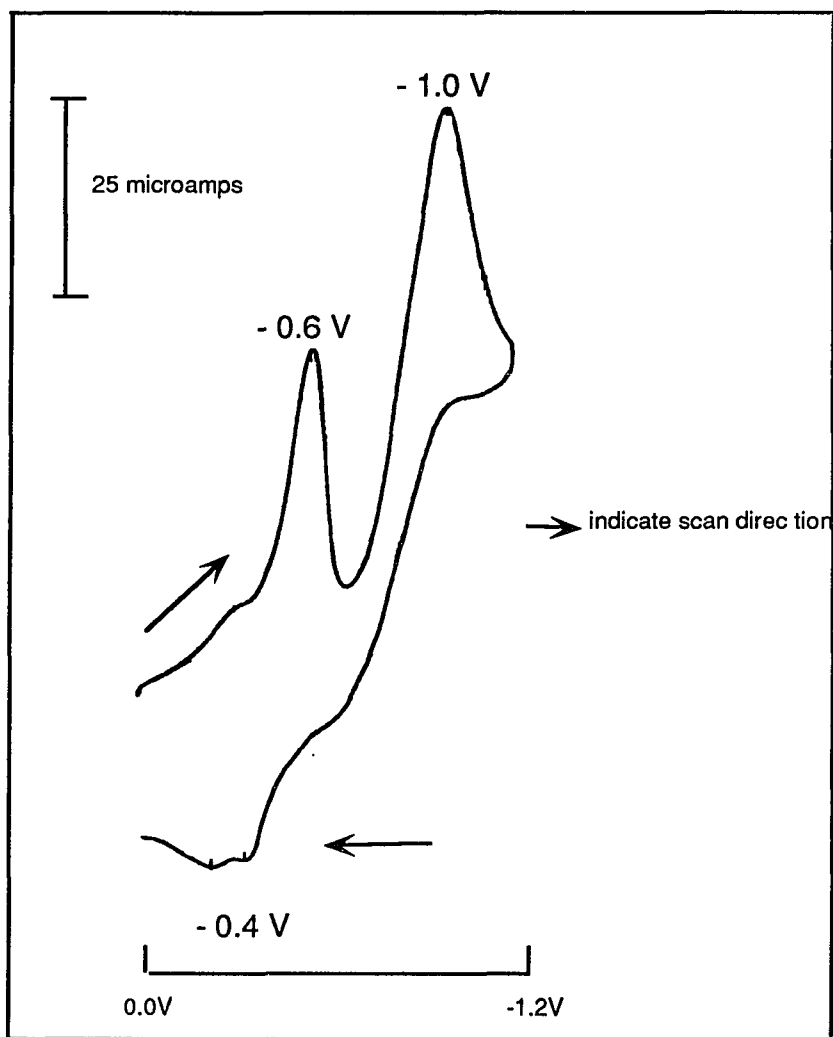


Fig.7 CV of TAPP dissolved in acetonitrile with TBAP as the supporting electrolyte. Potential range from 0.0 V to -1.2 V on a polished Ag electrode and scan rate of 500 mV/sec. Electrode area approx. 1.6 sq. mm

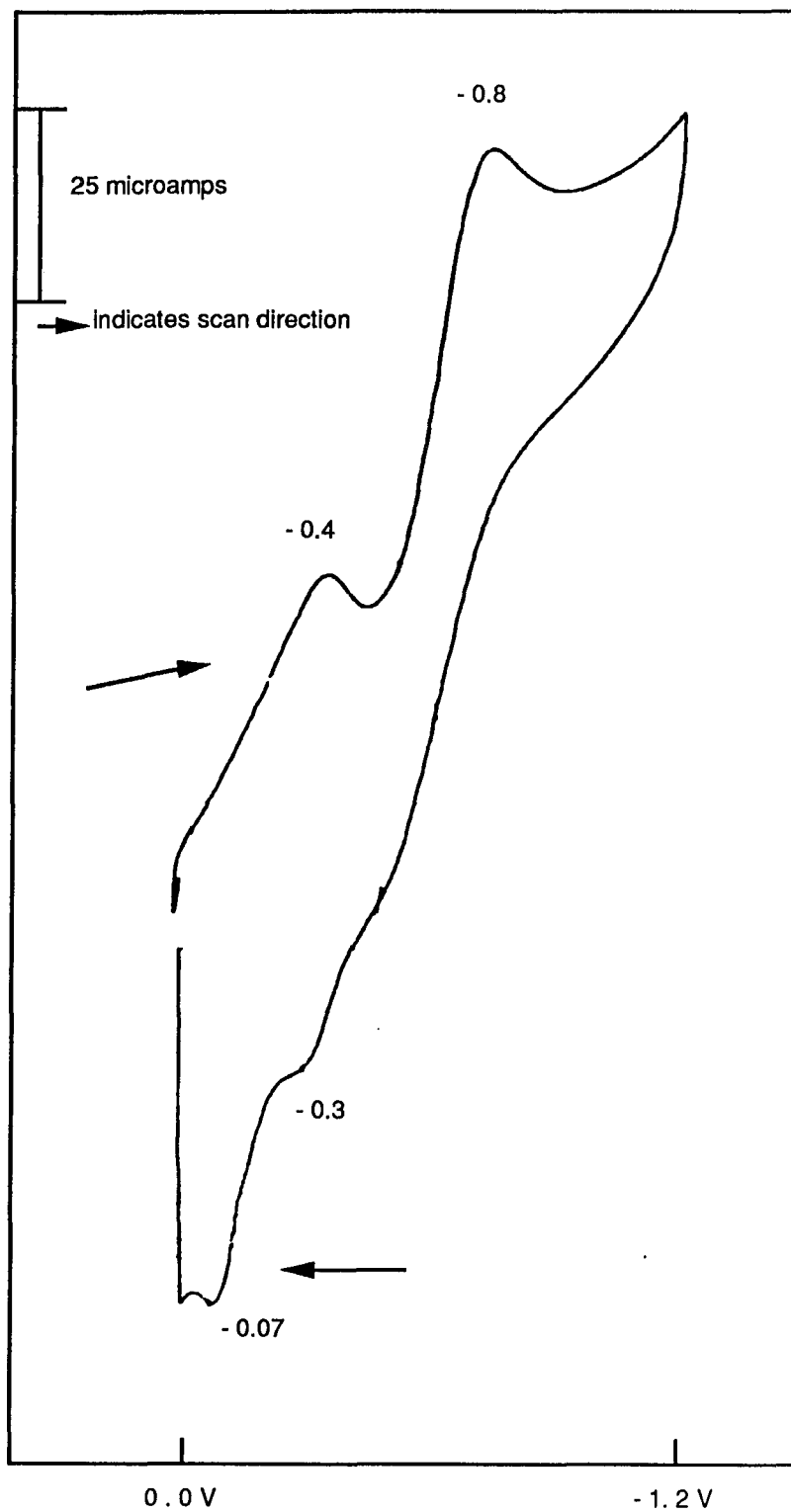


Fig.8 Cyclic Voltammogram of TAPP in acetonitrile with TBAP as the supporting electrolyte on a polished gold electrode .Scan rate 100 mV/sec . Electrode area approx. 1.6 sq.mm

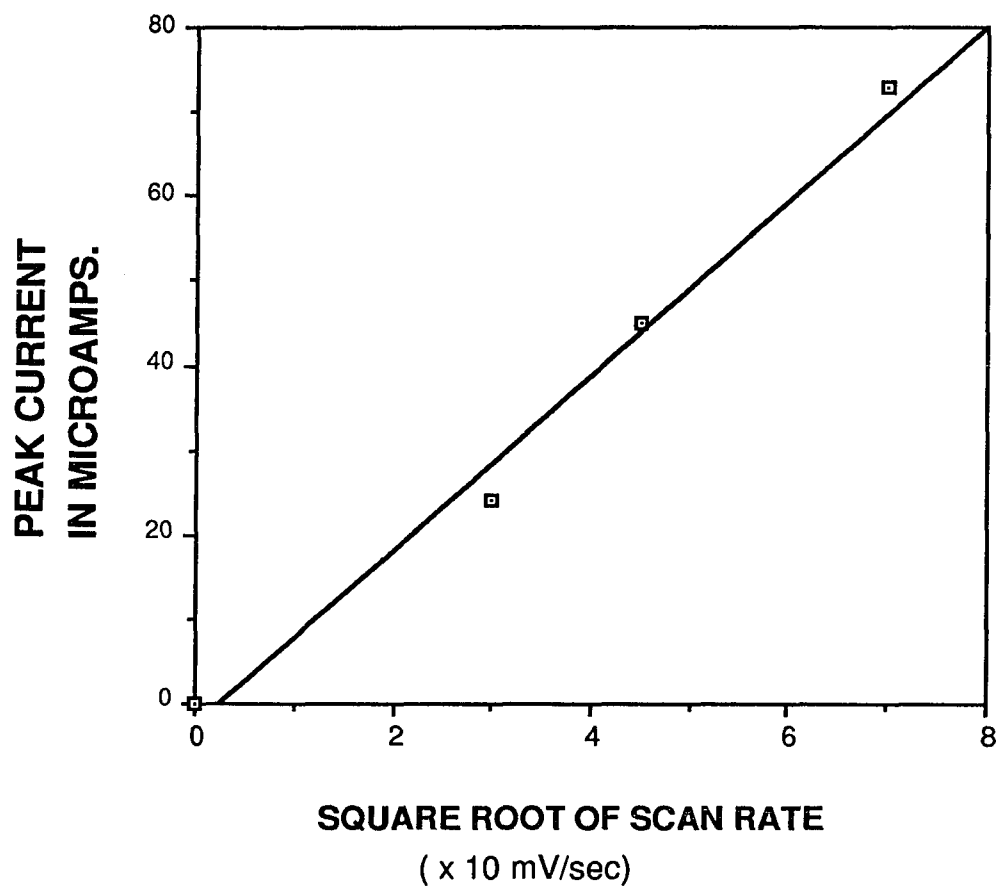


Fig.9 Plot of peak current vs the square root of the scan rate for the -1.0V peak of TAPP dissolved in acetonitrile on a silver electrode.

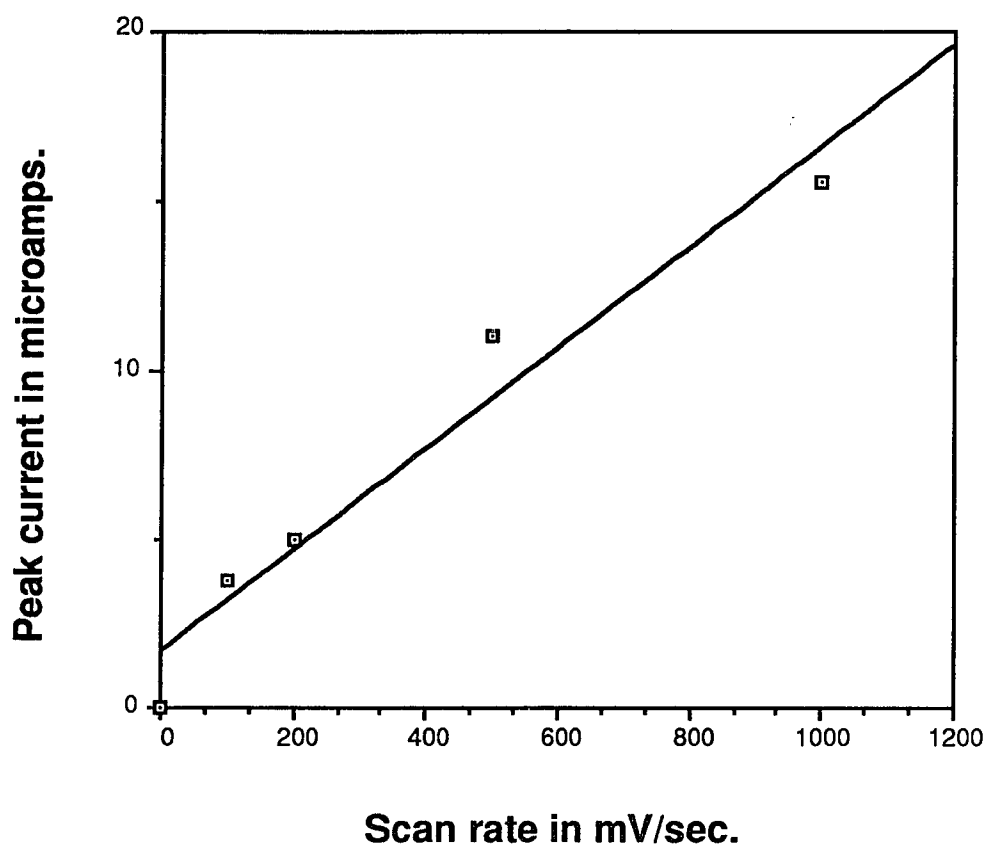


Fig.10 Plot of peak current vs scan rate for the -0.6V peak of TAPP dissolved in acetonitrile on a silver electrode.

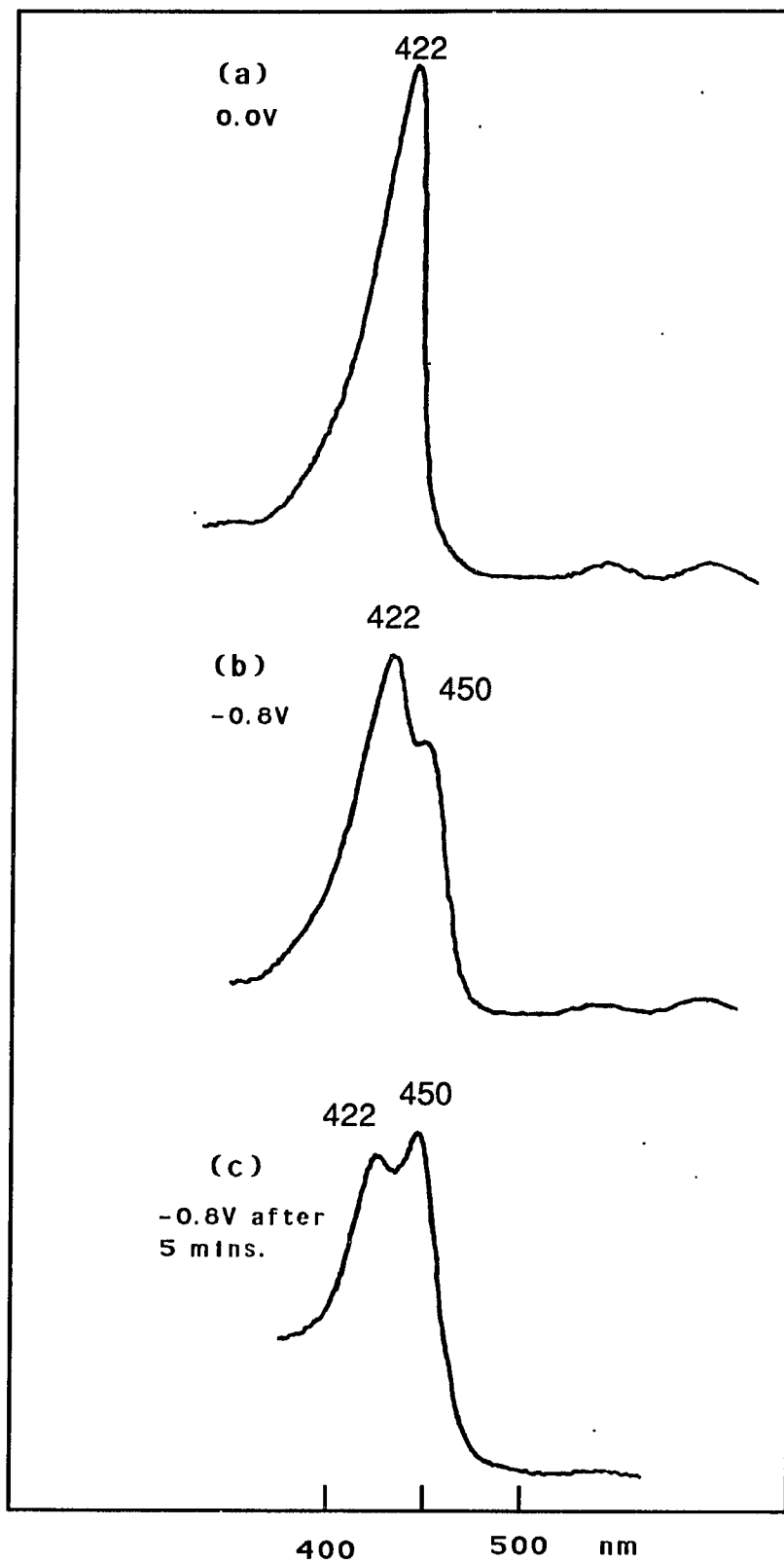


Fig.11 potential dependent absorption spectra.

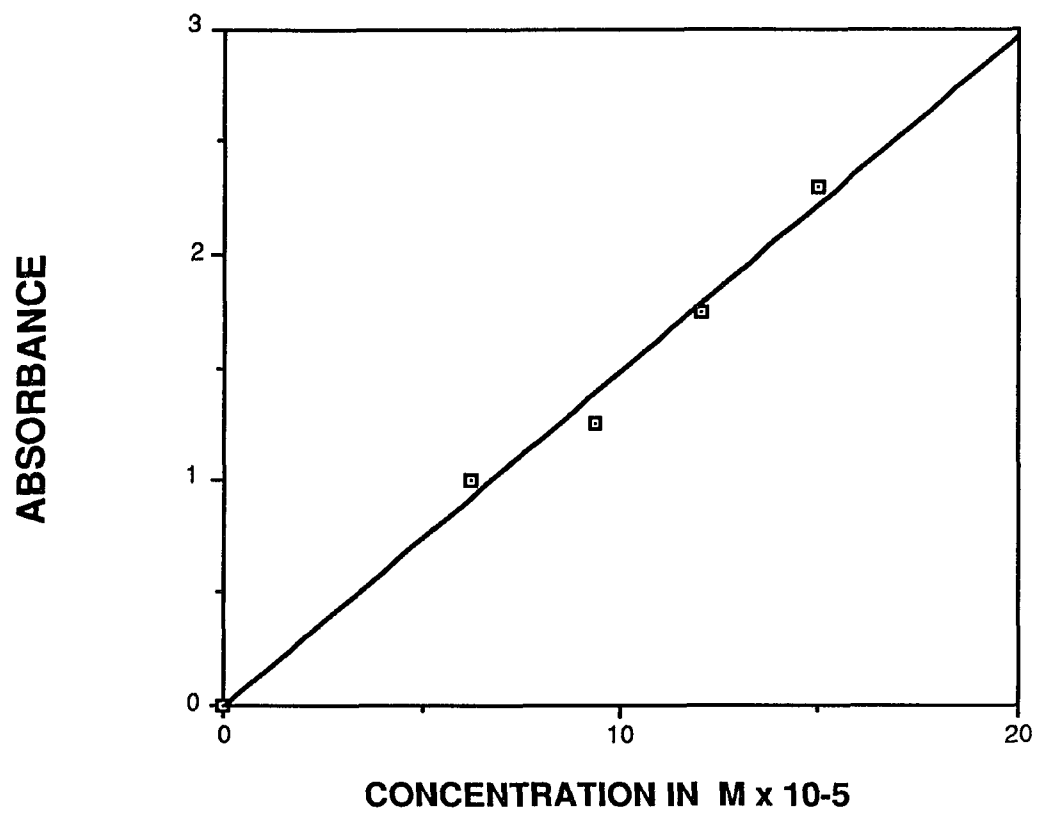


Fig.12 Plot of absorbance against concentration for TAPP dissolved on acetonitrile

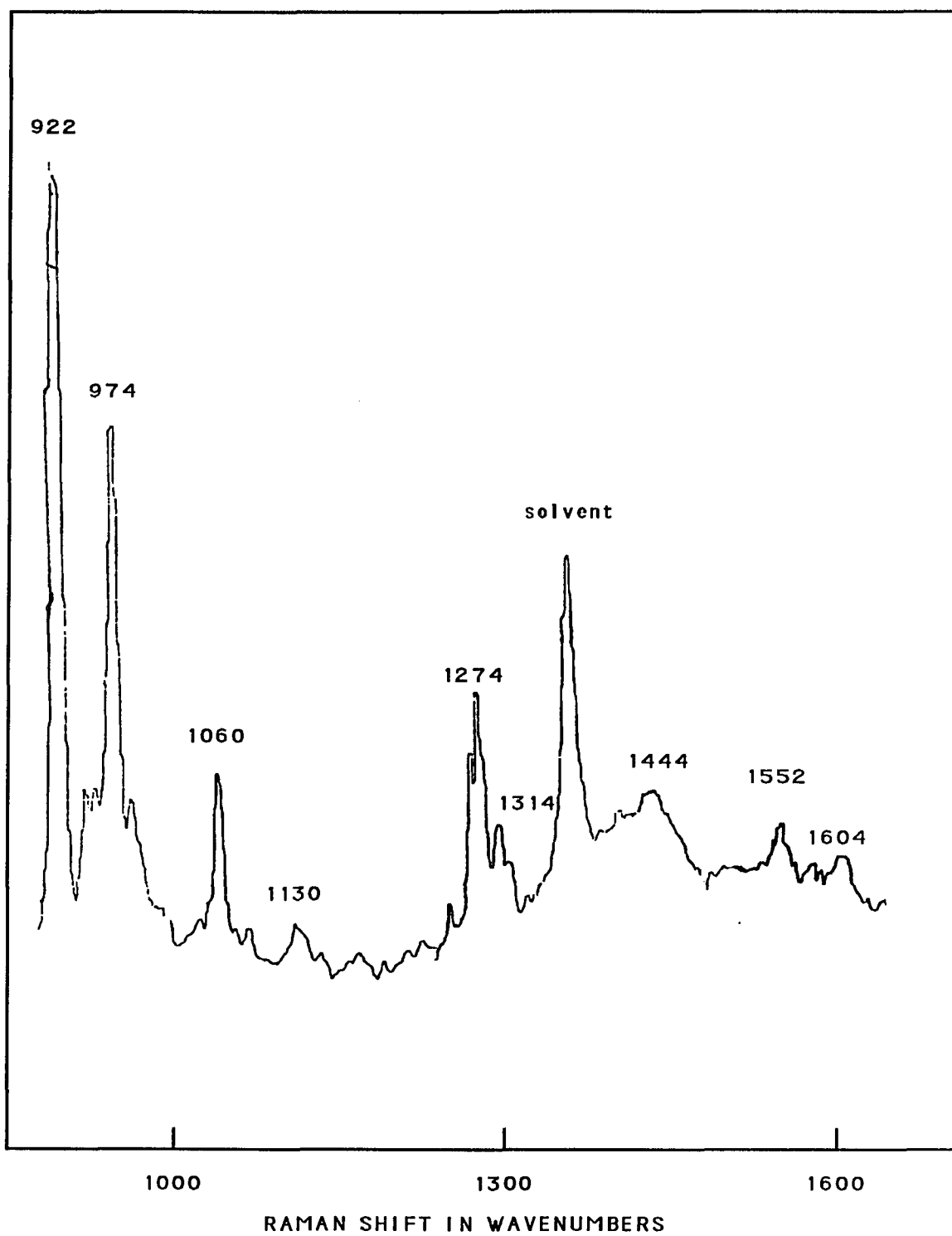


Fig.13 Normal Raman spectrum of TAPP in acetonitrile with 488 nm laser excitation .

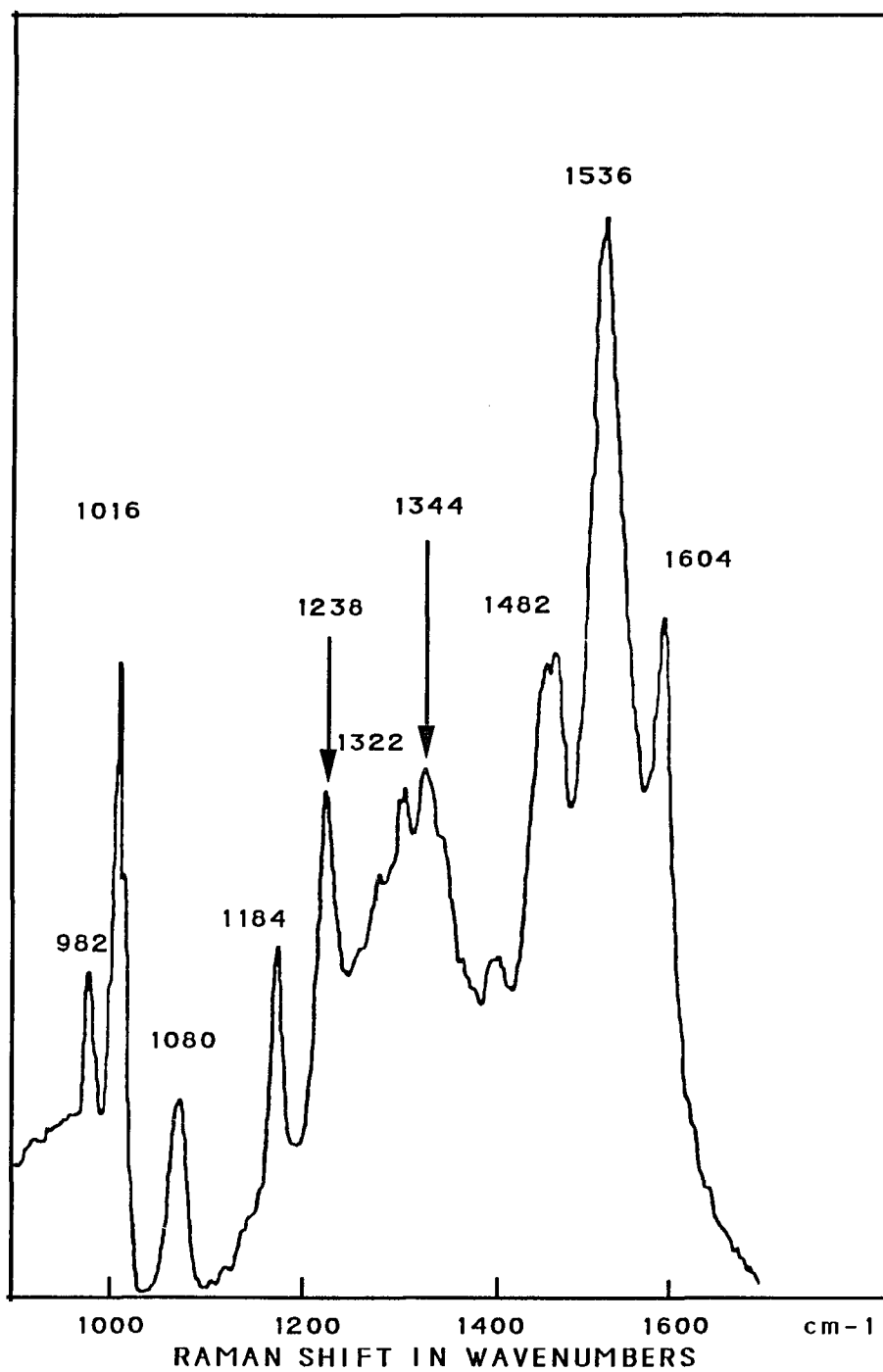


Fig.14 SERS from a silver electrode roughened in an acetonitrile solution of TAPP and left to dry. 488nm laser excitation .

Normal Raman	SERS
922	920
974	962
1060	1002
1130	1078
1274	1274
1314	1326
1552	1550
1604	1598

Table 2. Comparison of the normal Raman spectrum of TAPP with its SERS spectrum. 488 nm excitation. Raman shift in wave numbers. TAPP dissolved in acetonitrile.

RDE	In situ SERS	
	0.0V	-0.6V
982	962	962
1016	1002	1010
1080	1078	1078
1184	1174	1174
1238	1236	1234
1322	1326	1324
1344	1342	1340
1482	1486	1484
1536	1550	1534
1602	1598	1586

Table 3 A comparison of the SERS of TAPP on a roughened dried electrode against an in situ electrode at 0.0 V and - 0.6 V. 488 nm excitation Ag electrode

CHAPTER THREE

A SERS STUDY OF FIVE P-AMINO SUBSTITUTED TPP
COMPOUNDS IN AQUEOUS SOLUTION.

3.1 ABSTRACT

The intensity of the SERS spectra of a number of p-amino substituted tetra phenyl porphyrins is studied as a function of the number of amino groups on the molecule. A linear increase in intensity is observed as the number of amino groups on the molecule increases. One porphyrin deviates from this trend. The cis disubstituted molecule(AAOO) shows an anomalously large SERS spectra intensity. This deviation is explained as being due to a difference in the orientation of the adsorbed AAOO molecule relative to that of the other porphyrins.

The SERS spectra of the porphyrins are also studied as function of excitation frequency and electrode substrate. It is established that in aqueous acid solution electropolymerization of the tetrasubstituted porphyrin(AAAA) occurs. We present the spectrum of the polymer and compare it with that obtained when electropolymerization was performed in CH_2Cl_2 .

3.2 INTRODUCTION

Since its discovery over seventeen years ago¹ surface enhanced Raman spectroscopy(SERS) has been used to obtain detailed structural information concerning electrode-molecule interactions. In this study SERS is used to investigate electrode-porphyrin interactions.

It is virtually impossible to overemphasize the importance of porphyrins^{2,3}. They are found in cytochromes, in heme proteins and in the chloroplasts of green plants. Porphyrins act as important conduits for electrons in the charge transfer reactions occurring in living systems⁴.

A number of publications have indicated that SERS can be used to obtain information concerning a) porphyrin orientation⁵ b) porphyrin electrode interaction⁶ c) intermediates in the oxidation - reduction of porphyrins⁷ and d) the oxidation state of the metal-ligand in metallated porphyrins⁸.

This study is part of a larger one which is attempting to understand the primary photochemical process in photosynthesis. In photosynthesis charge transfer from an excited chlorophyll system to a quinone is a very important step. It is not fully understood why the reverse charge transfer reaction is so much less efficient. It is postulated that a conformational change might occur during the forward reaction resulting in a change in symmetry of the system, thus reducing the probability of the reverse reaction occurring. Because of the importance of symmetry in this process we decided to study a number of p-amino substituted tetraphenyl porphyrins. Fluorescence lifetime decay measurements have already been performed on these molecules⁹. Fig. 1 shows the structures of these p-amino substituted porphyrins.

Changing the number of p-amino substituents results in a change in the symmetry of the molecule. A study of the SERS spectra of these molecules allows for the investigation of the affect of symmetry on the SERS spectra.

The SERS spectra of the p-amino substituted TPP compounds on differing substrates, such as Ag and Au and with differing excitation frequencies, 488, 514 and 647 nm. are also reported. Finally it is shown that electropolymerization of porphyrin AAAA occurs from a solution of the porphyrin dissolved in 0.05 M HCl solution and we present the spectrum of the polymer.

3.3 Experimental

All the porphyrins used in this chapter were a gift provided by Prof. Guo of the Beijing Institute of Technology. For the SERS intensity measurements 1×10^{-5} M solutions of the porphyrins were prepared by serial dilution of a 10^{-2} M solution. The porphyrins were dissolved in 0.05M H_2SO_4 or 0.05M HCl solution. The acid solutions were reagent grade. Solutions were deaerated by nitrogen bubbling for twenty minutes.

The roughening of the Ag electrode was accomplished by applying a double step oxidation reduction cycle(ORC) from - 0.3 V to + 0.3 V in the presence of the porphyrin. The electrochemical system consisted of a silver working electrode, a platinum counter electrode and a saturated calomel electrode as the reference. All potentials in this chapter are reported relative to the saturated calomel electrode. After the ORC the potential was held at - 0.2V and the cell was physically washed with 0.05 M acid until there was no longer any porphyrin in solution.

For the relative intensity measurements the intensity of the laser line was used as the standard or reference throughout the experiment. Using an neutral density filter the intensity of the scattered radiation impinging on the entrance slit was set to within 5% for each experiment run by altering the focus and the position of the scattered radiation on the entrance slit. For each porphyrin the entire SERS spectrum was scanned with a Spex 1401 double monochromator instrument. Photon counting detection was used with an accumulation time of 0.6 s/cm^{-1} . Peak intensities were determined after background subtraction.

3.4 RESULTS AND DISCUSSION.

3.4 a Relative Intensity Measurements

It was necessary to have a reliable method to compare intensities in several experiments. An examination of the term which describes the intensity of the scattered radiation from a molecule, shows that one of the parameters upon which this intensity depends, is the intensity of the incident light, in this case the laser line. Since from one run to the next in the course of an experiment, the laser intensity changes due to factors such as changes in alignment or position of the scattered light on the slits, some method of cancelling out the changes in the laser line intensity had to be employed.

Two methods are commonly used. The first method involves adding an internal standard to the solution and determining the ratio of the intensities of the analyte peak with that of the standard. The intensity of the standard peak is compared for different experimental runs and the factor obtained is used as a correction factor for the other peaks.

For SERS, the requirements of the internal standard are numerous. It must adsorb onto the electrode and remain electrochemically inactive at the potential being used, its adsorption must be independent of the concentration of the analyte, and it must produce a clearly identifiable peak whose position must not overlap with that of the analyte peak. Finally the standard must have a spectrum with as few peaks as possible so as to prevent spectral interference between the standard and the analyte. These requirements are quite stringent and have severely limited the pool of available standards and their use.

The other method involves using the intensity of the laser line as the standard. The intensity of the laser line is set at the beginning of each run by setting the intensity of the scattered radiation that impinges on the entrance slits.

By changing the focus and position of this light on the slit, its intensity can be regulated and set for each experimental run.

SERS spectra of the five p-amino substituted porphyrins dissolved in 0.05M acid were obtained on a roughened silver electrode with 488 and 514 nm laser excitation. Fig 3 shows a plot of the laser intensity vs the intensity of the 1012 cm^{-1} SERS peak. The plot shows a nearly linear relationship between the laser line intensity and the intensity of the SERS peak over a wide range of scattered radiation intensity.

Figures 4 and 5 are plots of the number of amino groups on the porphyrin molecule against the corresponding SERS intensities for the 1012 cm^{-1} SERS band. Fig.4 was obtained using 514 nm. laser excitation and Fig.5 was with 488 nm. excitation. No SERS spectrum was obtained for TPP under the same experimental conditions as for the p-amino substituted TPP compounds. This sets the first point on the plot and establishes that when the number of amino groups on the porphyrin molecule is equal to zero, the SERS intensity is also equal to zero.

Figures 6 and 7 were obtained under the same experimental condition as for Figures 4 and 5 but are for the the 984 cm^{-1} band. In all the plots there is a linear increase in the intensity of the SERS band as the number of p-amino substituted groups on the molecule is increased. Examination of Figs 4 to 7 indicates that one porphyrin shows anomalous behavior; this is the cis disubstituted porphyrin (AA00) see Fig.1 for structure.

If two p-amino groups are substituted on to TPP then two compounds are possible; one has the porphyrins situated cis to each other and the other has the porphyrins trans to each other. These two compounds show significant differences in their SERS intensities. The SERS intensity of the cis compound is approximately four times that of the trans compound. Also the intensity of the

cis compound is greater than that of any of the other p-amino substituted compounds studied.

The symmetries of the porphyrins are as follows:

$AOOO = C_{2v}$, $AAOO = C_{2v}$, $AOAO = D_{2h}$, $AAAO = C_{2v}$, $AAAA = D_{4h}$

Porphyrins AAOO and AOAO have different symmetries. AAOO is C_{2v} and AOAO is D_{2h} . This difference in symmetry cannot be related to the differences in SERS intensities of the spectra because two other molecules AOOO and AAOO also contain the same symmetry as AAOO and should therefore show similar intensities.

Other factors which could account for the intensity results are differences in the number of molecules adsorbed on the electrode surface and differences in the strength of the adsorbate surface interaction. Results presented in chapter 2 show that the SERS intensity is also dependent on the strength of the interaction between the adsorbed molecule and the electrode surface. In acetonitrile the SERS spectra for AOOO were very weak and the molecule was desorbed from the electrode surface at potentials more negative than - 0.5 V. Also the SERS spectra obtained in acetonitrile as solvent all show an increase in intensity at - 0.6V. This increase was attributed to a more firmly bound adsorbate. We have explored the possibility that one or both of these processes provides an explanation for the data that we have obtained regarding the relationship between the SERS intensity and the number of amino groups on the porphyrin molecule.

Increasing the number of amino groups on the porphyrin molecule increases the number of points at which interaction can occur between the adsorbed porphyrin molecule and the electrode surface. It would be expected, and it is supported by our studies in acetonitrile, that AAAA would be more firmly bound to the electrode surface than would AOOO. We believe that a linear

relationship exists between the number of p-amino groups and the strength of the interaction between the adsorbed porphyrin and the electrode. We propose that it is the strength of this interaction which is responsible for the linear relationship between the SERS intensity and the number of p-amino groups on the porphyrin molecule.

The anomalous behavior of AAO relative to that of AOA is related, we believe, to the orientation of the adsorbed porphyrin molecules on the silver surface. It has already been shown that no SERS spectrum was obtained for TPP. Therefore interaction between the adsorbed TAPP molecules and the electrode surface must be through the amino groups on the phenyl ring. Examination of the structure of AAO and AOA shows that for maximum interaction between the amino groups and the electrode surface AOA would orient itself parallel to the electrode surface. This would result in both amino groups interacting with the electrode surface. If this molecule were oriented perpendicular to the surface then only one amino group would be capable of interacting with the surface. For porphyrin AAO both a flat and a perpendicular orientation of the molecule relative to the surface would result in interaction between the two amino groups and the surface. A perpendicular orientation would result in maximum overlap of the non bonding orbital of the nitrogen atoms and the electrode surface. Holze¹⁵ established that iron tetra p-methoxyphenyl porphyrin was oriented perpendicular to the silver electrode surface.

Monolayer^{16,17} studies of porphyrin esters such as uroporphyrin octamethyl ester have also shown that the porphyrin molecules are vertically orientated at the liquid air interface. We suggest that porphyrin AOA is adsorbed oriented parallel to the electrode surface whilst AAO is adsorbed perpendicular to the surface. These differences in orientation would lead to an

increase in the number of AAOO molecules that could be adsorbed on the same surface area relative to AAOO which is adsorbed flat.

We have attempted to quantify this difference by estimating the area of the TAPP molecule, oriented vertically and horizontally, from the results of monolayer studies¹⁷. In monolayer experiments the porphyrin is dissolved in a volatile solvent and then spread onto an immiscible liquid. The spreading solution should be above 10^{-3} M and the porphyrin should be dissolved in a highly volatile solvent such as chloroform. These two considerations were difficult to achieve for TAPP because of its very low solubility in solvents such as chloroform. As a result its area could not be directly determined by monolayer experiments.

Bergon¹⁶ found that the minimum area occupied by a porphyrin ring substituted with methyl groups at all of its corners was 145 \AA when the molecule was lying flat and 45 \AA when the rings were oriented vertically. Other workers¹⁷ have determined the area of substituted TPP to be about 200 \AA when the molecule is lying flat and 45 \AA when it is perpendicular to the surface. From these results it can be seen that 3.2 to 4.4 times as many molecules can be packed in the same area if TAPP is oriented perpendicular to the surface rather than parallel. Examination of our intensity data show that SERS spectra of AAOO is approximately 3.7 to 4 times as intense as that of AAOO. The close agreement between the two sets of results lead us to suggest that the differences in the SERS intensities of porphyrins AAOO and AAOO are due to differences in the geometries of the adsorbed porphyrins. It appears that porphyrin AAOO is adsorbed orientated perpendicular to the electrode surface whilst porphyrin AAOO is adsorbed parallel to the electrode surface.

Although these calculations show good agreement they are at best speculative since the SERS spectra of AAOO does not provide any information

that allows us to definitively conclude that it is oriented differently to that of AOA. Confirmation of this difference in orientation could be obtained by comparing the relative intensities of the amino vibration and the C-H vibrations of the two compounds. Examination of the 2000-4000 cm^{-1} region of the spectra failed to show any peaks which could be attributed to these vibrations.

Identification of the orientation of these two compounds is an area for further research. Chronocoulometry experiments would allow for the calculation of the number of molecules adsorbed on the electrode surface whilst monolayer experiments would more accurately determine the area of the TAPP molecules. The results from these experiments would provide information which would allow for a more definitive explanation of the data which is presented here.

3.4 b Spectroscopy

The Raman spectrum of TAPP has not been published; as a result one of the first goals of this study was to determine whether the spectra obtained were those of the TAPP or of an impurity. This was accomplished by comparing the spectra of TAPP with the spectra of TPP, meso-tetrakis(4-sulfanato phenyl)porphine (TSPP) and meso-tetrakis(4carboxyphenyl)phenyl(TCPP). TAPP, TSPP and TCPP all contain the same TPP structure but possess different substituents on the phenyl groups. TAPP has amino substituents, TSPP sulfanato and TCPP carboxy. Because they all contain the same TPP structure only slight differences would be expected in their Raman spectra.

Good agreement is observed between the spectra of TAPP and the other two porphyrins confirming that the spectrum is that of a phenyl substituted porphyrin (in this case TAPP) Figure 16. Only minor differences are observed in the spectra and these are found either in the low frequency region or for bands

having very low intensities. In the 1500-1560 cm^{-1} region of the spectra there is some variation in the spectra. The most intense peak in the SERS spectra of TAPP occurs at 1536 cm^{-1} which agrees with that found by Itoh¹⁸ for TSPP in 0.05 M H_2SO_4 . Cotton¹⁹ however observed this peak at 1555 cm^{-1} with a shoulder at 1565 cm^{-1} . No shoulder was observed in the spectra of TAPP in the 1500 to 1560 cm^{-1} region. The 1536 cm^{-1} band in the TAPP spectrum is very broad and it is possible that this one band might represent two poorly resolved peaks.

Fig. 8 shows the SERS spectra for the five p-amino substituted TPP compounds at 488 nm laser excitation on an *in situ* roughened silver electrode. The porphyrins were dissolved in 0.05M HCl and the SERS cell was washed with an electrolyte blank solution until all the porphyrin molecules in solution were removed. The spectra were recorded at -0.2V and are of the surface species. Except for differences in the intensities of the spectra, (which has already been discussed) the spectra show little differences. Only in the 1240 to 1420 cm^{-1} region are there any differences in the spectra and these are due to the reduced intensity of the SERS spectrum of porphyrin AOOO relative to that of the other compounds.

Fig.9 shows the potential dependent spectra obtained for porphyrin AAAA. The other four porphyrins showed similar potential dependent behavior so that Fig.4 is characteristic of all five p-amino substituted porphyrins. There were no potential dependent changes in the spectra from 0.0V to -0.6V for any of the porphyrins. Poorly defined spectra were obtained at -0.6 V. No spectra were obtained at potentials more negative than -0.6 V. This is due to the evolution of H_2 gas on the electrode from the acidic solution resulting in the desorption of the porphyrin from the electrode.

Figures 10 and 11 show the SERS spectra obtained from porphyrin AAAA on a roughened Ag electrode in 2 M HCl solution. Fig.10 shows that the intensity of the SERS spectra decreases at -0.4 V and no spectra were obtained at potentials more negative than -0.4 V. When the hydrochloric acid concentration was increased from 0.05 M to 2M, the SERS spectra (d), porphyrin AAOO shows a new peak at 1000 cm^{-1} , Fig.11.

3.4 c 488 vs 514 nm excitation

The spectra of the p-amino substituted TPP compounds obtained on a silver electrode show no changes in the relative intensity or the frequencies of the bands when the excitation frequency is changed from 488 to 514 nm. An examination of the absorption spectrum of TAPP, Fig.2, shows that the Soret or B band has its maximum at 424 nm. The 488 nm excitation is to the red of the Soret band. It is closer to the weak Q_y band which is observed at 520 nm. Excitation with 488 and 514 nm results in Q band excitation of the molecule. It would be expected that the spectra would be dominated by modes which are enhanced by B term enhancement. The spectra should therefore contain anomalously polarized bands i.e. bands with a stronger intensity in perpendicular rather than parallel polarization. Depolarized bands should also be observed. SERS spectroscopy cannot distinguish these bands because the depolarization ratio for all SERS bands is between 0.6 and 0.75. This characteristic of SERS is independent of whether the vibrations are totally symmetric or non totally symmetric. The spectra obtained with 488 and 514 nm laser excitation are therefore resonance enhanced and are surface enhanced resonance Raman scattered (SERRS).

3.4 d Porphyrins adsorbed on Ag and Au

The spectra on Au were obtained from a roughened Au electrode surface. The ORC for gold was performed in the presence of the porphyrin molecules, *in situ*, by the application of triangular sweeps, 100mV/sec, from an initial potential of 0.0V to a switching potential of 1.3V. A Spectra Physics Model 2000 Krypton ion laser provided 647 nm laser excitation. The laser power at the electrode surface approximately 50 mW.

Spectra on both Ag and Au surfaces with 647 nm laser excitation were compared. Three of the Porphyrins show similar behavior and are discussed in this section. They are AAOO (Fig.12), AAO (Fig. 13), and AAAO (Fig. 14).

Only minor differences are observed between the spectra obtained on Ag and on Au with 647 nm. laser excitation. One difference is the shift by 6 cm^{-1} of the band found at 1366 cm^{-1} on Ag and 1372 cm^{-1} on Au.

The band at 1372 cm^{-1} has been assigned as a $\nu(\text{C}_\alpha-\text{N})$ and $\delta\text{C}_\beta-\text{H}$. The down shift of the 1366 cm^{-1} band on the silver electrode indicates a greater interaction between the metal and the molecule on the silver electrode relative to the gold electrode. Similar shifts are observed for the other porphyrins with the exception of porphyrin AAAA. The spectrum of porphyrin AAAA is discussed in the following section.

3.4 e Porphyrin (AAAA) : A comparison on Au and Ag at 647 nm.

An examination of Fig. 15 shows that there are differences between the spectra on Au and on Ag obtained at 647 nm laser excitation. The 1064 cm^{-1} band on silver is shifted to 1076 cm^{-1} on gold and the band at 1236 cm^{-1} on silver is absent on the gold surface. Instead a band is observed at 1286 cm^{-1} . There were two differences in the experimental conditions for the spectra obtained on Au and on Ag. First there was a difference in the nature of the

electrode surface and secondly the pretreatment conditions used for obtaining SERS active surfaces were quite different for Ag and Au. For Ag one two second pulse from 0.0V to 0.3 was used. For Au the electrode was cycled 20 to 30 times, between a potential of 0.0V and 1.2V. Both pretreatment procedures were performed *in situ*.

Fig.16 shows the SERS spectra of porphyrins AAAA, AAOO, AOAO and AAOO on a Au electrode with 647 nm laser excitation. No spectrum was obtained for porphyrin AOOO. Bands which appear at 984 and 1286 cm^{-1} for AAAA are weak or absent from the spectra of the other porphyrins. The 1014 and 1236 cm^{-1} vibrations which are found in the other porphyrins are missing from the spectrum of AAAA and the 1476 cm^{-1} band in porphyrin AAOO, AOAO and AAOO is shifted to 1480 cm^{-1} in the spectrum of AAAA and shows a large increase in intensity. The band at 1286 cm^{-1} for AAAA is absent in the spectra of the other porphyrins.

Table2 compares the spectra obtained from polymerizing AAAA in CH_2Cl_2 on a gold electrode along with the spectrum of porphyrin AAAA obtained on a Au electrode. Good agreement is found between the two spectra.

The significant differences in band frequencies and intensities between the spectrum of AAAA and that of the other porphyrins along with the similarity between the spectrum of AAAA on Au and the spectra of polymerized AAAA leads us to the conclusion that the spectra of AAAA on a Au electrode presented here is that of the polymerized porphyrin and not of the monomer.

Ex situ ORC of the gold electrode followed by dipping of the roughened electrode in a solution of porphyrin AAAA and then obtaining the spectrum in porphyrin free solution provided poor quality spectra. This experiment, had it provided intense spectra, would have conclusively identified the spectrum as either that of the polymer or monomer. However the fact that

electropolymerization of $\text{Co}(\text{o-NH}_2)\text{TPP}$ has been performed²⁰ in aqueous acid solution on a glassy carbon electrode lends further support to the conclusion that the spectrum is that of the polymer and that porphyrin AAAA has been electropolymerized in the HCl solution.

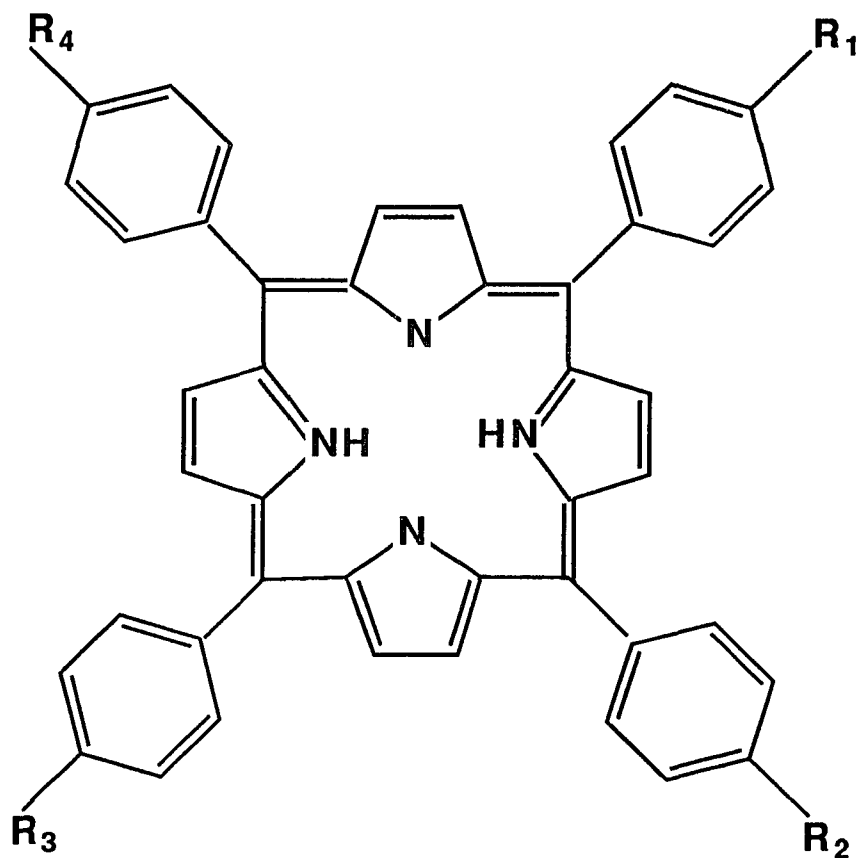


Fig. 1 Structure of p-amino substituted TPP

TPP	R_1, R_2, R_3 and R_4 are equal to H
A000	$R_1 = \text{NH}_2$, R_2, R_3 and R_4 are equal to H
AA00	R_1 and $R_2 = \text{NH}_2$, R_3 and R_4 are equal to H
AOAO	R_1 and $R_3 = \text{NH}_2$, R_2 and R_4 are equal to H
AAAO	R_1, R_2 and $R_3 = \text{NH}_2$, R_4 is equal to H
AAAA	R_1, R_2, R_3 and R_4 equal to NH_2

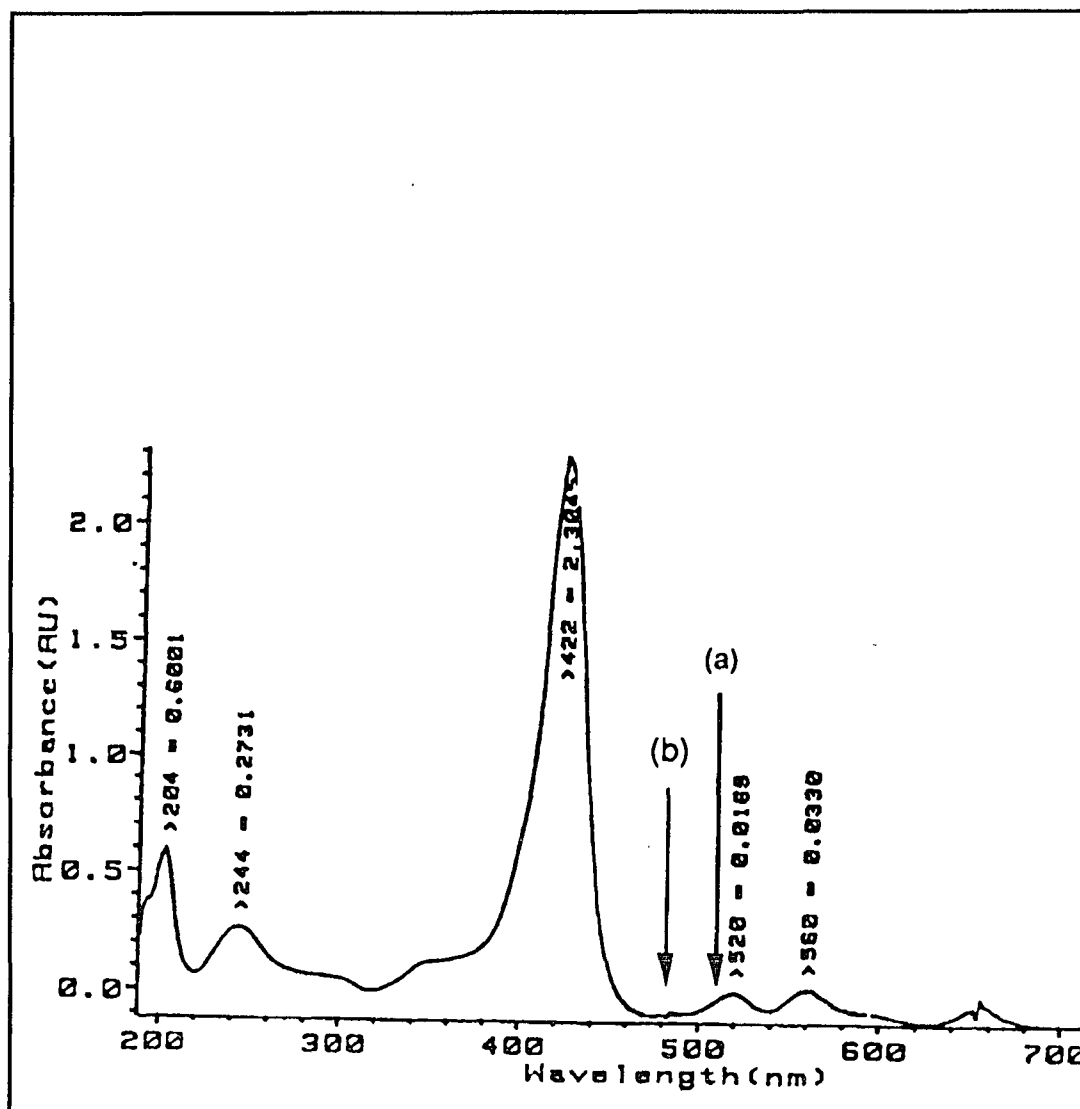


Fig.2 Visible absorption spectrum of TAPP in 0.05M HCl
(a) Represents laser excitation frequency 514 nm and (b) 488 nm

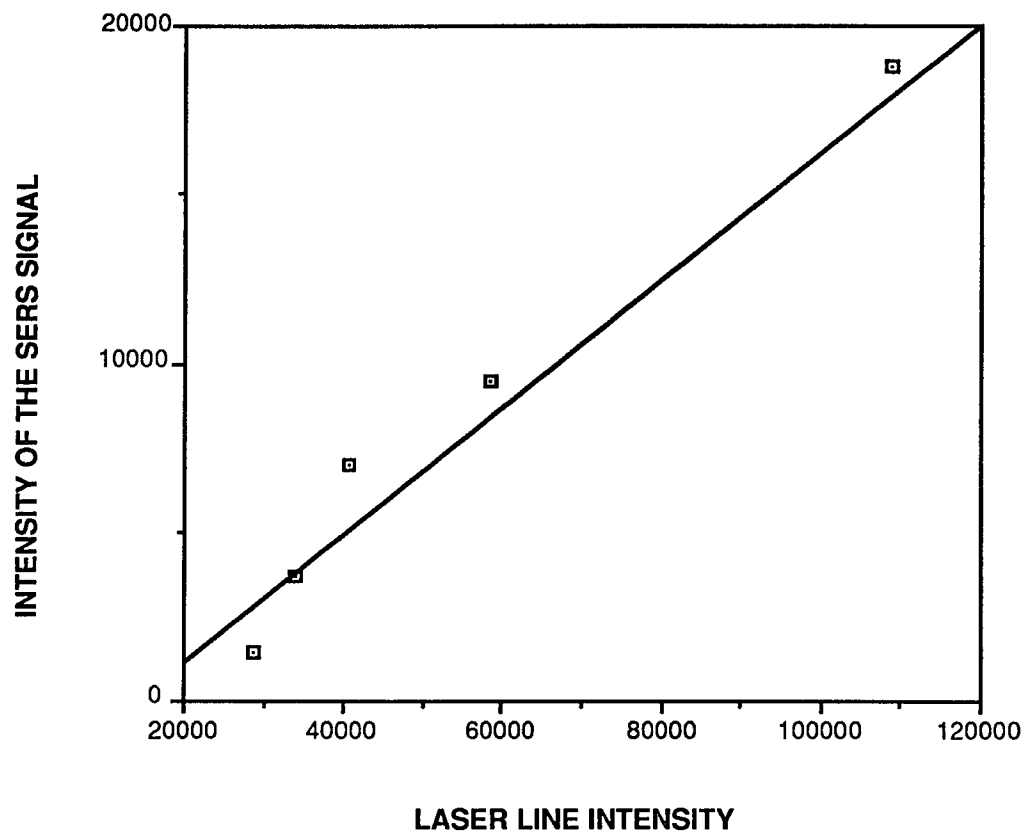


Fig.3 Laser line intensity vs intensity of the SERS signal

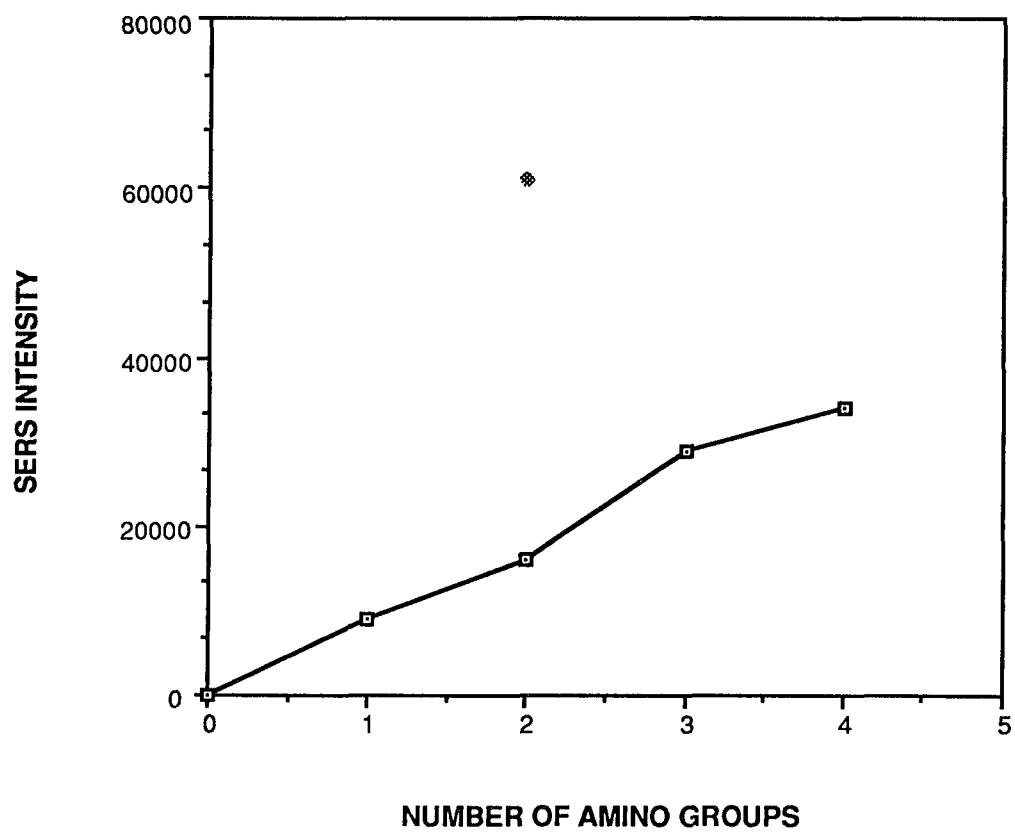


Fig.4 Plot of SERS intensity of the 1012 band vs the number of amino groups on the molecule. 514 nm laser excitation

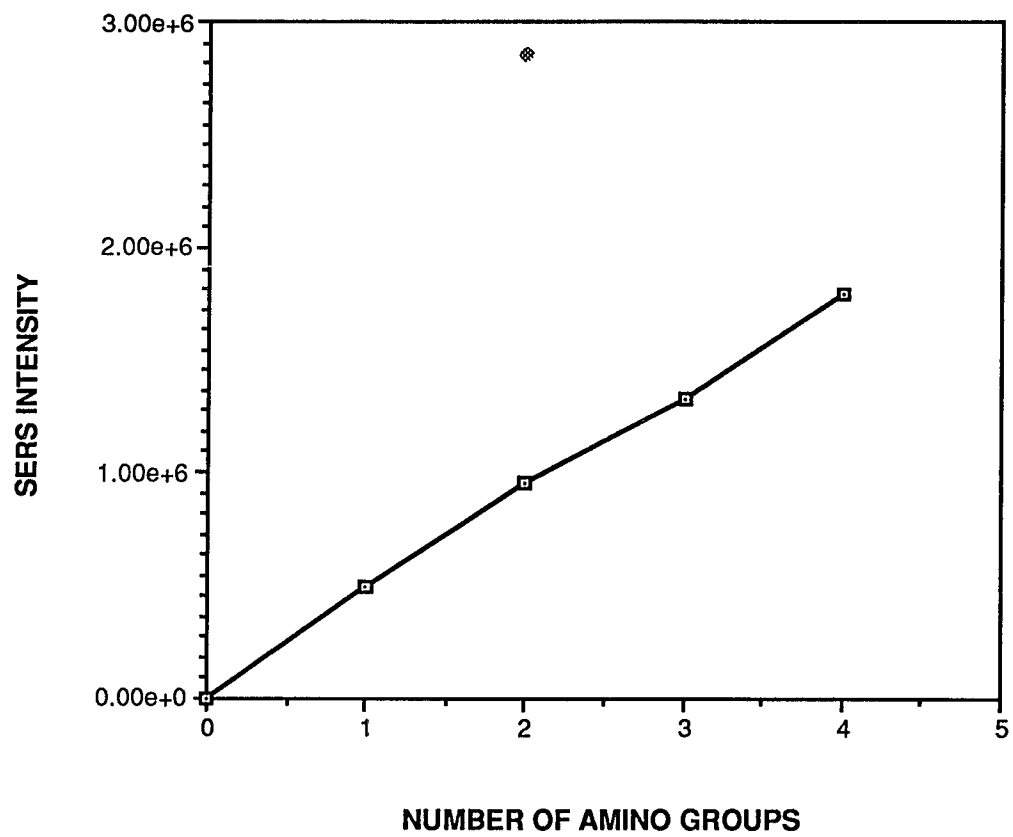


Fig.5 Plot of SERS intensity vs the number of amino groups on the molecule for the 1012 band with 488 nm laser excitation.

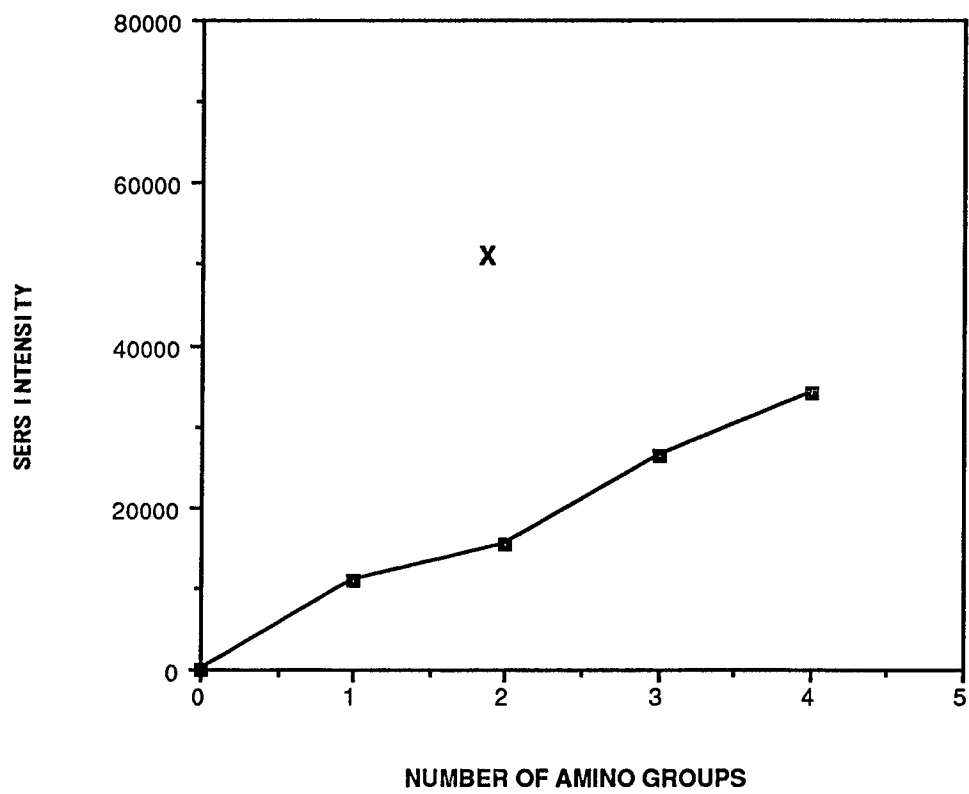


Fig.6 Plot of number of amino groups on the porphyrin molecule vs the SERS intensity of the 984 band. Laser excitation was 488 nm.

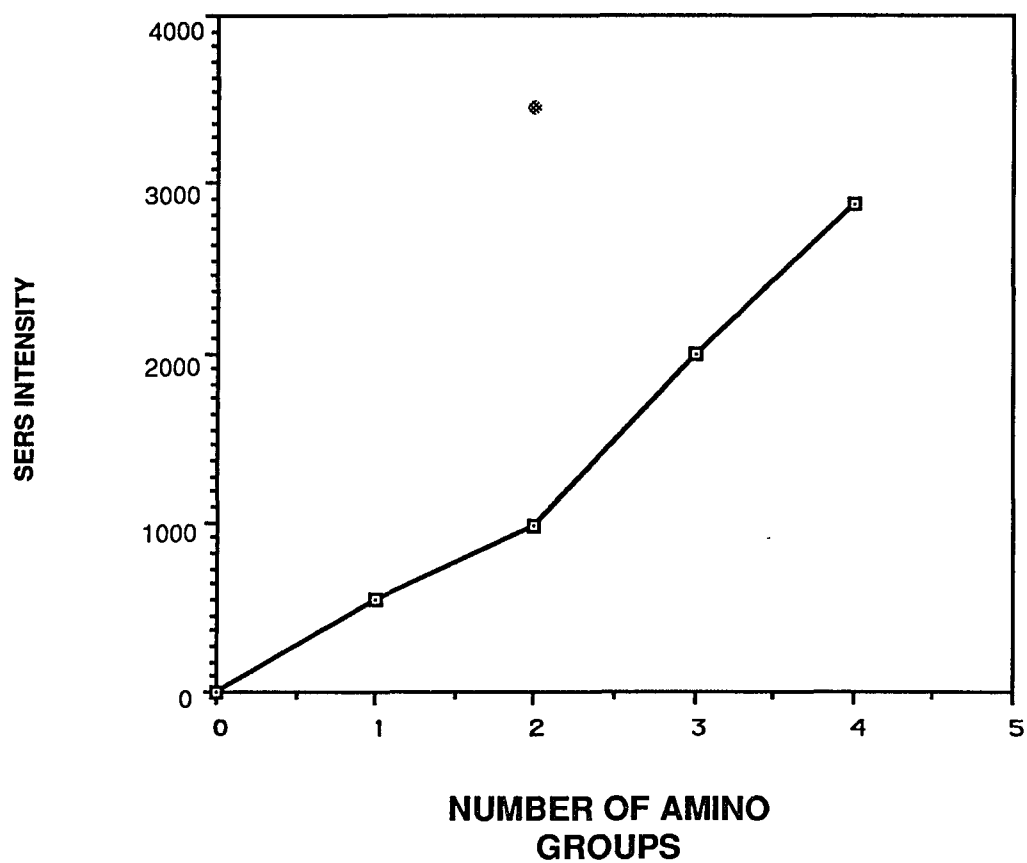


Fig. 7 Plot of number of amino groups on the porphyrin against the SERS intensity for the 984 band. Laser excitation frequency was 514 nm.

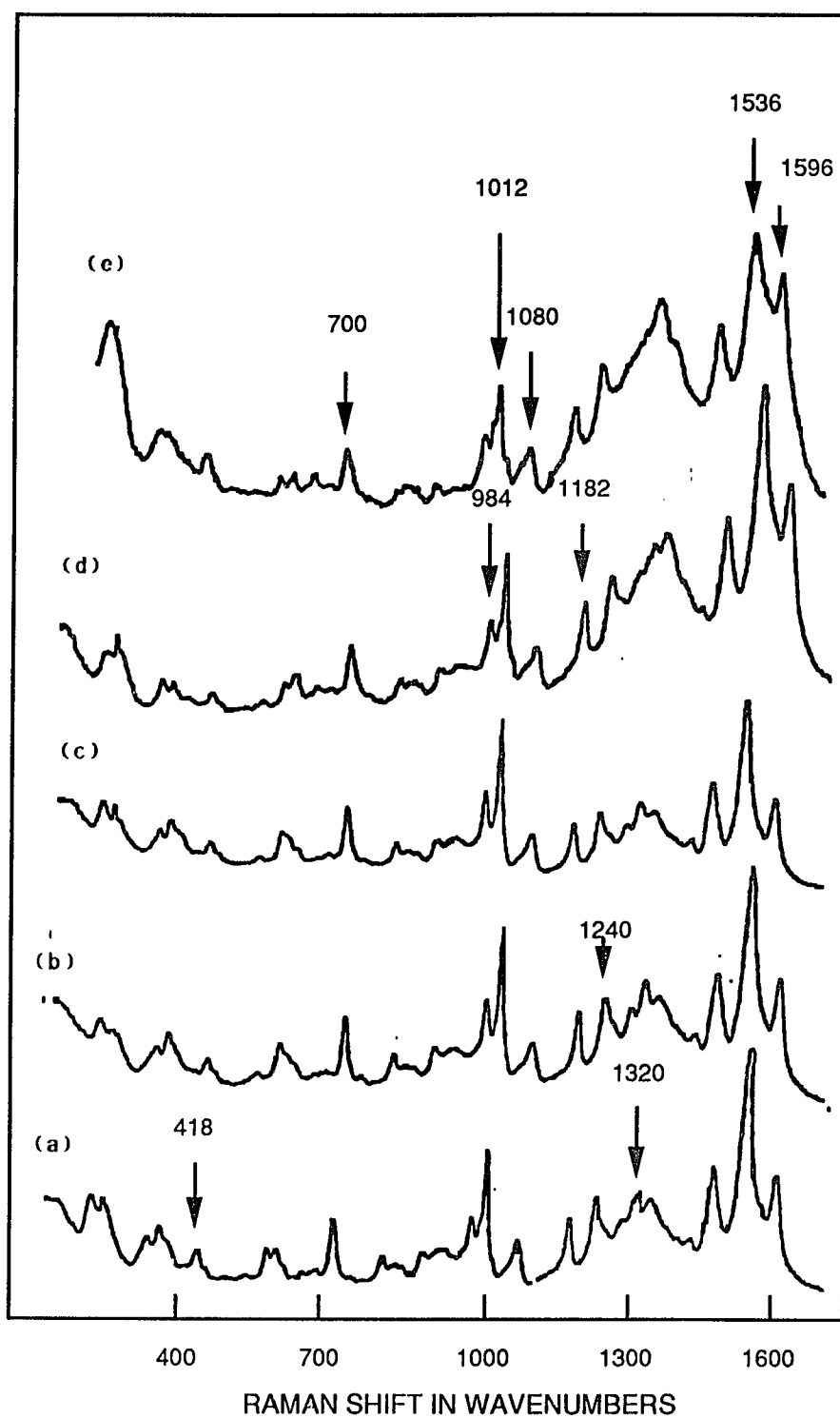


Fig.8 SERS of five p-amino substituted TPP on a Ag electrode.488 nm (a) Por.AAAA (b) AAOO (c) AAAO (d) AAOO and (e) AOOO

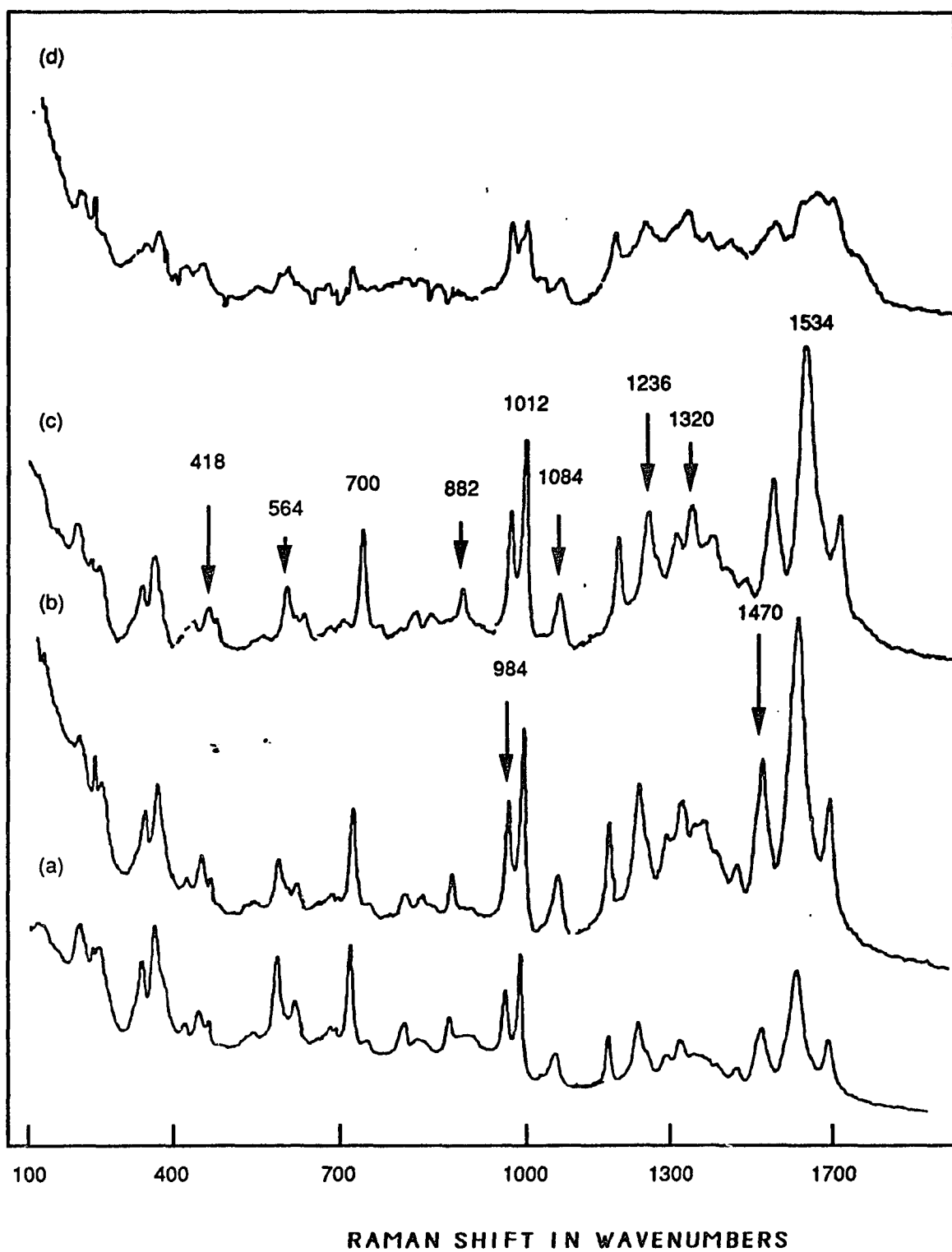


Fig.9 SERS of 0.01M TAPP in .05 M HCl on a silver electrode with 488 nm laser excitation .a) at o.o V b) at - 0.2 V c) at - 0.4 V and d) at -0.6 V

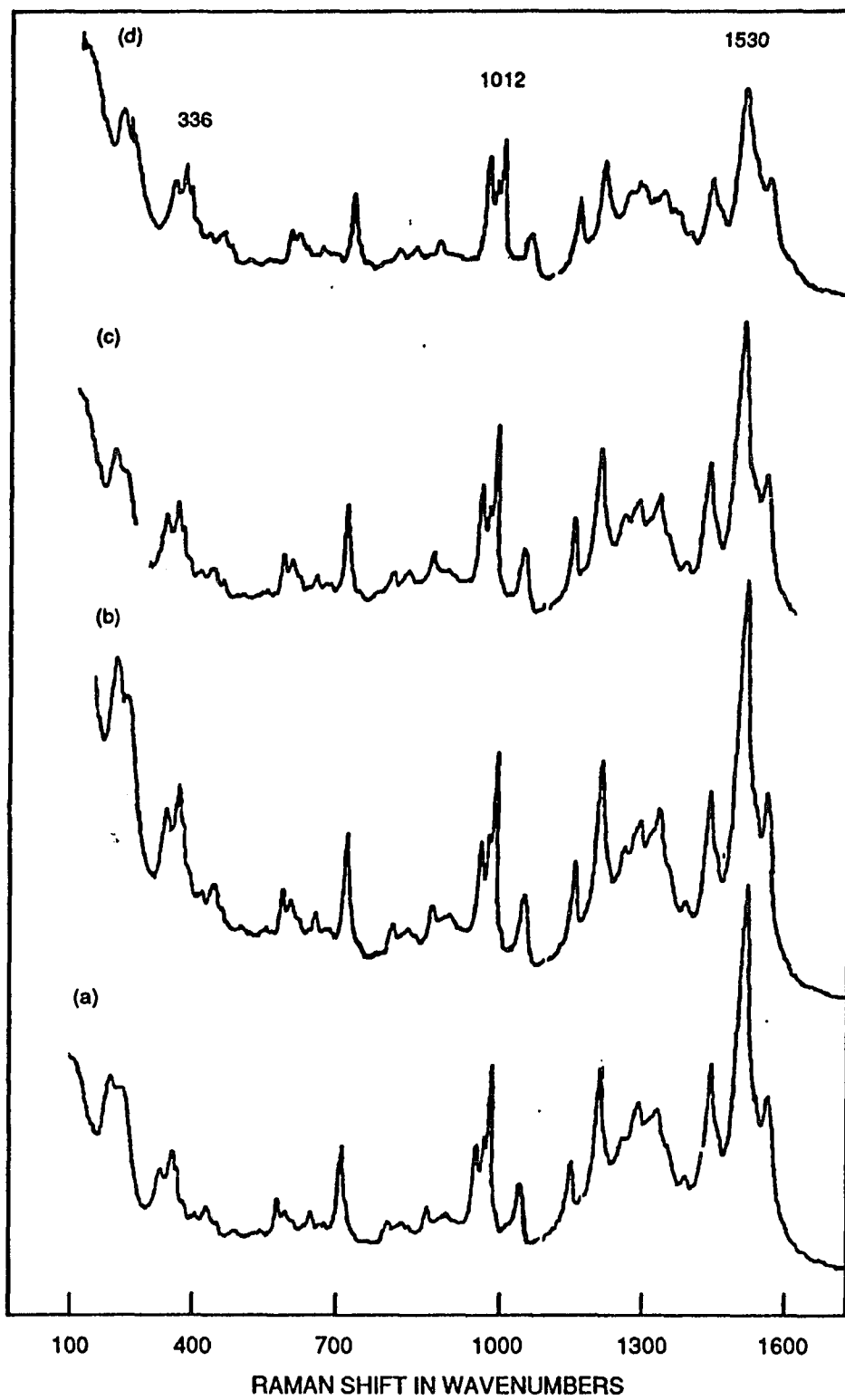


Fig.10 SERS of TAPP in 2 M HCl on a Ag electrode with 488 nm laser excitation.
a) No externally applied potential b) 0.0V c)-0.2V d) -0.4V

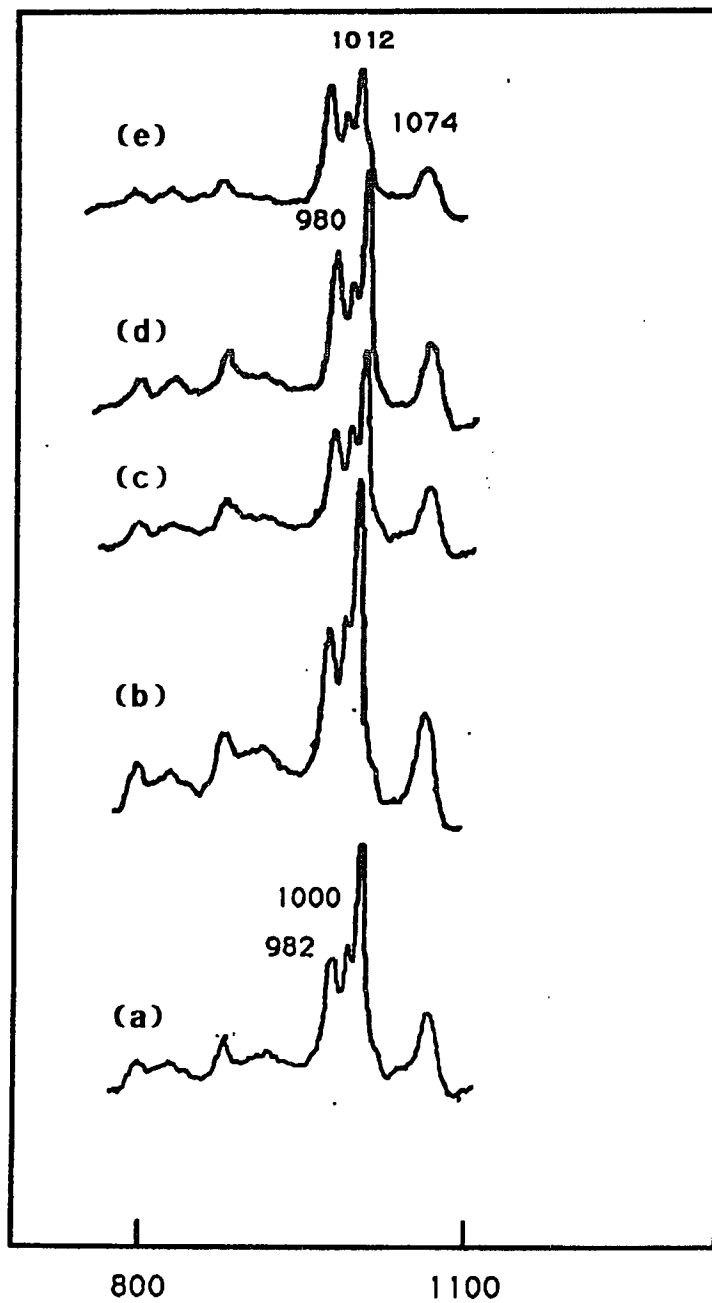


Fig. 1 Potential dependent SERS spectra of TAPP in 2M HCl on a AG electrode with 488 nm laser excitation. a) 0.0V b) -0.1V c) -0.2V d) -0.3 e) -0.4V

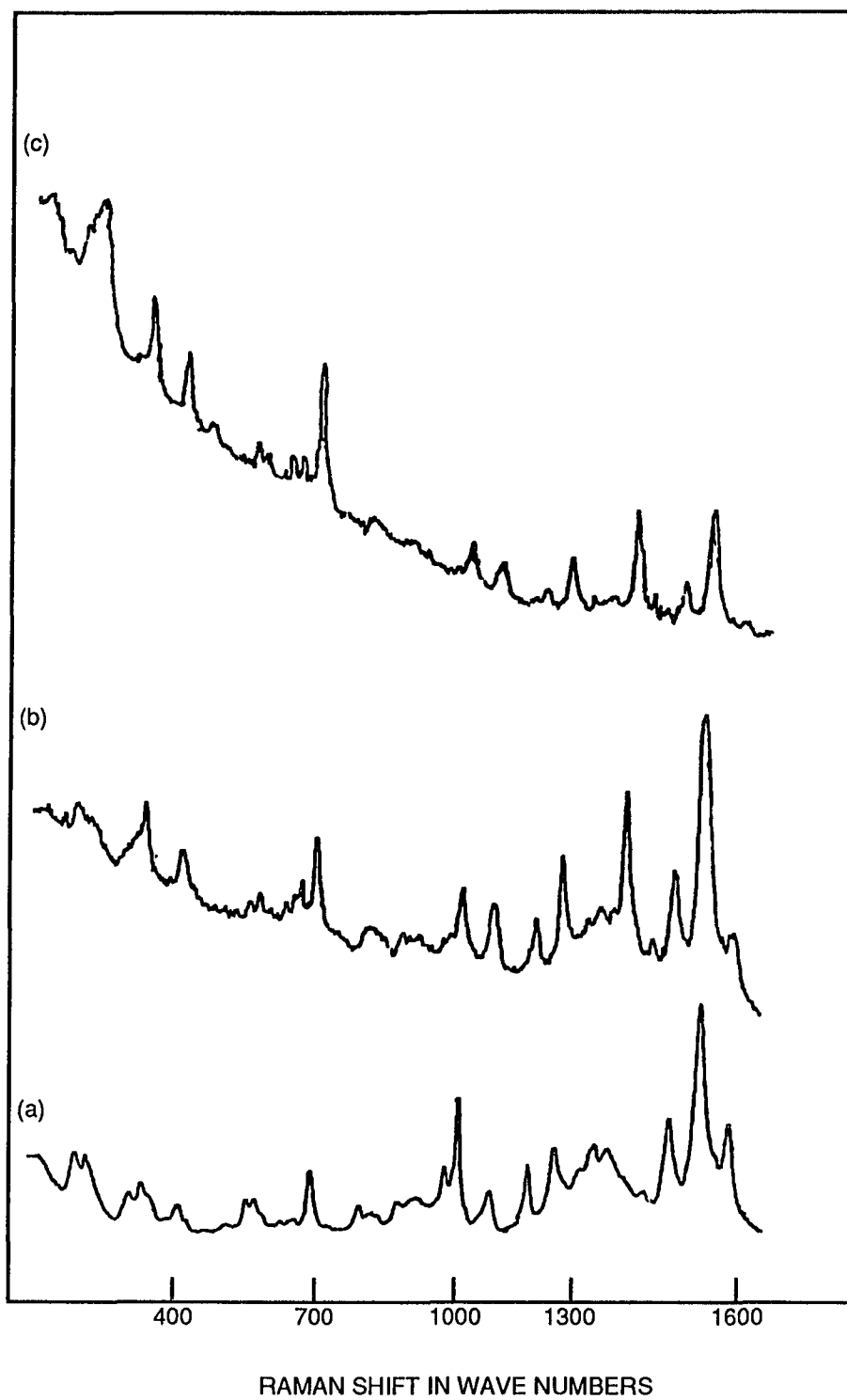


Fig.12 SERS of Porphyrin AAO . (a) on a silver electrode with 488 nm excitation (b) on a gold electrode with 647 nm laser excitation and (c) on a silver electrode with 647 nm laser excitation.

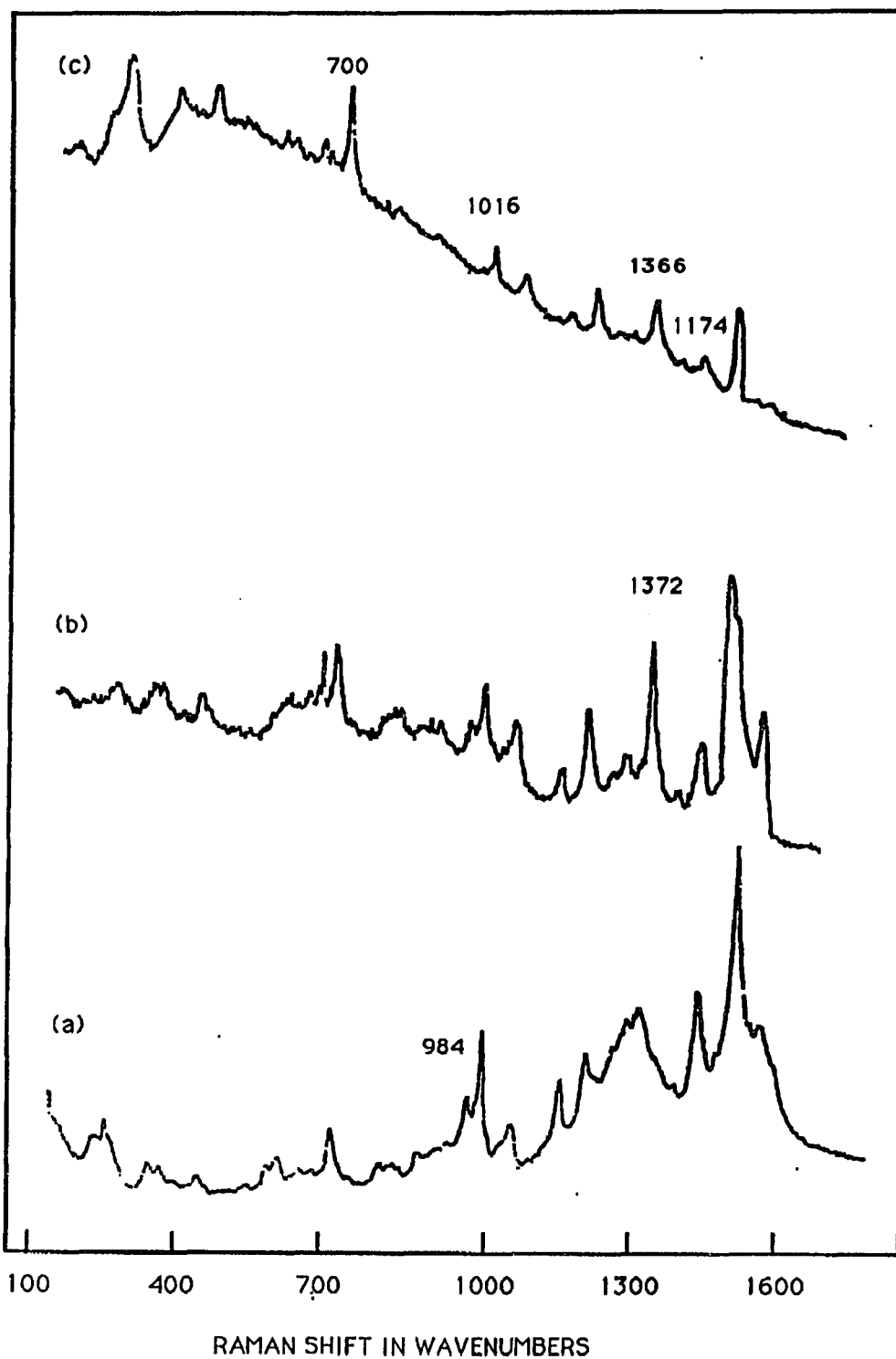


Fig. 13

SERS spectra of Por. D in 0.05 M HCl. (a) Ag electrode at 488 nm
(b) Au electrode at 647 nm and (c) Ag electrode at 647 nm laser excitation
Compound AOO

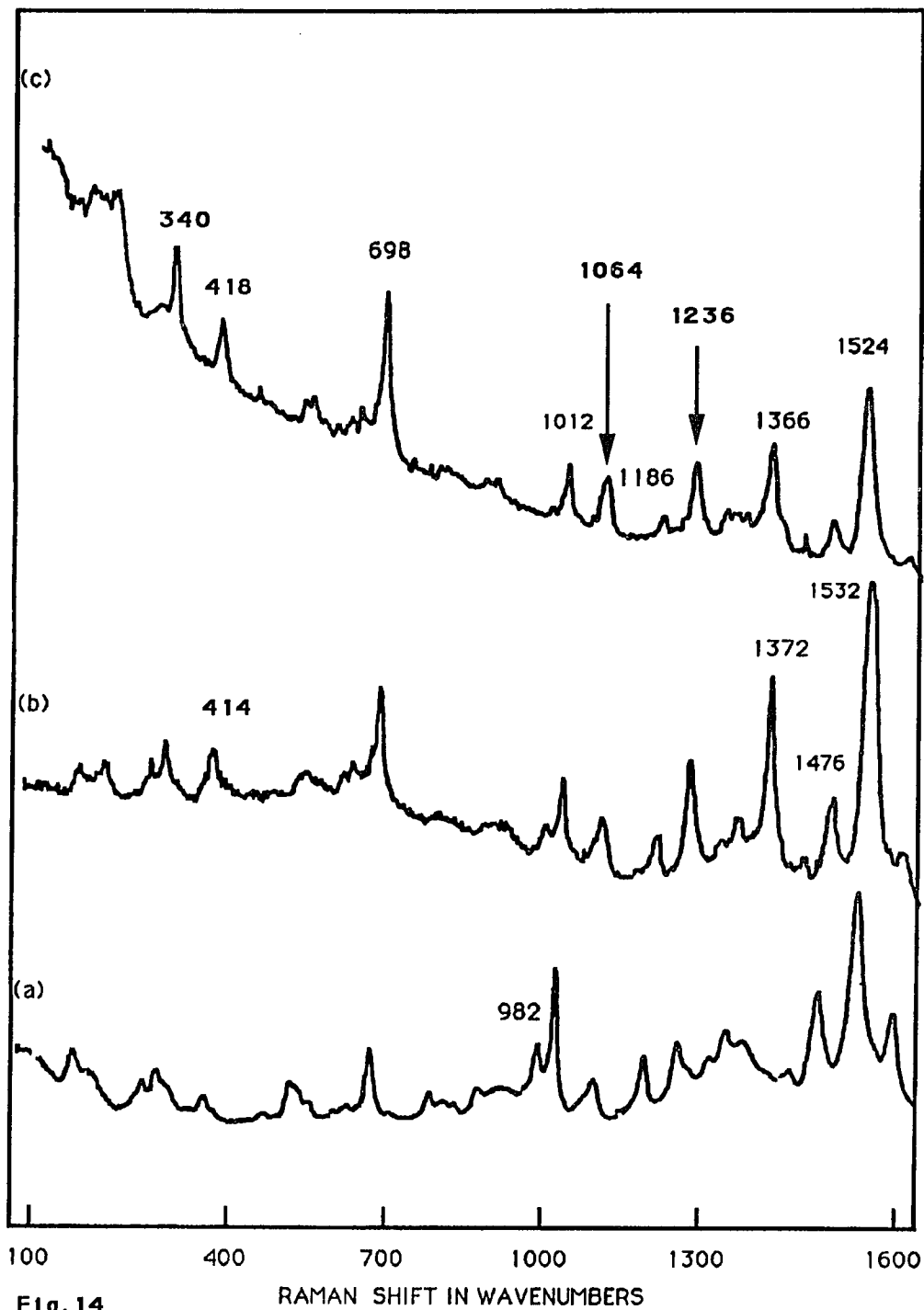


Fig. 14

SERS spectra of Por. B in 0.05 M HCl solution. a) Ag electrode 488 nm.

b) Au electrode 647 nm c) Ag electrode 647 nm laser excitation.

Compound AAO

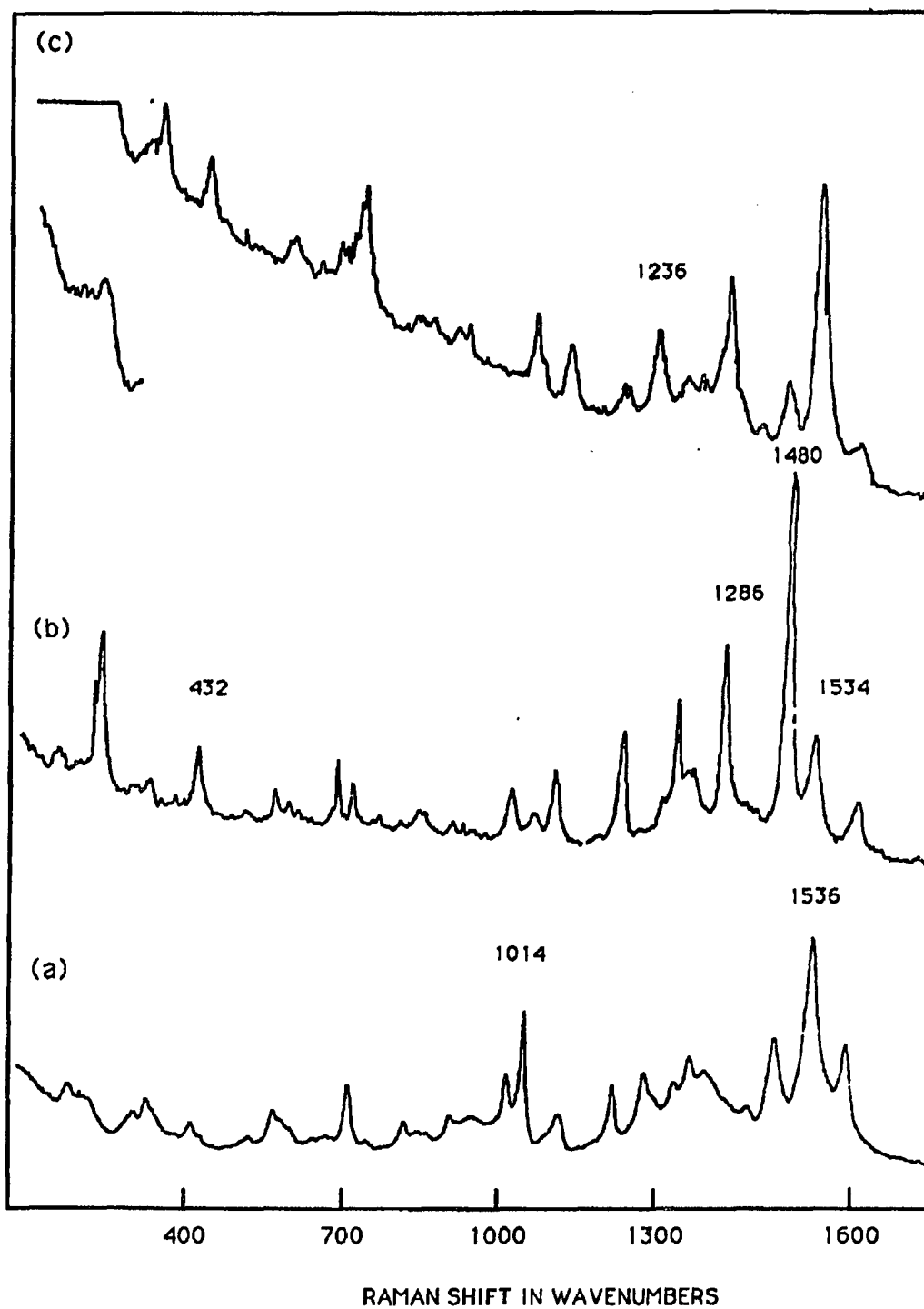


Fig. 15 SERS spectra of TAPP . (a) on a Ag electrode with 488 nm excitation (b) on a gold electrode and (c) on a silver electrode both with 647 nm laser excitation .

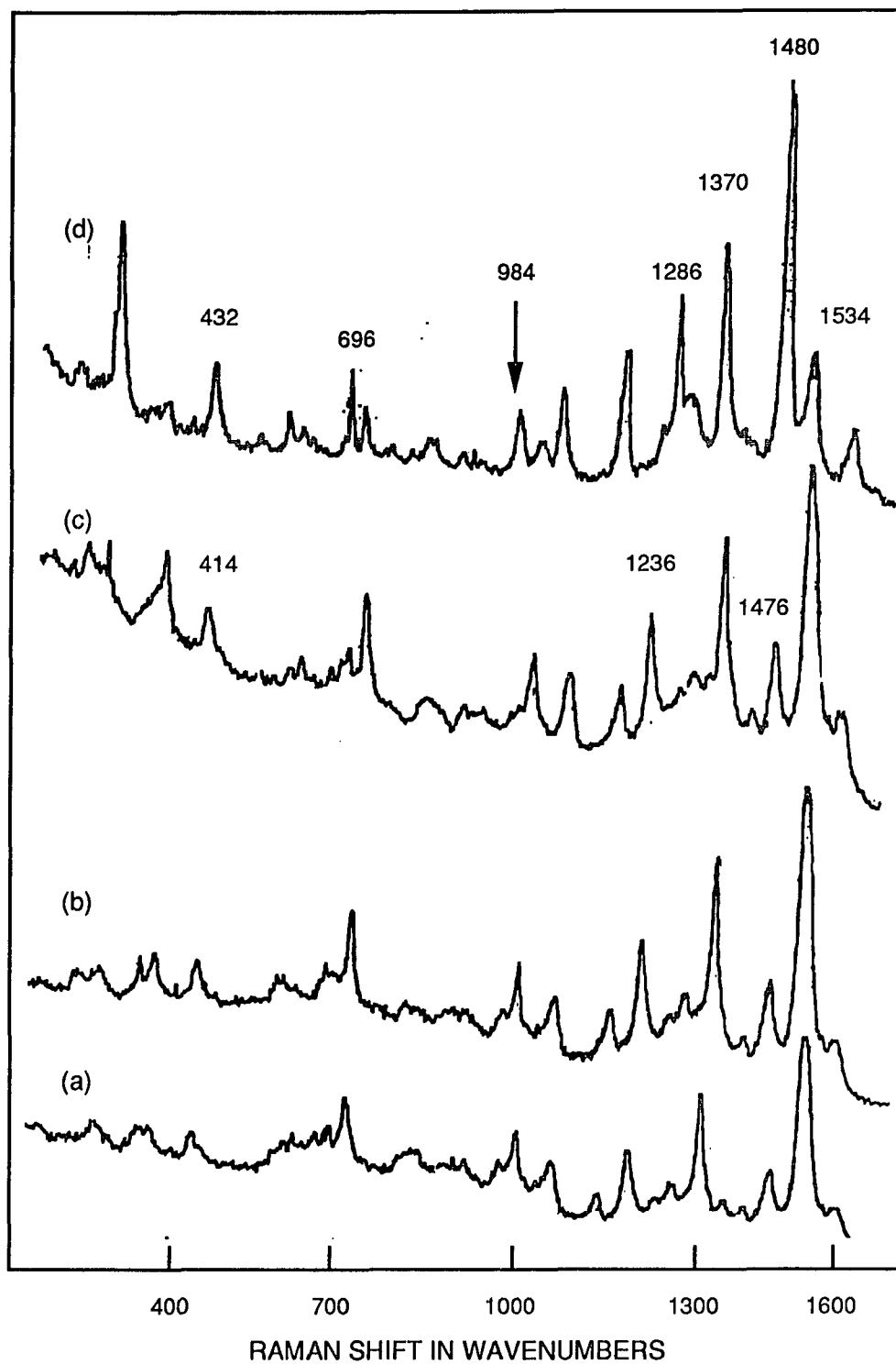


Fig.16 SERS spectra of five TAPPs on a roughened Au electrode with 647 nm laser excitation (a) AAO (b) AAO (c) AAO and (d) AAAA

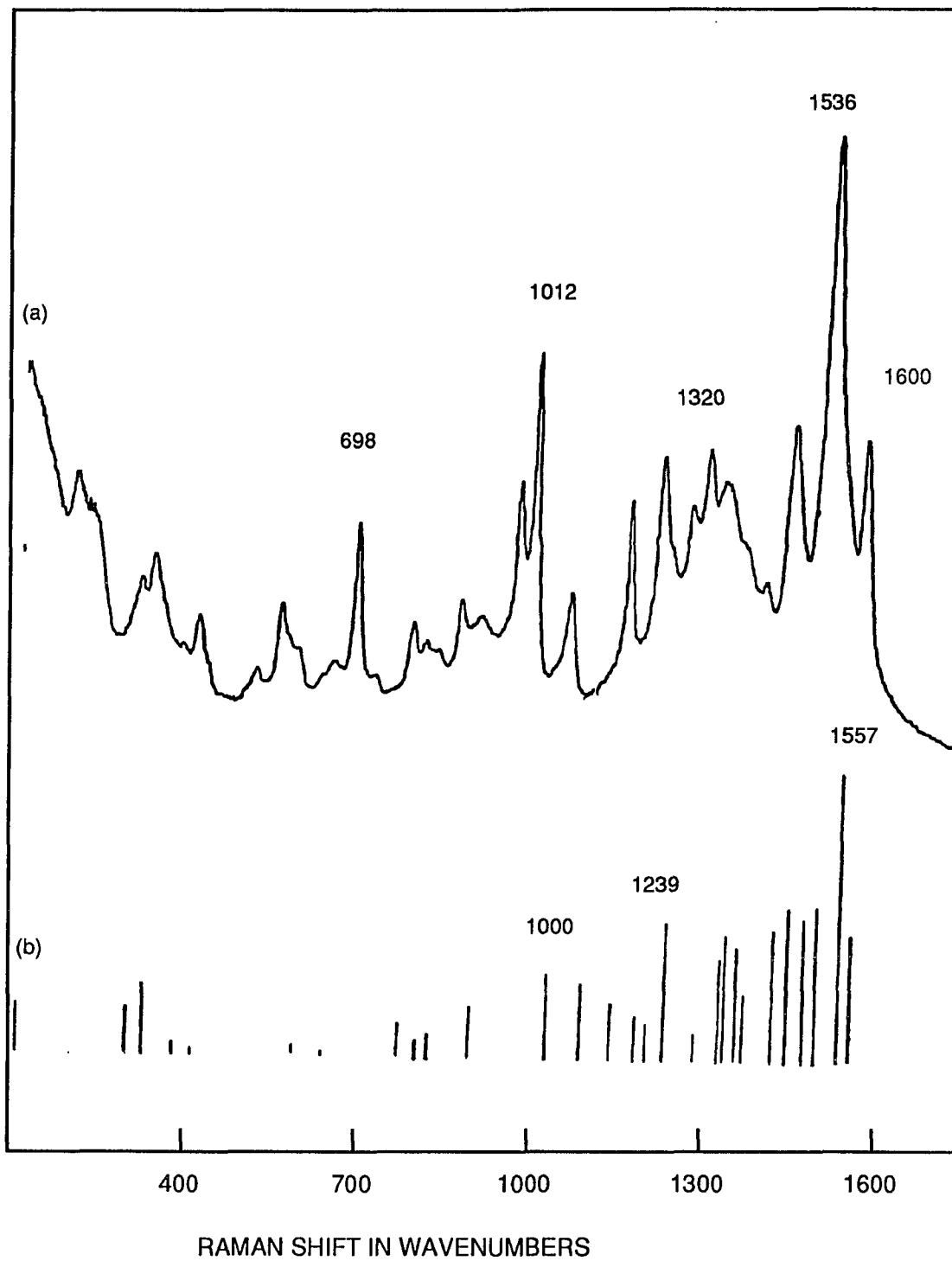


Fig. 17 (a) SERS spectrum of TAPP in 0.05 M HCl at 488 nm laser excitation and Ag electrode.(b) Normal Raman of solid TPP

CHAPTER FOUR
ELECTROPOLYMERIZED TAPP: STRUCTURE AND CATALYTIC
PROPERTIES

4.1 ABSTRACT

Surface Enhanced Raman Spectroscopy is used to characterize the constitutional unit structure of electropolymerized *meso*-tetrakis(4-aminophenyl)porphine(TAPP). TAPP electropolymerization was performed in both aqueous and non-aqueous solvents. Intense SERS spectra are obtained for the surface bound polymer on an electrochemically roughened gold electrode. The spectroscopic evidence shows that electropolymerization results in bond formation between the amino group of one monomer and the carbon atom of another. The presence of an intense band at 1480 cm^{-1} in the polymer spectra indicates that the monomer units are held together by a $\text{C}=\text{N}$ bond in the polymer.

The ability of TAPP to catalyze the reduction of NAD and NMN as well as the oxidation of NADH was also investigated.

4.2 INTRODUCTION

Considerable interest has been shown in attaching electroactive molecules to electrode surfaces^{1,2,3}. These modified electrode surfaces can have their electroactive compounds bonded or adsorbed as monolayers^{4,5} or electropolymerized⁵. The resulting modified electrode surfaces have been used to catalyze useful redox reactions^{6,7,8}.

Porphyrins, especially metalloporphyrins are ideal candidates for electrocatalytic studies because of the porphyrin aromatic system and the ability to attach axial ligands on to the porphyrin molecule. Spiro⁹ electropolymerized Zn(II) and Fe(III) protoporphyrin IX (PP) complexes from CH_2Cl_2 solutions of the porphyrins. In aqueous solution the PP film became inactivated, resulting in its inability to electrocatalyse O_2 reduction.

Electropolymerization of p-amino substituted TPP compounds resulted in modified electrodes which catalyses O_2 reduction. Electropolymerized Co(III) tetra(o-aminophenyl) porphyrin showed pronounced catalysis of O_2 reduction¹⁰. Dissolved, electropolymerized and adsorbed iron(III) tetrakis(o-aminophenyl) porphyrin, p-amino and iron(III) tetrakis (p-N,N'-dimethyl aminophenyl) porphyrin¹¹ showed efficient catalysis of dioxygen reduction. Catalytic efficiency was highest in acidic solution where the overvoltage for the O_2 reduction was reduced by approximately 450 mV. In the basic solution the reduction was about 50 mV. Similar levels of catalytic efficiencies were obtained for ruthenium(II) tetra(o-aminophenyl) porphyrins¹².

4.3 EXPERIMENTAL

(a) polymerization of TAPP

1 - 5 mM porphyrin solutions of TAPP, Mn TAPP and Et_2TAPP in CH_2Cl_2 with TBAP as the supporting electrolyte were used. N_2 gas was dried by passing it through a desiccant, $CaCl_2$, and then through a solution of CH_2Cl_2 prior to bubbling through the porphyrin solution. Electropolymerization was achieved by repeatedly cycling the potential of the working electrode between 0.0 V and +1.2 V at a scan rate of 100 mV/ sec, in the porphyrin solution. The electrochemical system consisted of the conventional three electrode cell with a platinum counter electrode, a platinum or gold working electrode and a saturated calomel electrode(SCE) as the reference. The reference electrode was separated from the rest of the electrochemical system by a bridge.

(b) SERS of electropolymerized TAPP

Polymerization was accomplished on a gold electrode instead of on a platinum electrode because of the ability to obtain SERS spectra from a roughened Au electrode surface. The gold electrode was roughened in 0.1 M KCl solution by applying 20 to 25 triangular sweeps at 100 mV/sec. from an initial potential of 0 V to a switching potential of +1.2 V. The roughened electrode was then removed from the KCl solution, washed with CH_2Cl_2 or CH_3CN , dried and then placed in a 0.5 to 1 mM porphyrin solution in CH_2Cl_2 or CH_3CN with tetrabutyl ammonium perchlorate (TBAP) as the supporting electrolyte. A number of oxidation reduction cycles were performed on this roughened surface and polymer growth was monitored by plotting the cyclic voltammogram on an XY recorder. After 5 to 7 cycles the electrode was removed from the polymer solution, washed with CH_2Cl_2 or CH_3CN and transferred to a solution of the solvent. The SERS spectrum was obtained from this polymerized surface using 647 nm excitation from a krypton ion laser. The rest of the instrumental set up has been described before.

c) catalysis

Electropolymerized electrodes were prepared as described in section (a). These electrodes were then washed with solvent. The washed electrode was placed in a degassed solution of the electroactive species, e.g. NAD, NADH or N methyl nicotinamide(NMN) and cyclic voltammetry performed. Solutions of NAD, NADH and NMN were in water with 0.1M KCl as the supporting electrolyte. All solutions had a concentration of 0.1 - 1 mM and were prepared on the day the experiment was performed. Solutions were deaerated by nitrogen bubbling for twenty minutes.

4.4 RESULTS AND DISCUSSION

(a) Electropolymerization

The reports that aniline could be electrochemically polymerized^{13,14,15} led to the investigation of the oxidative electropolymerization of substituted H₂TAPP and several of its metallated derivatives¹⁶

Fig 1 shows the cyclic voltammogram (CV) curves obtained for the oxidation of H₂(p-NH₂)₂TPP (TAPP). The potential range was from 0.0 V to 1.2 V with a scan rate of 100 mV/sec. The CV curves obtained here are similar to those obtained by other workers for H₂(o-NH₂)₂TPP¹⁶. Two waves are observed in the CV curves on the positive scan, one at 0.6 V and another beginning at 1.0 V. The first wave occurring at +0.6 V represents the oxidation of TAPP to form the porphyrin radical cation and the second wave is due to aniline oxidation. If the potential is cycled just passed the first wave, to about +0.8 V or 0.9 V, no polymer formation is observed. The system must be cycled to a potential at which aniline oxidation begins, for polymer formation to occur. This indicates that both aniline oxidation and porphyrin oxidation to the radical cation are necessary for polymerization of TAPP.

The cyclic voltammograms Fig.1, also show an increase in the oxidation reduction current with each successive scan. This growth of the oxidation reduction current envelope with each successive potential cycle is indicative of non passivating electropolymerization where the polymer film remains electroactive in the electropolymerization potential range. Similar behavior has been observed for amino substituted ruthenium complexes¹⁷⁻²².

Fig 2 shows CV curves for Mn TAPP in the potential range 0.0V to 1.6V on a platinum electrode at a scan rate of 100 mV/sec. While a number of peaks are observed at potentials of 0.6 and 1.3 V on the positive scan and 1.25 and

1.0 V on the negative scan successive CV scans are contracting rather than expanding.

A number of amino substituted macrocycles have been electropolymerized¹², among them Fe(p-NH₂) TPP, Co(o-NH₂)TPP and ruthenium porphyrin compounds of the type Ru(o-NH₂)TPP(CO) and Ru(oNH₂)TPP(L)₂ where L= pyridine, acetonitrile or tetrahydrofuran. All of these macrocycles were polymerized on glassy carbon electrodes except for the polypyridyl complexes of ruthenium which were electropolymerized on Pt, SnO₂ and vitreous carbon electrodes. In the results presented in this chapter attempts at the electropolymerization of MnTAPP, ZnEt₂NTPP and FeTAPP on a Pt or Au electrode using cyclic voltammetry were unsuccessful.

Since polymerization was not achieved on a Pt electrode, the electropolymerization was then attempted on a carbon electrode. The electrode used was not a glassy carbon electrode but graphite. The CV curves were also contracting with each successive cycle. Fig.3 shows CV curves obtained for ZnEt₂N(TPP) on a graphite electrode at a scan rate of 100mV/sec. in the potential range 0.0V to 1.6 V. Examination of the electrode surface after as many as 20 CV scans indicates that no polymerization occurred. Fig.4 shows CV curves for ZnEt₂NTPP on a Pt electrode. The concentration of the solution was 8-9 mM. The peak currents are larger than those obtained from less concentrated solutions but again the successive curves are contracting and no polymer formation was observed.

Attempts at electropolymerization of Fe (p-NH₂) TPP on a gold surface were also unsuccessful. Fe(p-NH₂) TPP was polymerized by Murray²³ on a glassy carbon electrode under experimental conditions similar to those used in this study. It appears that the type of working electrode, whilst not essential for electropolymerization of metal free TAPP is important in the

electropolymerization of metallated porphyrins. This is probably due to the ability of the polymer to bind to the electrode surface .

b) Polymer Characterization

Spiro²⁴ obtained visible and Raman spectra of electropolymerized H₂(*o*-NH₂)TPP. Both spectra indicated that the porphyrin ring remained unchanged in the polymer and that polymerization involved the aniline group. The Raman spectra of the polymer was dominated by porphyrin bands and the frequency and relative intensity of these bands were the same in solution and for the polymer. Two new bands, both very weak, were however observed in the Raman spectra of the polymer. One band at 1547 cm⁻¹ is characteristic of para substituted aniline and the other band at 1522 cm⁻¹ is equivalent to the band found in phenylenediamine at the same frequency and is characteristic of the N=N vibration. These results confirm para substitution but since polymerization of H₂(*p*-NH₂) TPP, in which the para position is occupied by the amine group, has been shown to occur, these result do not rule out other sites for polymerization, e.g. the ortho and meta positions in H₂(*p*-NH₂) TPP

Our results show that electropolymerization of TAPP does not occur unless the potential for aniline oxidation is attained. This establishes the importance of aniline oxidation in the electropolymerization of TAPP. Consequently an examination of the structure of electropolymerized aniline should assist in the elucidation of the structure of electropolymerized TAPP.

Aniline polymerization has been extensively studied^{25,26,27} and various structural compositions for the polymer have been proposed among them 1) head to tail polymerization resulting in the formation of a *p*-C=N bond²⁵ or a *m*-C=N bond²⁸ 2) head to head polymerization resulting in a N=N linkage and 3) tail to tail polymerization resulting in the benzidine linkage²⁹. Emeraldine,

Fig.5, has also been proposed as one of the possible products in aniline oxidation. Polymerized TAPP could therefore contain a variety of imine, diazo and unreacted amine sites.

Raman studies of azobenzene have shown a very strong band at 1442 cm^{-1} in solid³⁰, CCl_4 and methanolic³¹ solutions which has been assigned to the $\text{N}=\text{N}$ stretching vibration. The oxidative electropolymerization of a number of amino polypyridyl complexes of ruthenium have also been studied³² in an attempt to determine the structure of the polymer. IR spectra indicate that νNH_2 stretching vibrations of the amino group appear at 3320 and 3200 cm^{-1} for the monomer. These bands are not present in the polymer, instead they are replaced by a new band at 1695 cm^{-1} which is stronger in the intact polymer than in the KBr pellets. These two features, the loss of the νNH vibration and the appearance of the 1695 cm^{-1} band suggest the conversion of the amine groups into imine³³ groups.

Recently Harada^{34,35} and Brahma³⁶ have studied the vibrational spectra of polyaniline and a number of its derivatives including emeraldine. Harada correlated resonance Raman spectra of polyaniline and its derivatives with their structure. He proposed four unit structures for polyaniline. These structures are shown in Fig.6. The four structures are (a) Imino-1, 4 phenylene (IP) (b) imino-1,4 phenylene salt (IP^+) (c) nitrilo-2,5cyclohexadiene-1,4 diylidene nitrilo-1,4 phenylene (NP) and (d) the radical cation of (IP) $\text{IP}^{\cdot+}$. Harada³⁴ synthesized these four constitutional units and obtained their Raman spectra. He then compared their Raman spectra with that of the Raman spectrum of polyaniline.

The structures of polyaniline proposed by Harada all assumed head to tail polymerization between the aniline molecules. Tail to tail polymerization is also possible. In analyzing our spectra we first attempted to determine which of these three possibilities, head to head, head to tail or tail to tail polymerization,

actually occurs when TAPP polymerizes. Head to head polymerization would result in the formation of a nitrogen to nitrogen bond. In the spectra this would be expressed by a band at 1400 cm^{-1} which is characteristic of the $\text{N}=\text{N}$ vibration. No Raman peaks are observed in the 1400 cm^{-1} region of our polymer spectra obtained from electropolymerization in $0.05\text{M H}_2\text{SO}_4$, Fig.7d. We therefore conclude that there is no head to head polymerization when electropolymerization occurs in HCl. Examination of Fig.8, the SERS spectra of TAPP electropolymerized in CH_2Cl_2 , shows a very weak band at 1418 cm^{-1} . Hucker³⁷ studied a number of azobenzene derivatives and identified a band between 1440 and 1380 cm^{-1} as due to the $\text{N}=\text{N}$ stretch. The band observed at 1418 cm^{-1} we believe to be the equivalent band and therefore could represent the $\text{N}=\text{N}$ stretch. Its reduced intensity suggests that in the polymer only a few of the linkages are of the $\text{N}=\text{N}$ type. The presence of this vibration indicates an azo linkage. We therefore conclude that there are some azo linkages in the polymer.

We excluded the possibility of tail to tail polymerization because of the inability to electropolymerize benzene and the absence of a peak in the spectra which can be assigned to the benzidine $\text{C}-\text{C}$ vibration. This left head to tail polymerization as the other possibility. Head to tail polymerization would result in either a $\text{C}-\text{N}$ or $\text{C}=\text{N}$ bond. The $\text{C}-\text{N}$ vibration in compound IP and IP^+ has been observed at 1221 cm^{-1} and 1231 cm^{-1} respectively. No band is observed in the polymer spectra Fig.8, at either of these frequencies indicating that structures IP and IP^+ are not present in the polymer.

A comparison of the monomer and polymer spectra, Table 1, shows that the monomer spectrum has a peak of medium intensity at 1476 cm^{-1} while in the polymer an intense peak is observed at 1480 cm^{-1} for the polymer in HCl and 1476 cm^{-1} for the polymer in CH_2Cl_2 . The polymer peak is about five times

as intense as that of the monomer. We believe that the 1480 cm^{-1} polymer peak is a combination of the 1476 cm^{-1} monomer peak and the 1471 cm^{-1} polymer peak shifted to higher frequencies. This peak is characteristic of the $\text{C}\equiv\text{N}$ vibration. We therefore conclude that this represents the $\text{C}\equiv\text{N}$ vibration in the polymer.

Table 2 shows the characteristic frequencies for each of the constitutional unit structures of polyaniline. Of the constitutional unit structures proposed by Harada an intense band at around 1480 cm^{-1} is characteristic of structure NP, Fig.6c. This leads us to conclude that when TAPP is electrochemically polymerized from a HCl solution and from CH_2Cl_2 the predominant product is compound NP Fig.9.

Two other features of the polymer spectrum, Fig.4d are the intense band at 1286 cm^{-1} and the absence of the 1236 cm^{-1} band. It is not possible to determine whether the 1286 cm^{-1} band represents a new band or whether it is the 1236 cm^{-1} band upshifted by 50 cm^{-1} . There has been some ambiguity as to the assignment of this 1236 cm^{-1} band. Cotton³⁸ has assigned the 1236 cm^{-1} band to a $\text{C}_\alpha - \text{N}$ vibration for tetra sulfonato phenyl porphyrin .

c) Catalysis

Modified electrodes have been widely used to catalyze electrode reactions of organic compounds. In these cases the electroactive compound polymerized on the electrode acts as a mediator, oxidizing or reducing the substance and reducing its overpotential.

The exchange of electrons between the active site of biological redox compounds and the naked metal of the electrode occurs slowly. Coating the electrode with a chemical mediator e.g. a porphyrin should increase the rate of

electron transfer. Transition metal complexes have been used to catalyze ascorbic acid oxidation, oxygen^{39,40} and carbonyl compound reduction⁴¹.

Because of the role of iron and cobalt macrocyclic complexes, particularly the porphyrins and phthalocyanines, in oxygen transport and storage as well as in charge transfer, a number of studies have been performed in an attempt to characterize the complex formed between iron porphyrins and dioxygen^{42,43}. These studies were extended to examining the effect of monomeric iron and cobalt porphyrins in the electrocatalytic reduction of dioxygen^{44,45}. Attachment of the porphyrins to the electrode surface by covalent bonding or chemisorption lead to electrocatalytic studies of the adsorbed monomer⁴⁶⁻⁵⁰. When Spiro⁹ oxidatively electropolymerized metalloprotoporphyrin (IX) on to a metal substrate research into the electrocatalytic properties of electropolymerized porphyrins was born. Most of the subsequent studies of electropolymerized TAPP catalytic ability centered on their ability to reduce dioxygen to H₂O₂.

We believe that the presence of the extended π system in porphyrins results in them possessing favorable electron transfer characteristics, and that this would make them ideal candidates for electrocatalytic studies. In an attempt to expand the range of catalytic activity of TAPP, we performed experiments which investigated the catalytic activity of polymerized TAPP on NAD, NADH and NMN. In these experiments the peak potentials for the reduction of NAD and NMN, and the oxidation of NADH were compared for the naked platinum electrode and for the polymer coated electrode.

d) Catalysis of NADH oxidation

Au or Pt surfaces coated with electropolymerized TAPP were tested for catalytic activity in solutions of NADH. Fig.10(a) shows the CV curves for the

electropolymerization of TAPP to form the polymeric films used in the experiments described. Fig.10c shows the CV curves for the polymer coated electrode in 1 mM NADH solution. The potential scan was from 0.0 V to 1.2 V at a scan rate of 100 mV/sec. Similar results were obtained at other scan rates. Peaks are observed at 0.44 V on the positive scan and 0.34V on the negative scan. The beginning of an oxidation peak is observed at 1.2V. A comparison with Fig.10b, obtained from a similarly polymerized electrode immersed in 0.1M KCl shows an oxidation peak at 0.46 V and a reduction peak at 0.36 V. The fact that the oxidation peak which is observed at about 0.46V occurs in the presence and absence of NADH means that it represents a process which is independent of NADH. It probably represents the degradation of the polymer film. The intense peak observed at around 1.2V is the oxidation of NADH to NAD. The assignment of the wave at around 0.46 V to an electrochemical process involving the electropolymerized poropyrin film and the absence of any significant shift in the oxidation potential of NADH indicates that the oxidation of NADH is not catalysed by electropolymerised TAPP.

e) Catalysis of N methyl nicotinamide reduction (NMN)

Prashad⁴¹ has shown that catalytic oxygen reduction occurs on an electrode surface roughened in the presence and in the absence of porphyrin. In an attempt to expand the catalytic activity to substances other than oxygen, the effect of (a) a silver electrode roughened in KCl and (b) a silver electrode roughened in a porphyrin solution, on the reduction potential of N methyl nicotinamide was investigated.

The CV curves for a 5×10^{-2} M solution of N methyl nicotinamide on a polished silver electrode is presented in Fig.11a. The potential range is from 0.0

V to -1.6 V at a scan rate of 100 mV per second . A peak is observed at -1.1V on the negative scan and one at -0.15V on the positive scan. When the Ag electrode is roughened in 0.1 M KCl and then placed in a solution of NMN the CV curves obtained from this roughened electrode, Fig.11b, shows peaks at -1.0V (reduction) and -0.15 V (oxidation). When the electrode is roughened in a solution containing the porphyrin and then transferred to the N methyl nicotinamide solution the CV curves which are obtained are shown in Fig.11c,d.

The oxidation and reduction potentials obtained from the electrode roughened in KCl and the electrode roughened in a porphyrin solution are similar to those obtained on the smooth silver electrode surface. The absence of any shift in the reduction potential to more positive values indicates that neither the roughened silver surface or the silver surface roughened in the presence of the porphyrin monomer acts as a catalyst for the reduction of N methyl nicotinamide.

4.5 CONCLUSION

The ability of electropolymerized TAPP to catalyze the electrochemical oxidation and reduction of a number of biologically significant molecules was investigated using cyclic voltammetry. The results show that electropolymerized TAPP does not catalyze the reduction of NAD and N methyl nicotinamide in aqueous solution and the oxidation of NADH.

The results presented here have also illustrated the application of SERS to the elucidation of the molecular structure of electropolymerized TAPP. The increased intensity of the SERS signal compared to that of the normal Raman has allowed for the acquisition of very intense spectra. The data have shown how the high specificity of Raman spectroscopy can be applied to the

determination of the type of linkage holding monomer units together in electropolymerized TAPP. The SERS spectra indicate that in both types of solvents, electropolymerization results in the formation of a $\text{C}=\text{N}$ linkages between the monomer units. The use of SERS in determining the structure of a modified electrode surface is established.

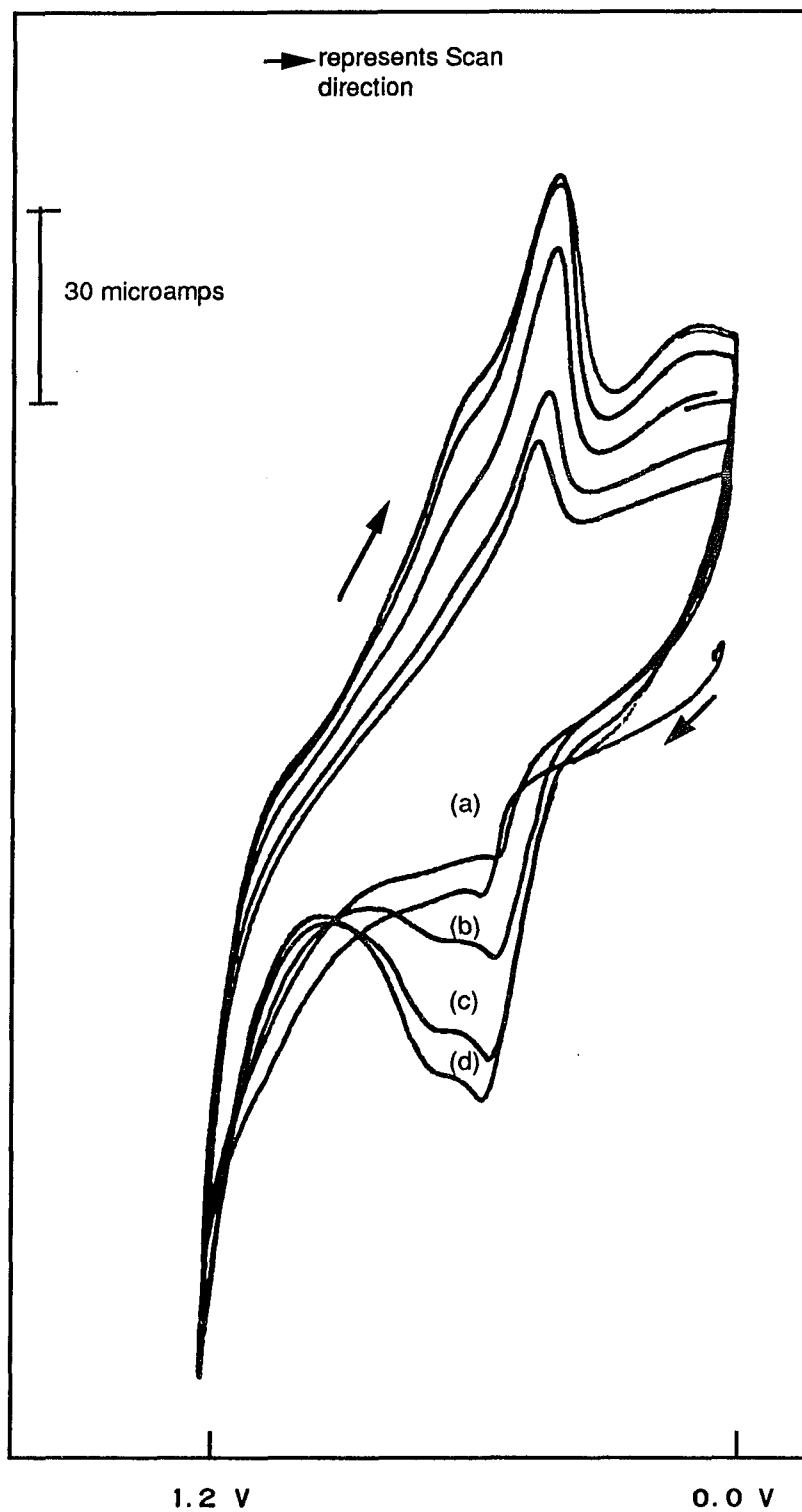


Fig.1 Cyclic voltammograms for the electropolymerization of TAPP on a Au electrode. (a) scan 2 (b) scan 10 (c) scan 15 and (d) scan 20. The unlabelled line represents the first scan.

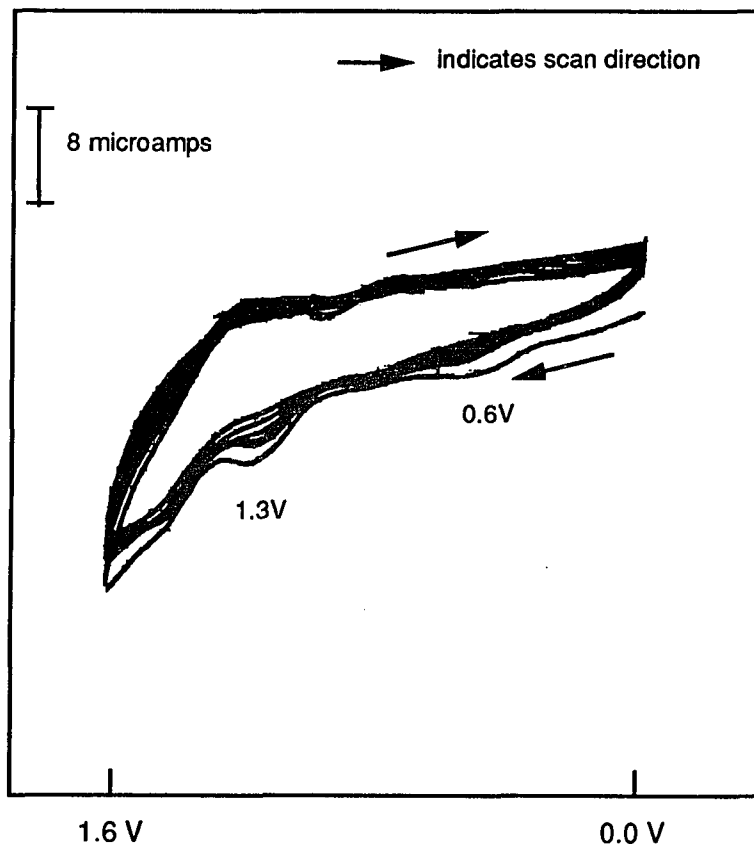


Fig.2 Cyclic Voltammograms for Mn TAPP on a Pt electrode. Scan rate 100mV/sec.

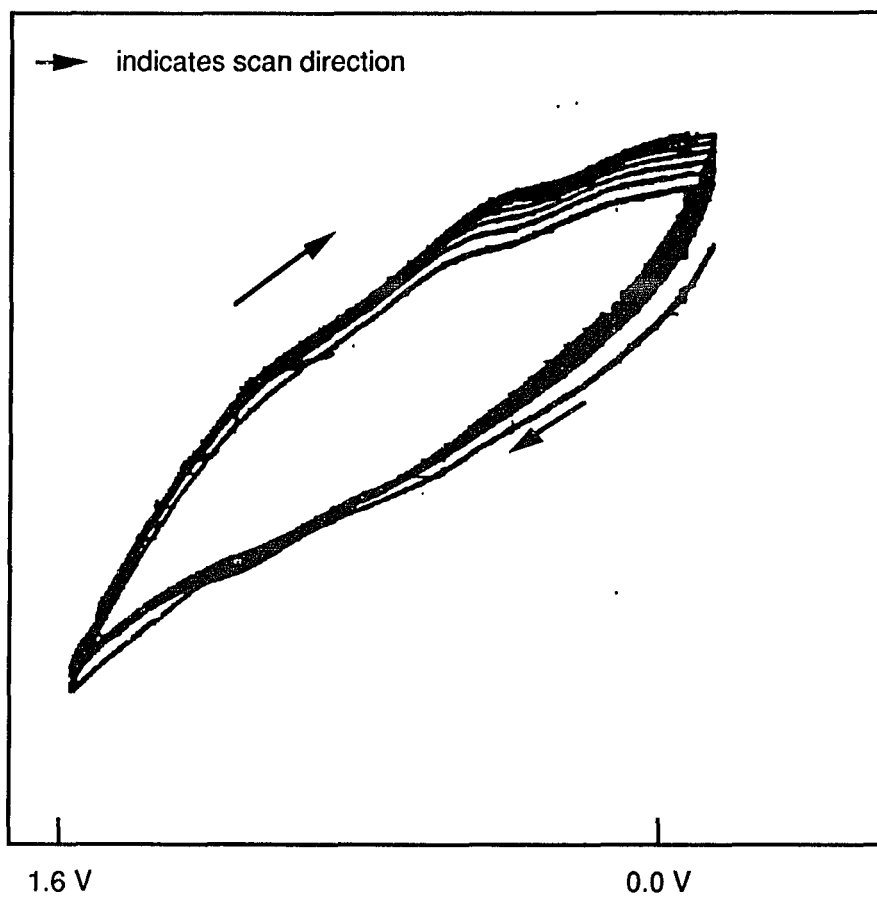


Fig.3 CV for ZnEt₂n TPP on a carbon electrode with methylene chloride as solvent. Scan rate 100 mV/sec.

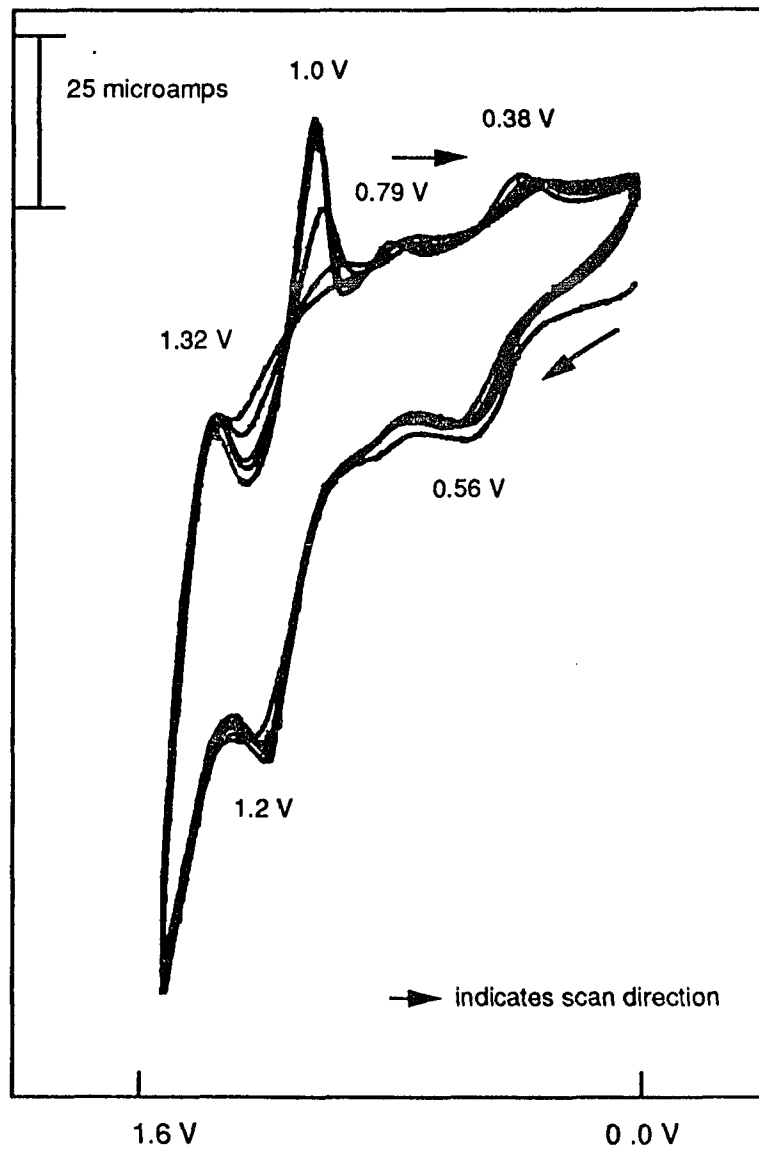


Fig.4 Cyclic Voltammograms for the electropolymerization of ZnEt₂N TPP on a Pt electrode. Scan rate of 100 mV/sec.

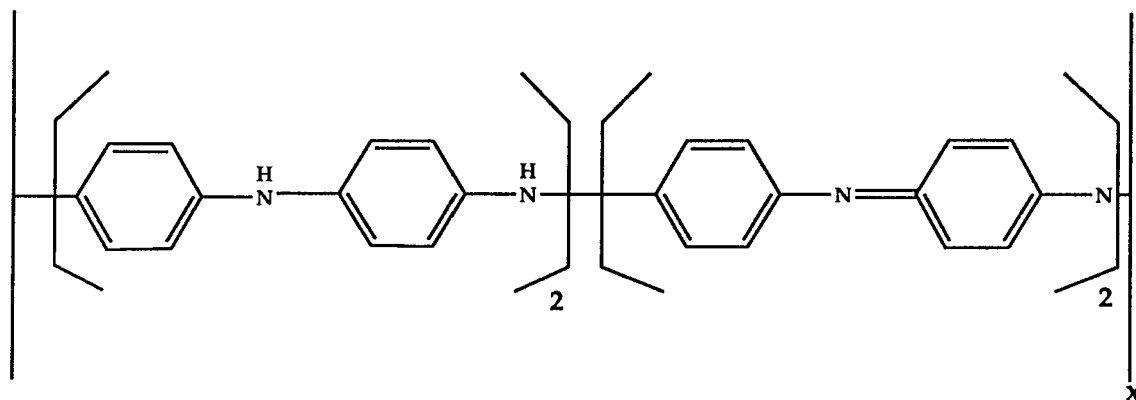


Fig.5 Structure of emeraldine

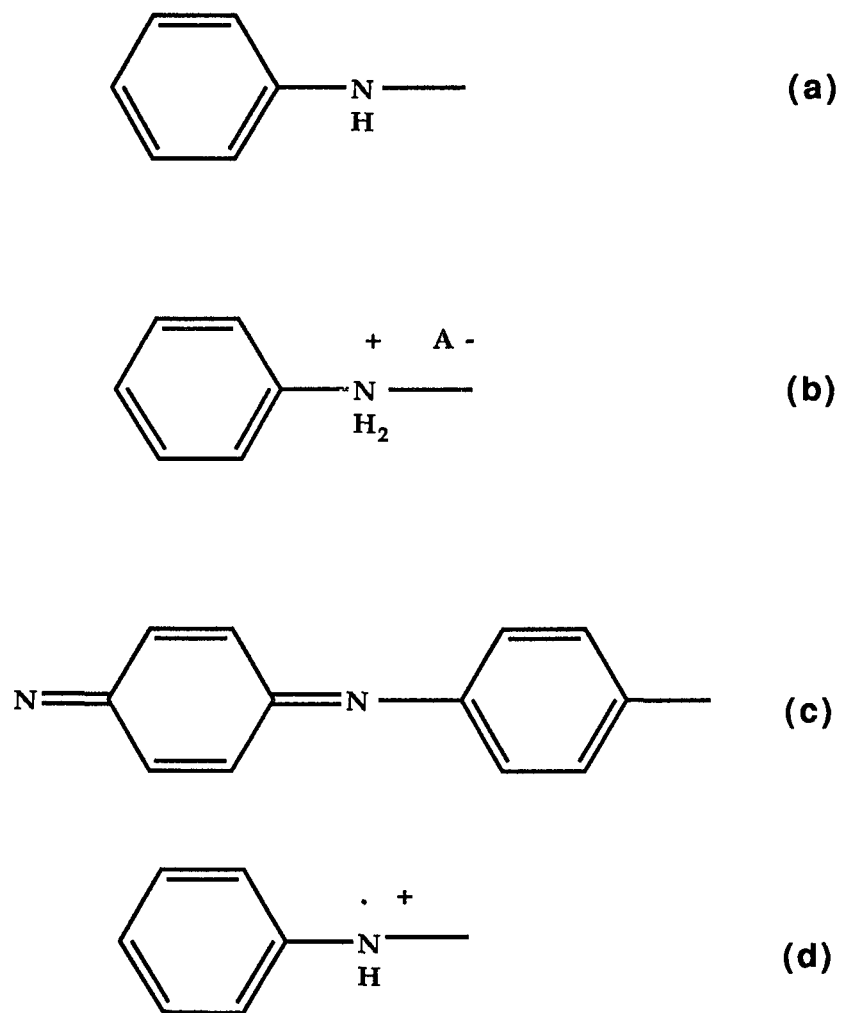


Fig6 Diagram of the constitutional unit structures of polyaniline.
 (a) Imino-1,4-phenylene , IP , (b) Imino-1,4-phenylene salt , IP + ,
 (c) Nitrido-2,5-cyclohexadiene-1-4diylidene-nitrilo-1,4-phenylene , NP, and
 (d) Radical cation of (a)

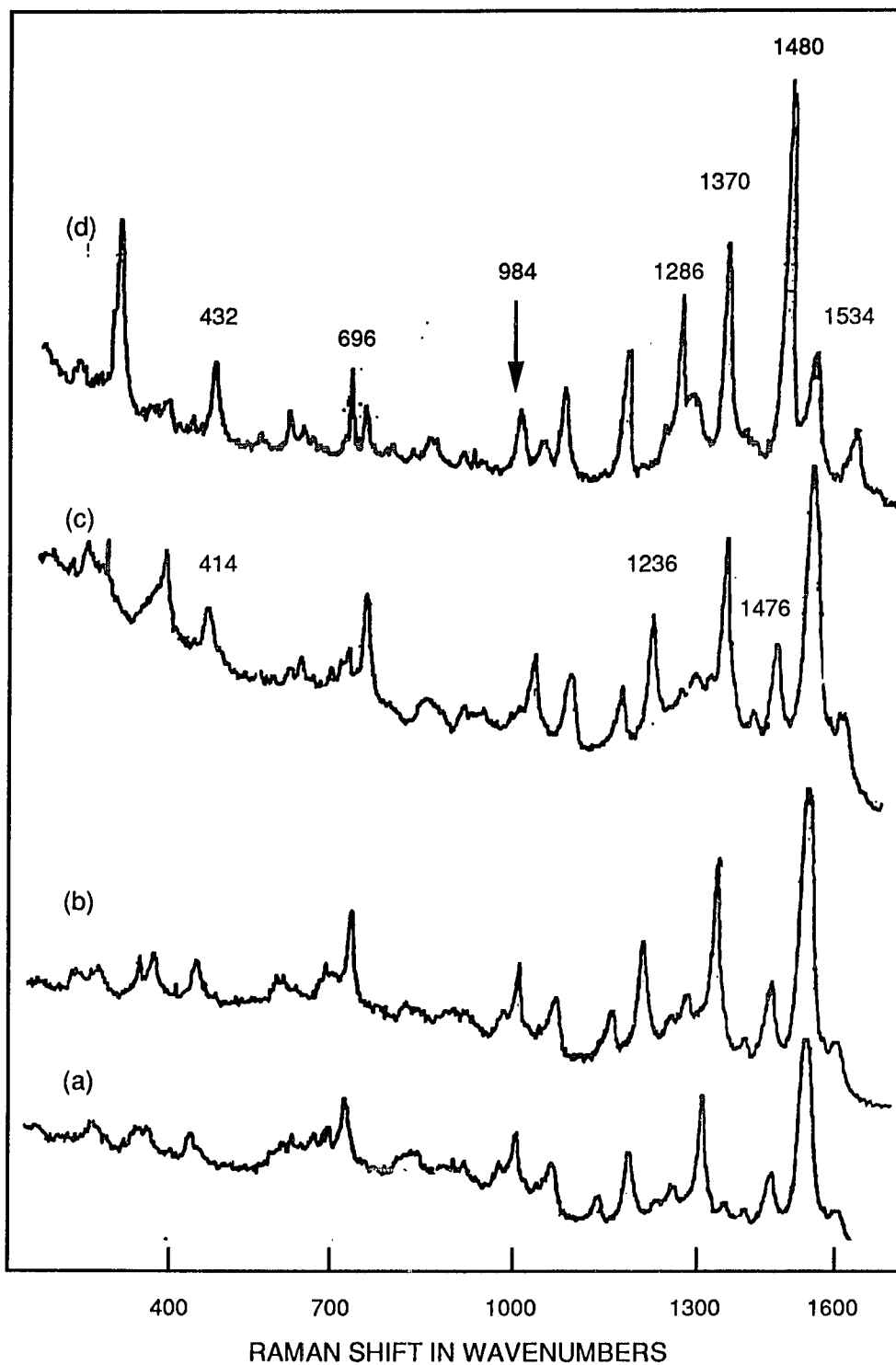


Fig.7 SERS spectra of five TAPPs on a roughened Au electrode with 647 nm laser excitation (a) AAOO (b) AAAO (c) AAOO and (d) AAAA

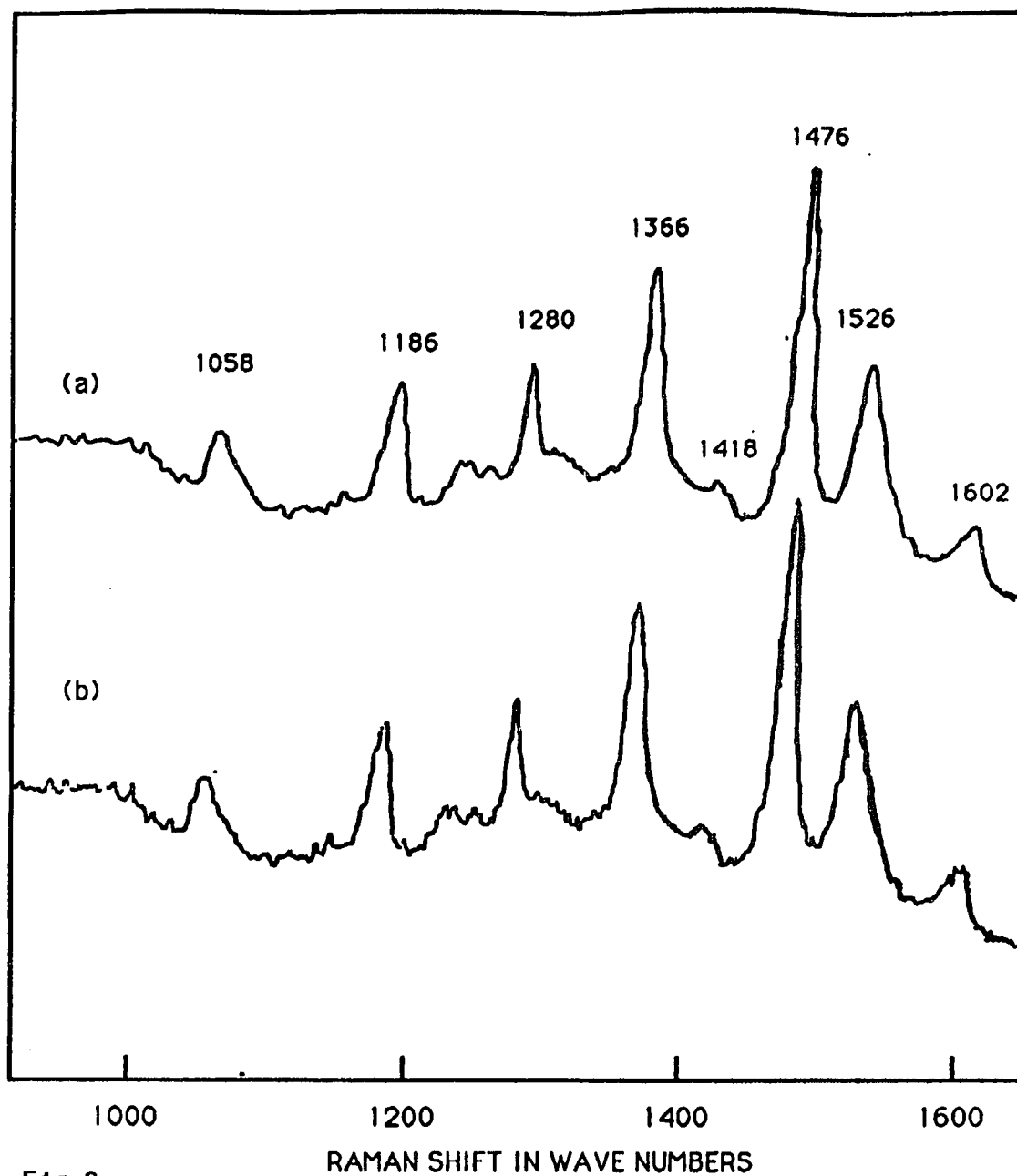


Fig. 8

SERS spectrum of TAPP electropolymerized on a roughened Au electrode, with 647 nm laser excitation. Spectrum (a) was digitally smoothed whilst spectrum (b) was not.

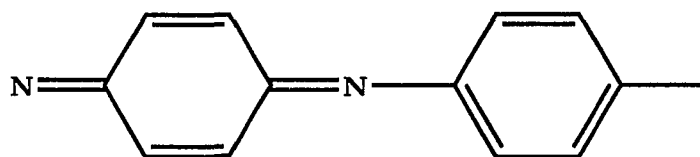


Fig.8 Structure of the constitutional unit structure of poly TAPP
Nitrilo-2,5-cyclohexadiene-1-4diylideneitrilo-1,4-phenylene (NP)

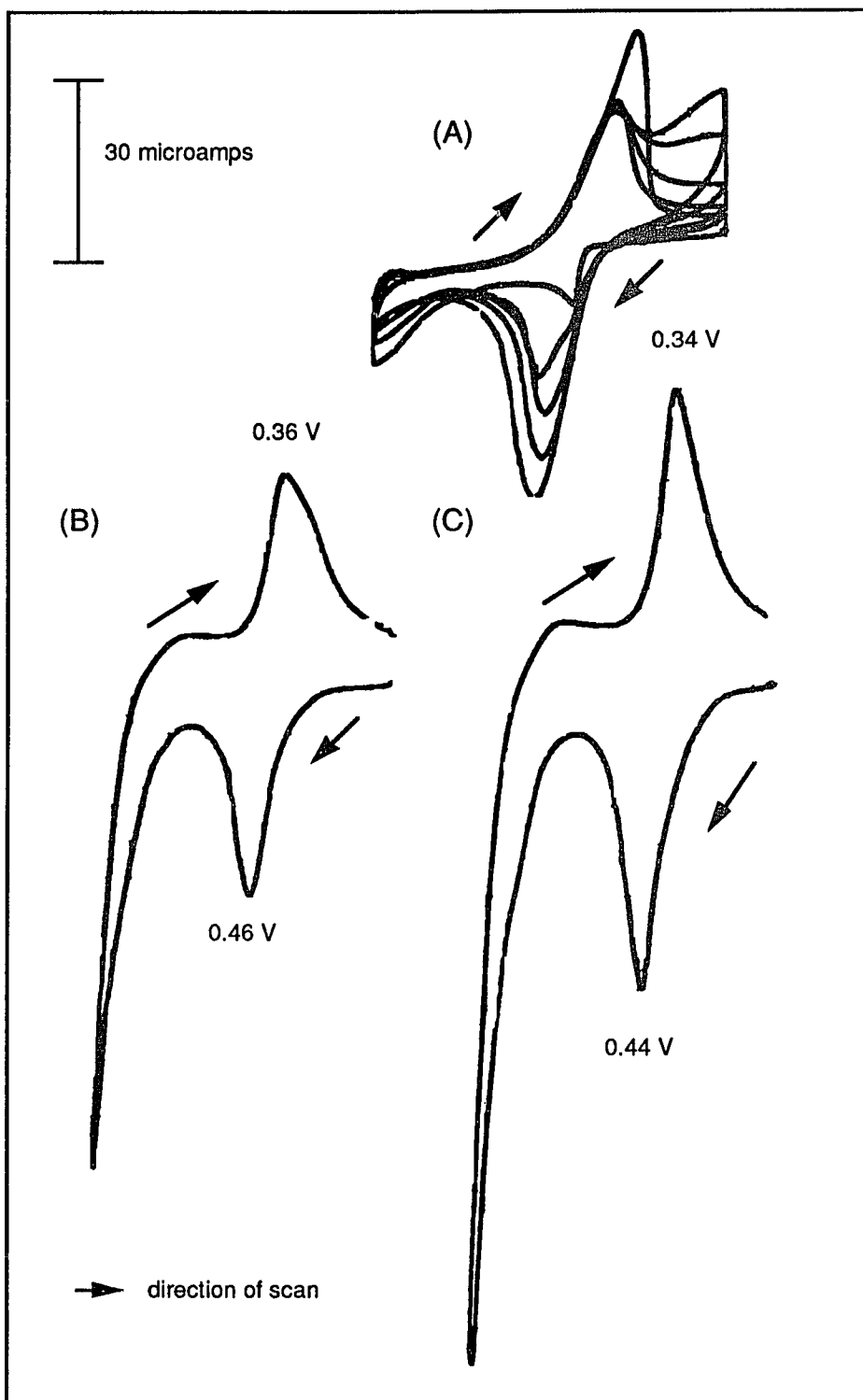


Fig.10 Attempts at catalysis of NADH by polymerized TAPP.
(a) shows the CV obtained during electropolymerization of TAPP.
(b) CV for polymer coated electrode in 0.1 m KCL solution.
(c) CV for polymer coated electrode in 1 mM NADH solution.

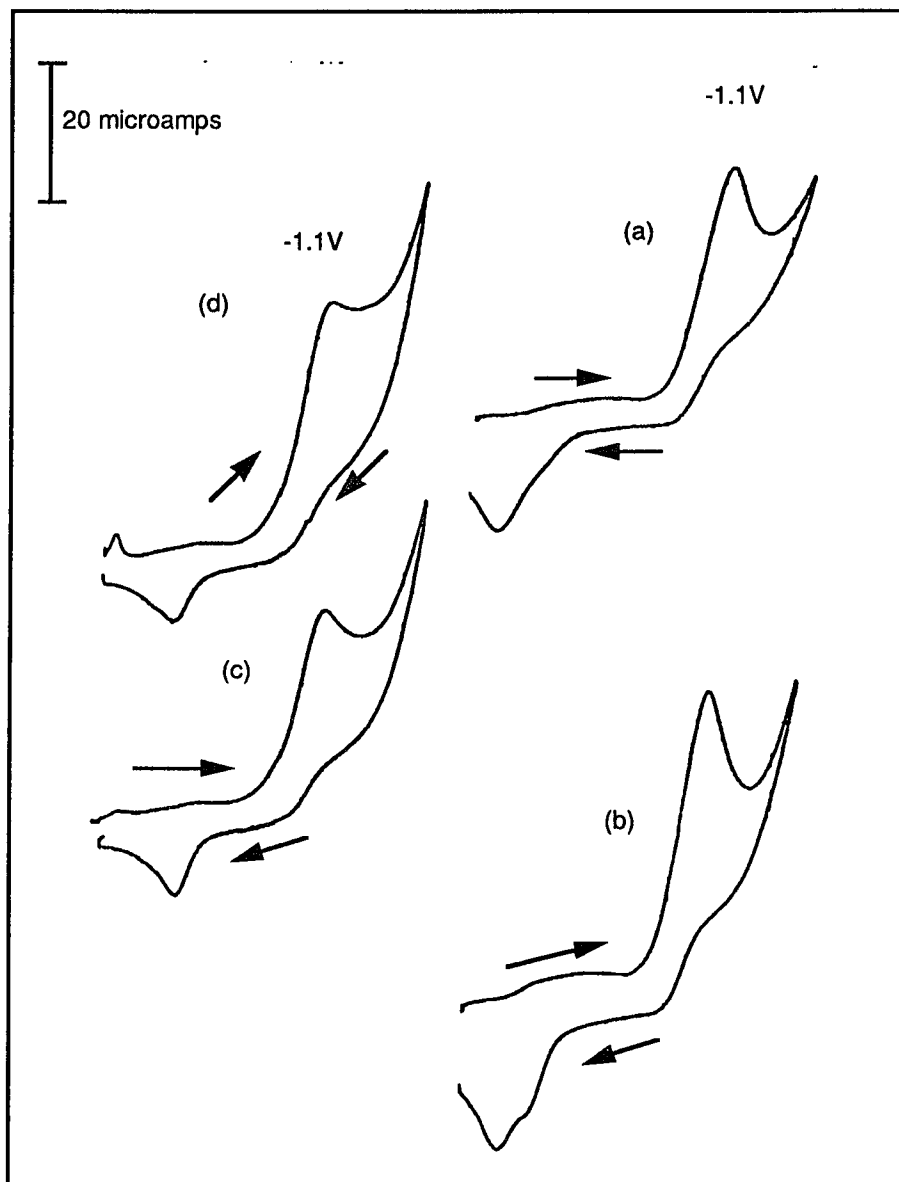


Fig.11 Cyclic Voltammograms of N-methyl Nicotinamide from 0.0 V to - 1.6 V .
 (a) on a polishd Ag electrode (b) on a roughened Ag electrode
 (c) on a Ag electrode roughened in TAPP and then washed and
 (d) on a Ag electrode roughened in TAPP and left to dry .
 Scan rate 100 mV/sec.

A	B	C
abs.	984	abs.
v. weak	v. weak	1014
1058 int	1064int	1078
1186	1190	1184 w
abs.	abs.	1236
1280	1286 int.	abs.
1476	1480	1472
1602	1612	1600

Table1 SERS bands of polymerized and unpolymerized TAPP

- A SERS bands for TAPP electropolymerized from an acetonitrile solution
- B SERS bands for TAPP electropolymerized from a HCl solution
- C SERS bands for TAPP on a roughened Ag electrode

MODE	IP	IP+	NP	IP.+
C - N str.	1221	abs.	abs.	abs.
C - N + str.	abs.	1239	abs.	abs.
C - N.+ str.	abs.	abs.	abs.	1344
C = N str	abs.	abs.	1471	abs.

Table 2 Characteristic frequencies in wave numbers for the bands of the four unit structures of polyaniline.

From I. Harada, Y. Furukawa and F. Ueda
 Synthetic Metals 29 E303 1989

CHAPTER FIVE

THE EFFECT OF pH, ELECTRODE POTENTIAL AND SOLVENT
POLARITY ON THE ORIENTATION OF ADSORBED NAD

5.1 ABSTRACT

The surface enhanced Raman scattering (SERS) spectra of nicotinamide adenine dinucleotide (NAD) at different pH values and electrode potential were investigated at a silver electrode. Good quality spectra are reported at an excitation frequency of 488 nm. NAD adsorbs spontaneously on the electrode at all of the pH values studied. The molecule desorbs before its reduction potential at - 1.2 V and as a result, the spectrum of the reduced form of the molecule is not observed.

The SERS spectra show that the manner of adsorption of NAD differs depending on the conformation of the molecule in solution. At physiological pH values NAD adsorbs on the silver electrode through the external amino group on carbon 6 and through nitrogen 7 on the imidazole ring. When the solvent is changed to methanol, NAD adsorbs in a side-on orientation through nitrogen 3 of the adenine part of the molecule. The ribose and phosphate parts of the molecule are also involved in adsorption.

The applicability of SERS as a technique for investigating the orientation of adsorbed molecules possessing multiple locations for adsorbate-surface bonding is established.

5.2 INTRODUCTION

Since the discovery of its role in electron transfer in biological systems^{1,2}, nicotinamide adenine dinucleotide, NAD, has been the subject of intense scientific investigation. Biochemists have studied its biosynthesis^{3,4} and catalytic activity^{5,6,7}. Its orientation in solution has been investigated using fluorescence⁸⁻¹⁰ and NMR techniques^{11,12}. Electrochemists^{13,14} have

investigated its oxidation reduction characteristics in an attempt to explain its biological activity.

In living systems NAD/ NADH normally binds to a protein prior to the transfer of an electron or proton. This realization has led to studies of the orientation of NAD at an electrode interface, with the hope that the NAD/ protein conformation could be mimicked at the electrode solution interface.

Since its discovery by Fleischmann *et.al.*¹⁵ one of the applications of SERS has been in the determination of the orientation of adsorbates at an electrode surface, mainly silver and gold electrodes¹⁶⁻¹⁹. Although the information on orientation that is provided by SERS is of a qualitative nature, when it is combined with the information obtained from other techniques, it can give a very detailed picture of molecular orientation.

Taniguchi²⁰ studied the SERS of NAD adsorbed on a silver and gold electrode. He concluded that NAD was adsorbed via the adenine group with the adenine ring perpendicular to the electrode surface. In the reported spectra only two bands were observed, at 735 cm^{-1} and 1330 cm^{-1} . A study of NAD on silver sols²¹ revealed more detailed spectra with vibrations assigned to the phosphate, ribose and nicotinamide portions of the NAD molecule being observed. The poor sensitivities of the spectra obtained on a solid electrode led us to re-examine the SERS of NAD on a silver electrode.

In this study we present well resolved, intense spectra of NAD adsorbed on a silver electrode. We have studied the effect of pH on the orientation and conformation of adsorbed NAD. Also we have investigated the effects of *in-situ* vs *ex-situ* ORC and the effect of the number of *in-situ* oxidation reduction cycles on the SERS spectra. Finally we examined the effect of solvent polarity on the conformation of adsorbed NAD. We establish that at pH values close to physiological pH, NAD retains its solution conformation when it is

adsorbed on a silver electrode. The interaction between the adsorbed NAD and the electrode surface is via the adenine group. When the solvent is changed to a mixture of methanol and water, the NAD is adsorbed in the extended conformation.

5.3 EXPERIMENTAL

Nicotinamide Adenine Dinucleotide (NAD) Grade IIIc was purchased from Sigma Chemical Company and used without further purification. 1×10^{-3} M solutions were used. Buffer solutions of differing pH values were prepared by combining varying volumes of 0.15 M solutions of disodium hydrogen phosphate and potassium hydrogen phosphate. Solutions were deaerated by bubbling purified grade nitrogen for 20 to 30 minutes. Solutions were prepared on the same day of the experiment.

The oxidation reduction cycle(ORC) was carried out in the buffered solution containing the sample and consisted of a two second potential pulse from 0.0V to +0.3V. The electrochemical potential was controlled by a Princeton Applied Research model 175 Universal Programmer and model 173 Potentiostat /Galvanostat. The sample cell consisted of a silver working electrode with ca. 1.6 mm^2 surface area, a platinum counter electrode and a saturated calomel electrode(SCE) as the reference. All potentials reported in this chapter are quoted vs the SCE.

Prior to pretreatment the silver electrode was polished with a slurry of $0.03 \mu\text{m}$ alumina powder and sonicated in distilled water.

488 nm laser excitation was used as the excitation source and this was provided by a Spectra Physics 164 Argon ion Laser. The laser power at the electrode surface was approximately 60mW. The SERS spectra were recorded on a Spex 1401 scanning double monochromator. The spectra presented here

were obtained by photon counting detection with an accumulation time of 0.6s/cm⁻¹. The intensities were recorded digitally and are presented unsmoothed.

5.4 RESULTS AND DISCUSSION

a) SERS of N-methyl Nicotinamide

Fig.1a shows the structure of NAD in the extended conformation along with the labelling of the atoms that comprise the molecule. Fig.1b shows the structure of nicotinamide and Fig.1c the structure of adenine. The SERS spectrum of N methyl nicotinamide(NMN) on a silver electrode at pH 11.3 is presented in Fig.2, while Fig.3 shows the structure of N-methyl nicotinamide.

Although the SERS spectra of NMN has been reported in the literature ²², we have for comparison purposes measured the spectra under the conditions of our experiment, Fig.2. The most intense modes in the NMN spectra occur at 1032 cm⁻¹ and 1634 cm⁻¹. These are assigned to the ring breathing mode(1032 cm⁻¹) and to the carbonyl stretching mode of the carboxy amide(1634 cm⁻¹). Weaker bands are also observed in the SERS spectra at 682, 732, 1178, 1234, 1420, 1548 and 1584 cm⁻¹. The strong bands at 1634 and 1032 cm⁻¹ are characteristic of a flat orientation of the nicotinamide ring. The NMN SERS spectra obtained in this study have intense bands at 1032 and 1634 cm⁻¹ indicating that at pH 11.3, NMN is adsorbed flat on to the electrode surface .

b) SERS of NAD

Fig.4 is the potential dependent SERS spectra of NAD in phosphate buffer at pH 7.4 in the potential range from -0.2V to -0.8V on a roughened silver electrode. The potential dependent spectra were obtained at potential steps of -0.2 V starting at 0.0V. No SERS spectra were obtained at potentials more negative than -0.8V.

A comparison of our spectra with those reported by Taniguchi²⁰ under similar experimental conditions shows that in addition to bands at 736 cm^{-1} and 1336 cm^{-1} observed in both spectra, the spectra obtained at pH 7.4 contain peaks at 756 , 1220 , 1370 , 1424 , 1456 , 1582 , and 1618 cm^{-1} which were not observed by Taniguchi²¹ in his study of NAD adsorbed on a silver electrode. The differences in the spectra are related to the methods by which they were acquired. The spectra reported by Taniguchi were obtained by signal averaging while the spectra presented in this chapter were obtained from a single scan and were not averaged.

Table 1 lists the vibrational assignments for the NAD molecule. Most of the bands observed in the spectra are characteristic of the adenine part of the molecule. The 736 cm^{-1} band is the adenine ring breathing mode and the 1336 cm^{-1} band the imidazole, N7 - C5 vibration. Both of these bands have been reported by Taniguchi²⁰. The 1370 cm^{-1} band and 1618 cm^{-1} band are also assigned to the adenine group. The 1370 cm^{-1} band being the adenine ring δ C2-H vibration and the 1618 cm^{-1} the external amino scissors vibration. The weak band at 1500 cm^{-1} is observed at 1493 cm^{-1} in the SERS spectra of NAD on colloids. It is assigned as a C6 - amino vibration.

The spectrum also shows a band at 1582 cm^{-1} whose intensity increases as the potential is made more negative. Examination of Fig.2, the SERS of NMN, shows a band at 1584 cm^{-1} . We assign the 1582 cm^{-1} vibration in the

NAD spectrum to the nicotinamide portion of the molecule. No other vibrations characteristic of the nicotinamide group are observed in the spectra. This 1582 cm^{-1} vibration has not been observed in other SERS studies of NAD^{20,21}.

In Fig.4 along with the band at 736 cm^{-1} is found another band at 756 cm^{-1} . The intensity of this 756 cm^{-1} band decreases as the potential is made more negative. This 756 cm^{-1} band has been assigned as a ribose sugar vibration²¹. It provides information on the conformation of the ribose ring and indicates the presence of both C2 endo and C3 endo adenine ribose conformations. The plane of the sugar molecule is defined by C1- O - C4 all being horizontal (Fig.1a). Atoms lying above this plane are in the endo conformation. The C2 and C3 endo conformation result in a puckering of the ribose ring. This ribose arrangement of both C2 and C3 endo has been shown to exist when NAD is bound to some enzyme systems²³.

The reduction in intensity of the 756 cm^{-1} band with potential suggests that a single conformation becomes dominant in NAD as the potential is made more negative. Crystallographic analysis²⁴ of the lithium salt of NAD confirms puckering of the ribose groups in NAD, with the adenosine ribose displaying a C-2 endo conformation whilst the nicotinamide ribose is in the C3 endo and C2 exo twisted form.

In Fig.5 the SERS spectra of NAD at pH 6.4, in the potential range from 0.0V to -0.3V are displayed. No spectra were obtained at potentials more negative than - 0.3 V . The spectra obtained at pH7.4, Fig.4 and pH 6.4, Fig.5 show similar peaks at about 736 cm^{-1} , 756 cm^{-1} 1338 cm^{-1} , 1372 cm^{-1} , 1582 cm^{-1} and 1618 cm^{-1} . A band at 592 cm^{-1} which is very weak at pH 7.4, increases in intensity at pH 6.4. Fig.5 shows two poorly resolved peaks at 1074 and 1092 cm^{-1} . At pH 7.4 only the 1064 cm^{-1} peak is present and it is much weaker than at pH 6.4. The 1092 peak is assigned as the pyrophosphate PO_2 mode. Another

mode the phosphodiester P - O - P, has been observed at 800 cm^{-1} in sols²¹. This vibration has not been observed in our spectra.

The ratio of the intensities of the phosphodiester vibration to the phosphate vibration has been used to determine whether or not there is an ordered structure around the pyrophosphate linkage^{25,26}. When this ratio is equal to zero it indicates disorder in the rotational conformation.

Absent from the SERS spectra of NAD at pH 7.4 and 6.4 are vibrations in the $900 - 1000\text{ cm}^{-1}$ region of the spectra which are due to the ribose part of the molecule.

Fig.6 represents the potential dependent SERS spectra of NAD at pH 5.3. The spectra obtained at pH 5.3 show differences when compared to the spectra obtained at pH 6.4 and 7.4. The 736 cm^{-1} band is absent at pH 5.3. Instead an intense band is found at 748 cm^{-1} . As the potential is shifted to more negative values the 748 cm^{-1} band is reduced in intensity whilst a band at 760 cm^{-1} increases in intensity. Bands at 1338 cm^{-1} , 1370 cm^{-1} , 1586 cm^{-1} , and 1616 cm^{-1} are observed at pH 5.3 just as they are observed at pH 7.4 and 6.4

At pH 5.3 bands are also observed at 1278 cm^{-1} , 1338 cm^{-1} , 1470 cm^{-1} , and 1560 cm^{-1} . The 1278 cm^{-1} band has been assigned as an adenine ring vibration, $\delta\text{C8} - \text{H}$, whilst the 1328 cm^{-1} could be equivalent to the very weak 1346 cm^{-1} vibration seen in sols and assigned as an adenine vibration. The spectra also show a vibration at 1068 cm^{-1} which increases in intensity as the potential is made more negative. A very weak 1030 cm^{-1} ribose vibration is also observed in the spectra.

Fig.7 shows the SERS spectra of NAD at pH 3.5 over the potential range 0.0V to -0.4V. No spectra were obtained at potentials more negative than -0.4 V.

This is due to the acidity of the solvent resulting in hydrogen gas being evolved at -0.4V . The spectra at pH 3.4 is similar to those obtained at other pH values.

In the potential dependent spectra at pH 3.5 a number of bands show changes in intensity as the potential is changed from 0.0 to -0.2 V . The 760 cm^{-1} band shows a large decrease in intensity while bands at 736, 1328 and 1612 cm^{-1} all show large increases in intensity. The intensity of the 1076 cm^{-1} band also increases as the potential is made more negative, while the reverse is observed for the 1094 cm^{-1} band.

c) Conformation of NAD in solution

In solution NAD exists in two main structural forms: an extended form (Fig.8a) and a stacked form (Fig.8b). In the extended form the nicotinamide and the adenine rings are approximately 13 \AA apart and are at right angles to each other, whilst in the stacked form the rings are parallel to each other and separated by 3 \AA with the nicotinamide ring covering the adenine part of the molecule rather than the imidazole part.

Two stacked conformations have also been identified, one with the adenine on top of the nicotinamide and the other with the nicotinamide on top of the adenine. Proton NMR²⁷ studies have shown that the favoured conformation is the one with the pyridine ring above the plane of the adenine ring.

At pH 7.0 NAD exists in the folded form in solution (Fig.8b). As the acidity of the solution is increased there is a decrease in the interaction between the nicotinamide and adenine bases. Protonation of the adenine at N1 occurs with decreasing pH. The pK for the protonation of the N1 is 4²⁸. Therefore at pH values lower than pH 4 there is a positive charge on the adenine ring. This increase in electrostatic interaction causes a decrease in the interaction

between the two rings. Lowering the pH does not totally abolish the interaction holding the two rings together. Only on heating at pH 8 does the molecule unfold²⁸. Therefore for the experiments in aqueous solution in the pH range covered in this study, NAD in solution is in the stacked form.

d) CONFORMATION OF ADSORBED NAD

There are three sites on the NAD molecule which are capable of metal binding; the phosphate oxygens, the sugar alcohol oxygen and the adenine ring and amino nitrogen. These three sites are therefore ideal for the direct chemisorption of NAD to the silver surface.

The adsorption of adenine on a silver surface has received considerable attention. Otto²⁹ has shown using a number of substituted derivatives of adenine that the external amino group participates in the surface binding process. The ability of the amino group to act as a Lewis acid has been used to explain the orientation of adenine. Otto²⁹ concluded that when adenine is adsorbed onto a silver electrode it is not adsorbed parallel to the surface but perpendicular to it. Other studies³⁰ have proposed a number of orientations from a parallel arrangement to a side on arrangement with adenine and silver interacting through the N7 of the imidazole group. Watanabe³¹ came to the conclusion that adenine was oriented perpendicular to the surface when he observed peaks at 1330 cm^{-1} assigned to the N7 - C5 vibration, and at 736 cm^{-1} for the adenine ring breathing mode. Moskovits³², using surface selection rules, concluded that a high intensity of the 736 cm^{-1} band would be expected only when the ring is standing up or tilted with respect to the surface.

Except for the spectra obtained at pH 5.3, Fig.6, all the other spectra show peaks at 736 and 1330 cm^{-1} . The peak at 1618 cm^{-1} assigned as an amino vibration, has its equivalent in solution at 1548 cm^{-1} . This downshift of 30

cm^{-1} is indicative of an interaction between the amino group and the silver surface. The band at about 1338 cm^{-1} is due to an imidazole vibration, the N7 - C5 vibration. This suggests bonding between the adenine part of the NAD molecule and the silver surface. It also establishes that the adenine group has a side on orientation with interaction occurring between the external amino group, N7 - C5, of the imidazole ring and the silver surface. It has been shown³⁴ that the preferred point of binding between adenine and metals, e.g. Co^{2+} and Ca^{2+} is through the N7 of the heterocycle. Experiments with NAD in sols²¹ have shown a band at 1137 cm^{-1} which is associated with the N1-C2-N3 stretching mode. This suggests a side on orientation of adenine with bonding through N3. In the pH range studied in this chapter the 1137 cm^{-1} band is absent, indicating that binding was not through the N3.

The vibration at about 1584 cm^{-1} is the only vibration characteristic of nicotinamide, that is observed in the spectra at any of the pH values studied. The absence of the two strong NMN bands at 1032 and 1634 cm^{-1} which are characteristic of a flat nicotinamide orientation, along with the presence of the 1584 cm^{-1} band provides information regarding the orientation of the nicotinamide group. The absence of the 1032 cm^{-1} and 1634 cm^{-1} vibrations can be due to either the nicotinamide part of the molecule being too far away from the surface to have its vibrations enhanced, or, that the orientation of the nicotinamide is such that its intense vibrations are reduced because of surface selection rules.

Other workers^{21,34} have obtained SERS spectra of nicotinamide in which the bands around 1030 cm^{-1} and the 1680 cm^{-1} have been absent from the spectra. As a result there exists some doubt as to the significance of the presence or absence of these bands. Assuming that when NAD adsorbs on the surface the conformation of the adsorbed molecule is the same as in solution

then it adsorbs in the folded conformation. Studies using molecular models indicate that when NAD adsorbs in the folded conformation if the adenine moiety is adsorbed in a side on orientation then the nicotinamide group must also be side on. The presence of the 1582 cm^{-1} vibration is evidence of this side on orientation.

Other SERS studies^{20,21} of adsorbed NAD have only speculated at a perpendicular orientation for the nicotinamide part of the molecule. The absence of the vibrations characteristic of a flatly orientated nicotinamide group along with the presence of the 1582 cm^{-1} band confirms a perpendicular orientation of the nicotinamide group of the adsorbed NAD molecule and indicates that when NAD is adsorbed onto the silver electrode at the pH values used in this study the molecule retains its solution conformation .

Figures 4,5,6 and 7 all show an intense vibration around 1370 cm^{-1} which is assigned as an adenine ring vibration and a δ adenine C2 - H. This vibration is observed in the SERS spectra of adenosine when the potential is changed from -0.6V to 0.2V and also in the SERS spectra on sols³⁵ where it is observed at 1363 cm^{-1} . According to SERS selection rules, the 1370 cm^{-1} band is indicative of a flat orientation of adenine on the electrode surface. This 1370 cm^{-1} should also be accompanied by vibrations at 1163 , 1238 , 1304 , 1379 , 1417 and 1476 cm^{-1} which are all enhanced when adenine is lying flat on the surface. The absence of these vibrations along with the presence of the 1338 and 736 cm^{-1} vibrations all rule out a possible flat orientation and tend to support a side on orientation. It is possible that the 1370 cm^{-1} band is incorrectly assigned.

e) Effect of potential on the SERS spectra of NAD

For the potential dependent SERS studies of NAD at pH values of 7.4, 6.4 and 5.3, no significant changes are observed in the frequencies of the bands as a function of potential. Only a reduction in the intensity of the 756 cm^{-1} peak and an increase in the intensity of the 736 cm^{-1} peak is observed.

Fig.7 is the potential dependent SERS spectra for NAD at pH 3.4. A number of potential dependent changes are observed in the spectra. These changes occur when the potential is changed from 0.0V to -0.2V. The relative intensities of the bands at 736 cm^{-1} , 1332 cm^{-1} and 1612 cm^{-1} all increase whilst the bands at 530 cm^{-1} , 592 cm^{-1} and 760 cm^{-1} all decrease in intensity. At -0.4 V a new band is observed at 1344 cm^{-1} .

Watanbe³¹ studied the effect of the electrode potential on the SERS spectra of adenine, adenosine and adenosine monophosphate. He observed that at potentials more positive than -0.2V the 736 cm^{-1} mode showed a large decrease in intensity. He also observed new peaks at 680 cm^{-1} and 1380 cm^{-1} . For adenosine monophosphate the changes were less pronounced than for adenosine. These changes were attributed to a change in the orientation of adenine from a parallel orientation to a side on orientation.

The bands that show a reduction in intensity at potentials more positive than -0.2V are the bands at 736 cm^{-1} , 1328 cm^{-1} and 1614 cm^{-1} . These bands are all associated with a side on orientation of adenine. The changes observed here are similar to those shown by adenosine monophosphate³¹ and are related to a change in the conformation of the adsorbed adenine moiety. It appears that at potentials more negative than -0.2 V, NAD is attached to the surface side on through the amino group and the imidazole N7 as evidence by the intensity of the peaks at 736 cm^{-1} , 1324 cm^{-1} and 1612 cm^{-1} . At potentials more positive than -0.2 V the spectra do not provide enough data to

unequivocally conclude that adenine is now flat on the surface, but it suggests that adenine has an orientation between flat and perpendicular. The conclusion from these spectral changes is that at - 0.2 V there is a change of orientation by the adenine part of the molecule, and it adopts a perpendicular orientation at more negative potentials .

f) SERS SPECTRA OF NAD IN METHANOL/WATER

1) Comparison of the *in situ* vs *ex situ* spectra

The solutions of NAD in methanol/water were prepared by dissolving the NAD in as little water as possible (less than 5 ml) and then making the volume up to the required level of 25ml, by adding methanol. The solutions contained 80 - 90 % methanol. 0.1M KCl was used as the electrolyte and the solutions were deaerated by bubbling with nitrogen for twenty to thirty minutes. An examination of the spectra, Fig.9 , obtained by *in situ* and *ex situ* ORC, shows that in peak frequencies and relative intensities, the spectra are similar.

The spectra obtained from a silver electrode roughened *in situ* are approximately 10 times as intense as those obtained from the *ex situ* roughened electrode. This increase in intensity of the SERS spectra obtained from an electrode roughened *in situ* is expected and has been observed for other compounds e.g. porphyrins. The absence of any new bands in the spectrum obtained by *in situ* roughening indicates that the roughening process does not result in the electrochemical degradation of the compound nor does it result in a trapped adsorbate having an orientation strikingly different from that of the species physically adsorbed onto the surface. The SERS spectra of NAD dissolved in methanol were 50 to 100 times as intense as those obtained from aqueous solutions.

II) Orientation of Adsorbed NAD

It has been shown by Catteral²⁷ that on going to a methanol-water mixture, the dinucleotide NAD unfolds in solution and exists in the extended conformation. Other workers have suggested that both the folded and unfolded conformations exist, but that in a water- methanol mixture the ratio of the unfolded to folded increases. On the basis of the work by Catteral²⁷ we conclude that in a methanol solution NAD exists in the extended conformation .

Fig.8a shows the structure and orientation of NAD in the extended conformation. A comparison of the SERS of NAD in methanol against that of NAD in water should lead to important information on the effect of solvent polarity on the conformation of adsorbed NAD .

Table 2 lists the SERS peak frequencies and their assignments for NAD in methanol. The spectra of NAD in methanol, Fig.9 , contain bands at 846 cm^{-1} , 964 cm^{-1} , 1006 cm^{-1} , 1022 cm^{-1} and 1202 cm^{-1} . The phosphate vibration is observed at 846 cm^{-1} whilst a peak at 1022 cm^{-1} is assigned as due to the adenine part of the molecule. Peaks at 1140 cm^{-1} , 1262 cm^{-1} , 1310 cm^{-1} and 1624 cm^{-1} have been assigned to adenine ring vibrations. The pair of peaks at 678 and 702 cm^{-1} have been assigned as an adenine ring vibration and a sugar vibration respectively.

III) Adenine Vibrations

The 1140 cm^{-1} , 1262 cm^{-1} , 1310 cm^{-1} , and 1624 cm^{-1} vibrations have all been assigned as due to the adenine part of the molecule²¹. The 1140 cm^{-1} band has been assigned as a N1-C2-N3 stretching mode(Fig.1). It is observed at 1137

cm^{-1} in the SERS spectra of NAD on sols²¹ and it is an in plane mode. It is not the usually intense vibration of adenine or its derivatives in aqueous solution.

The 1022 cm^{-1} vibration indicates a side on adenine orientation. The 1262 cm^{-1} is the C8-H and the 1624 cm^{-1} is the adenine amino rock. Both the 1140 and the 1022 cm^{-1} bands suggest a side on adenine orientation with bonding through N3 to the silver electrode²¹. The 1624 cm^{-1} and 1262 cm^{-1} bands suggest interaction between the surface and the external amino group. The 1624 cm^{-1} band has its counterpart in solution at 1648 and at pH 7 this band is observed at 1618 cm^{-1} . This difference in downshift, 30 cm^{-1} in water and 24 cm^{-1} in methanol indicate differences in the degrees of affinity between the amino group and the surface in the different solvents.

Iv) Sugar Vibrations

The bands at 964 , 1006 and 1202 cm^{-1} have been assigned as sugar vibrations²¹. Their presence indicates, that in the extended conformation, the geometry of the adsorbed NAD molecule is such that interactions between the hydroxyl groups of the ribose parts of NAD and the silver surface are possible.

The P-O-P vibration is found at 846 cm^{-1} . A very weak band is observed at 1080 cm^{-1} and this is assigned as PO_2 vibration. The intensity ratio (P-O-P/ PO_2) provides information on the ordered structure about the pyrophosphate linkage. In the spectra presented here, Fig.9, this intensity ratio is larger than 500 and suggests that there is an ordered structure about the pyrophosphate linkage.

Absent from the SERS spectra are vibrations due to the nicotinamide part of the molecule which are observed around 1582 cm^{-1} in the aqueous spectra. When NAD adsorbs onto a silver electrode in the extended conformation, the nicotinamide part of the NAD molecule may be too far away from the surface to have its vibrational modes enhanced.

We therefore conclude that when NAD adsorbs on to a silver surface from a methanol/water solution it is adsorbed in the extended conformation. The P-O-P, sugar and adenine parts of the molecule interact with the surface whilst the nicotinamide part of the molecule is far away from the surface. This arrangement is similar to that observed for NAD bound to dehydrogenase. When NAD is bound to an enzyme, it adopts the extended conformation with the sugar and pyrophosphate groups bound to the amino acid side chains of the protein and the adenosine group inserted into a hydrophobic pocket of the protein.

The bonding geometry suggested here would require that NAD have the orientations shown in Fig.8a. Adsorption would be via the adenylic acid portion of the molecule with the nicotinamide 5 ribonucleotide part directed away from the surface. This would account for the absence of any signal from the nicotinamide moiety.

g) Effect of the number of ORC cycles on the SERS of NAD

In these experiments *in situ* ORC was performed. The number and duration of the electrochemical pulses used in the ORC were altered and the effect on the SERS spectra observed. The pulses were all from 0.0 V to +0.3 V and back to 0.0V. Fig.10 shows the number and duration of applied pulses as well as the corresponding spectra. The spectra were obtained in phosphate buffer at pH 7.4. In all of the spectra the frequencies of the main bands are independent of the number of applied ORC cycles. In the 700 - 1600 cm^{-1} region of the spectra, only the relative intensities of the bands increase with the number of oxidation reduction cycles.

The most intense spectrum in Fig. 10 was obtained using four two second pulses. The 1372 band in this spectrum is extremely intense. The increase in intensity of the 1100 cm^{-1} band with increasing number of ORC is the most striking feature in the 700-1600 cm^{-1} region. An examination of the low frequency region of the spectrum, from 300 to 700 cm^{-1} shows more significant changes. All these spectra show peaks at 530 and 590 cm^{-1} , although these peaks show increasing intensity as the number of ORC is increased. The band at 420 cm^{-1} behaves similar to those at 530 and 590 cm^{-1} . The main differences between the spectra in the low frequency region is the presence of a peak of medium intensity at 348 cm^{-1} in Fig.10.

Studies³⁵ on the effect of *in situ* ORC on the SERS vibrational frequencies have shown that only after 15 to 20 ORC cycles were there differences in the SERS spectrum and that these changes were minor. The main conclusion from these experiments was that for competitive adsorption studies *ex situ* ORC should be the pretreatment of choice .

Fig.10 shows that when the number of *in situ* oxidation reduction cycles is less than six the only change observed in the spectra are changes in intensity of the bands. When the number of ORC pulses is increased to 6 changes in the SERS spectra are observed. We have assigned the 1100 cm^{-1} band to a phosphate PO_2 vibration. The 348 cm^{-1} band is unassigned. Whilst we are unable to interpret the two new bands in detail, we believe them to originate either from trapping of the adsorbate or from complexation of silver with NAD during the ORC to form a Ag/NAD complex . NAD has been shown³⁹ to complex with Li^+ to form a dimer with Li positioned between two adenine groups possibly attached to N7 . We suggest that the 348 cm^{-1} band might represent the NAD - Ag - NAD vibration of the dimer .

5.5 CONCLUSION

We have presented a complete study of the effect of pH, electrode potential and solvent polarity on the orientation of NAD adsorbed on a silver electrode. Our results show that in aqueous solution at pH values close to physiological pH, NAD adsorbs onto the electrode by the adenine group in a side on arrangement through the external amino group and the N7 of the imidazole ring. The nicotinamide group is also bound to the surface side on. The ribose and pyrophosphate groups are directed away from the surface and no appreciable SERS signal is observed for them. At pH 3.4 protonation of N1 of the adenine group occurs. This results in a change in the orientation of NAD at potentials more positive than - 0.2 V. At - 0.2 V the molecule is adsorbed with the same orientation as at other pH values. In methanolic solution NAD exists in the extended conformation and is adsorbed with the pyrophosphate, adenine and sugar groups in contact with the silver electrode and the nicotinamide group far from the surface. In this conformation NAD mimics the orientation that it adopts when it binds to the dehydrogenases and acts as a biological catalyst. The very intense signal which is detected for NAD adsorbed from a methanol/water solution allows for an analytical application of this technique which should be capable of detecting 10^{-6} to 10^{-8} M NAD in a water methanol environment. This high sensitivity should allow for the application of SERS in the detection of low concentrations of NAD.

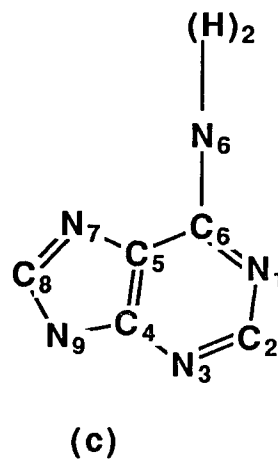
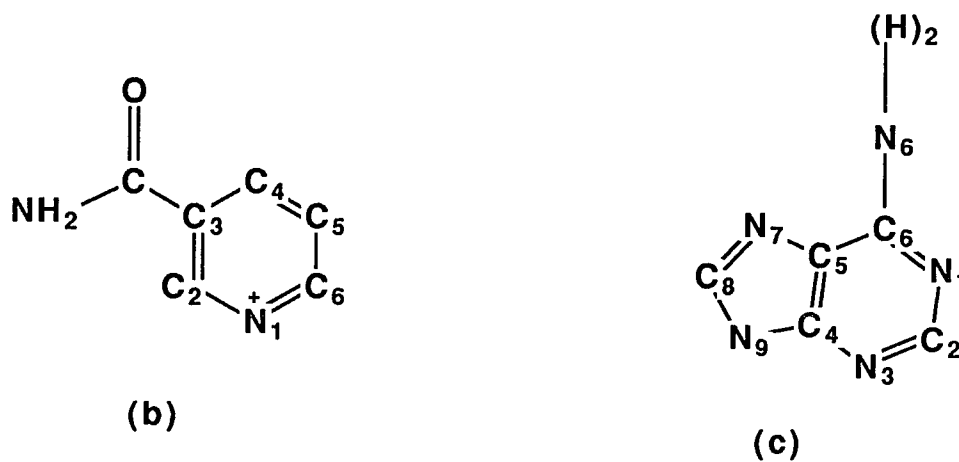
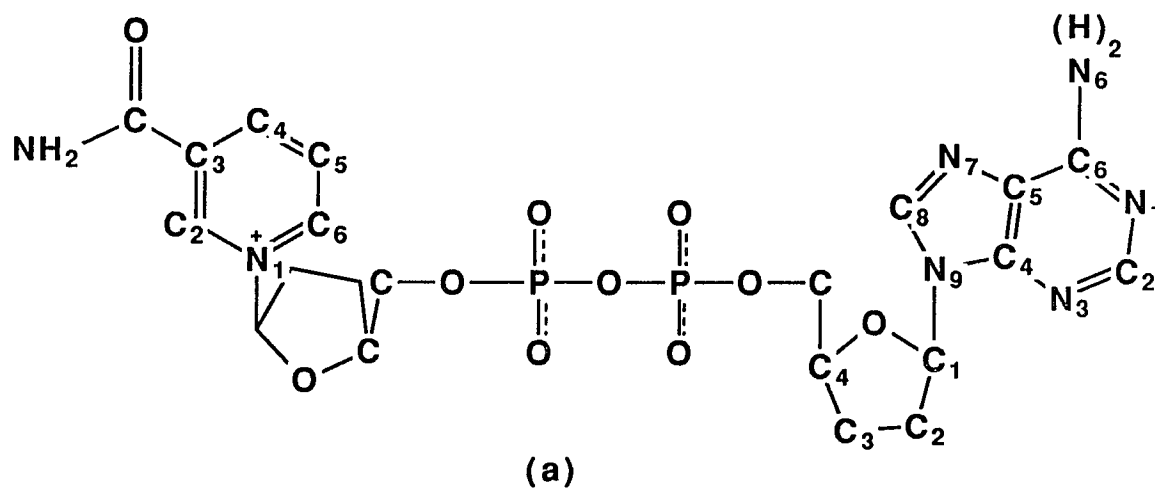


Fig.1 Diagram to show the structure of NAD (a) NAD (b) Nicotinamide part of the molecule and (c) adenine part of the molecule . Ribose carbons contain hydrogen and hydroxy groups to satisfy valence requirements.

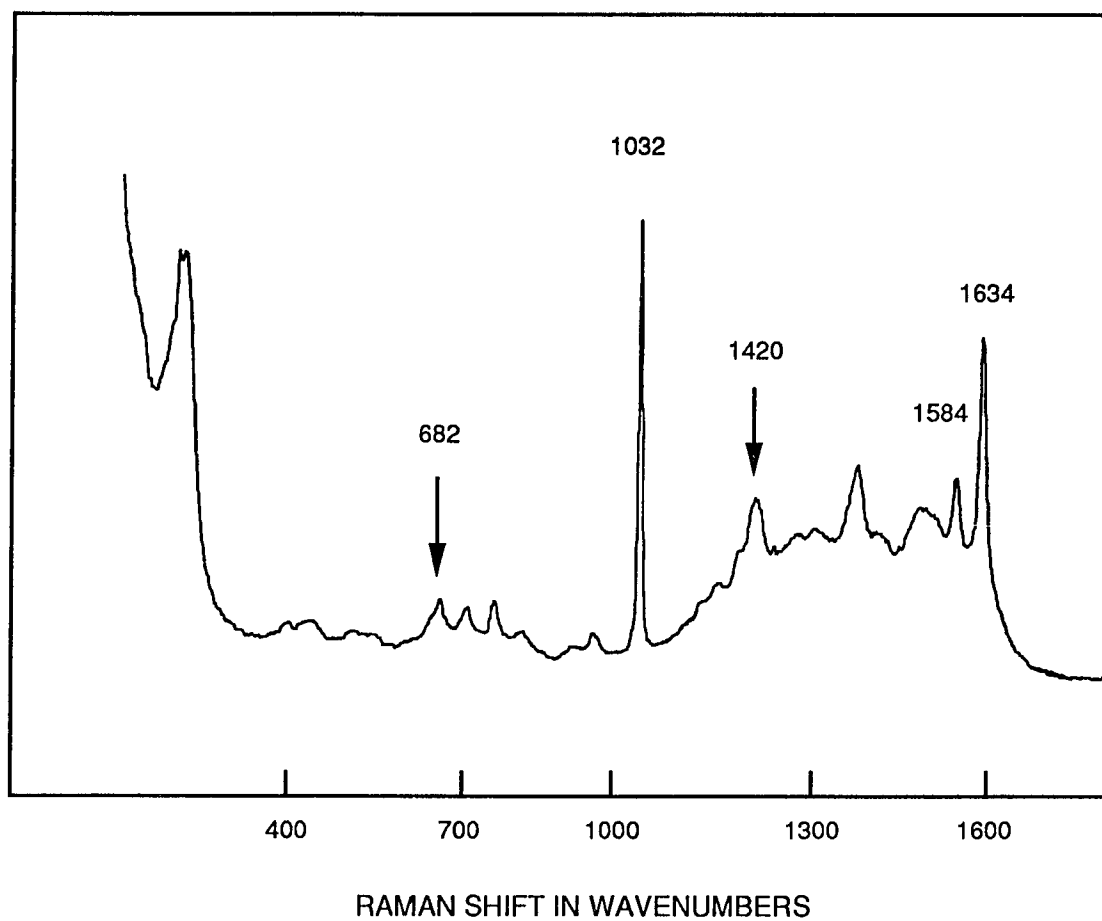


Fig.2 SERS of N methyl nicotinamide on a silver electrode with 488 nm laser excitation at pH11.3

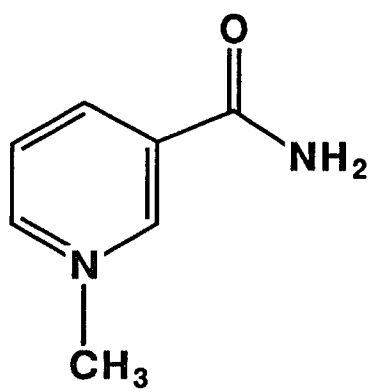


Fig.3 Structure of N-methyl nicotinamide

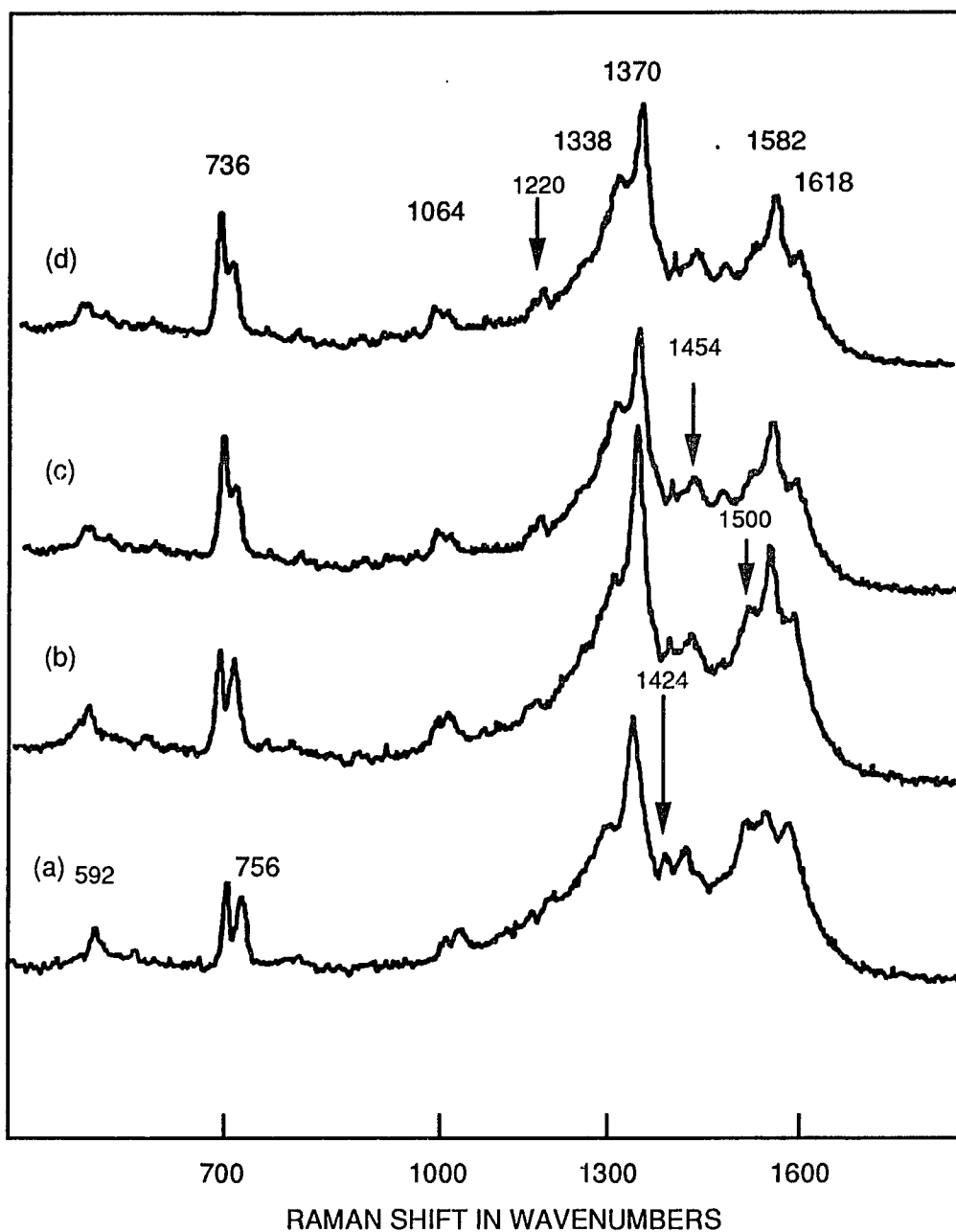


Fig.4 SERS of NAD on a silver electrode with 488 nm laser excitation at pH 7.4 (a) -0.2V (b) -0.4V (c) -0.6V and (d) -0.8V

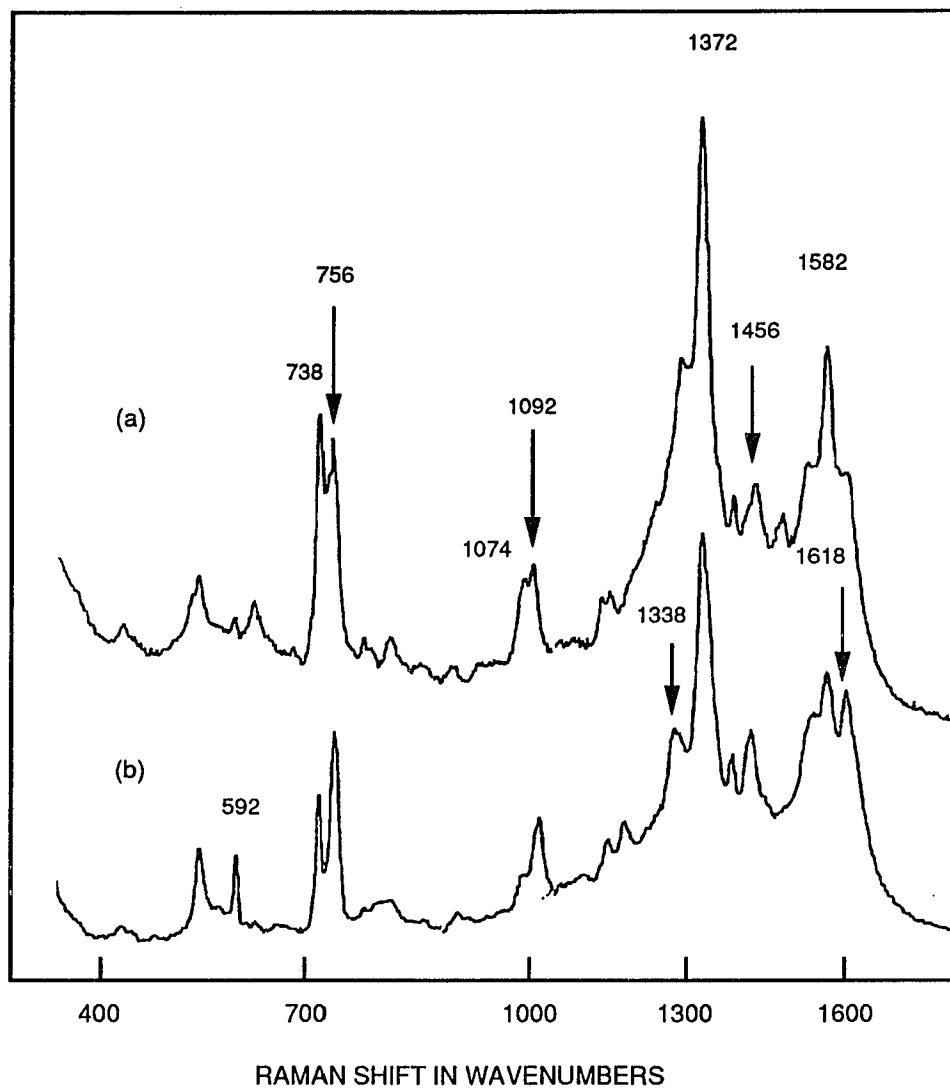


Fig.5 SERS of NAD adsorbed on a Ag electrode at pH 6.4 with 488 nm laser excitation . (a) at 0.0 V and (b) at -0.3 V

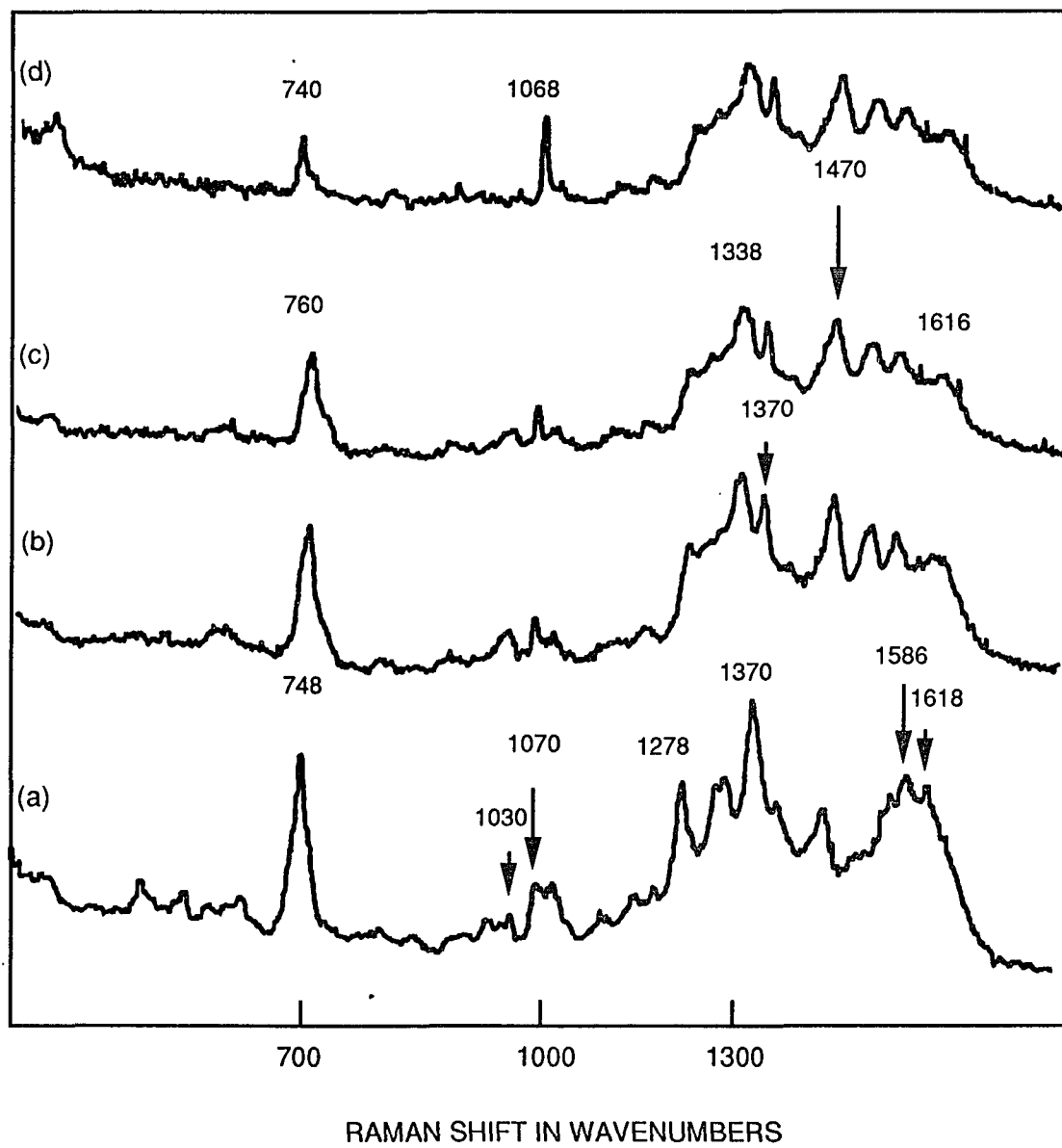


Fig.6 SERS of NAD on a silver electrode with 488 nm laser excitation at pH 5.3
(a) - 0.2V (b) - 0.4V (c) - 0.6V and (d) - 0.8V

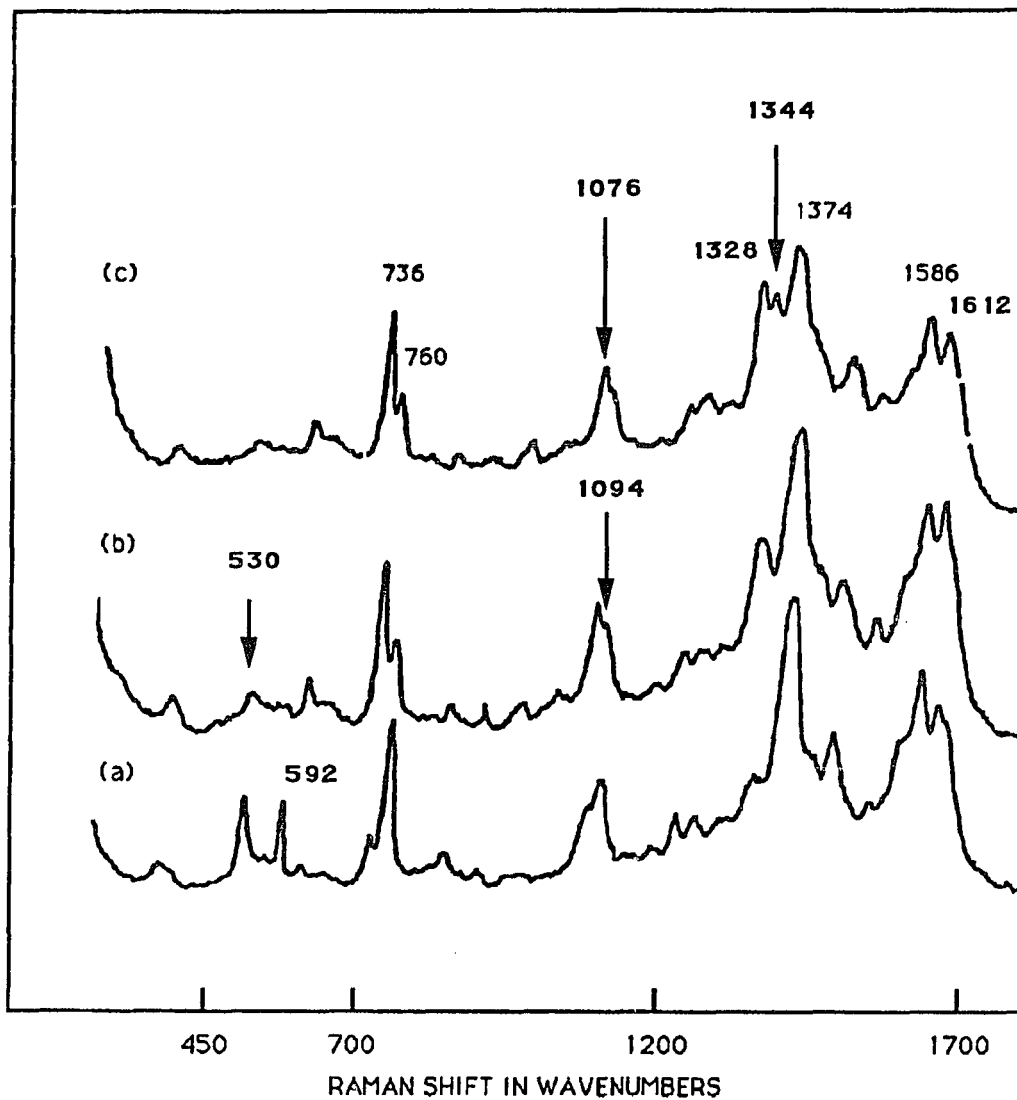


Fig. 7
SERS spectra of NAD on a silver electrode with 488 nm laser excitation, at pH 3.5
(a) at 0.0 V (b) at - 0.2 V and (c) at - 0.4 V.

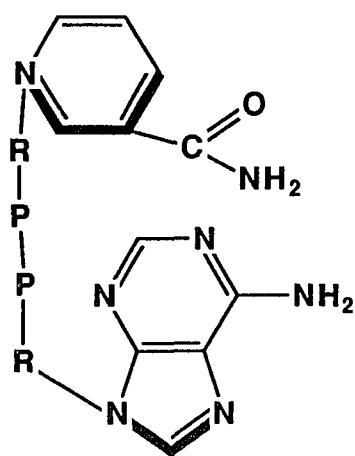
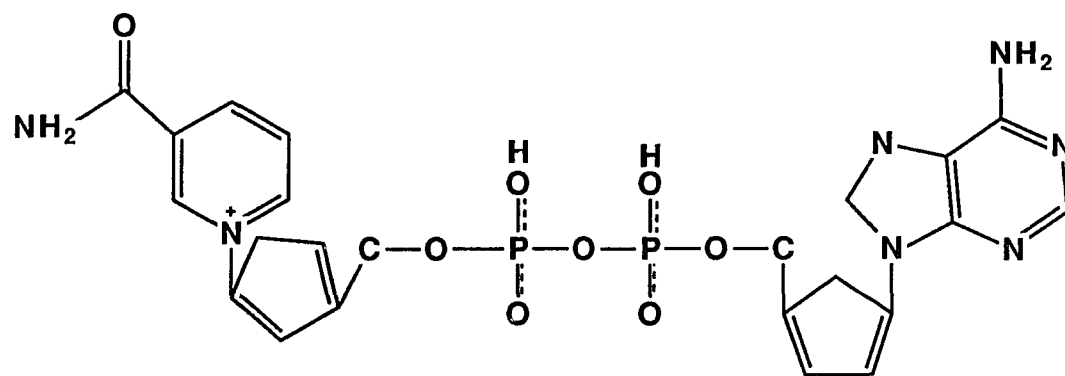


Fig.8 Conformation of NAD (a) the extended conformation and (b) the folded conformation

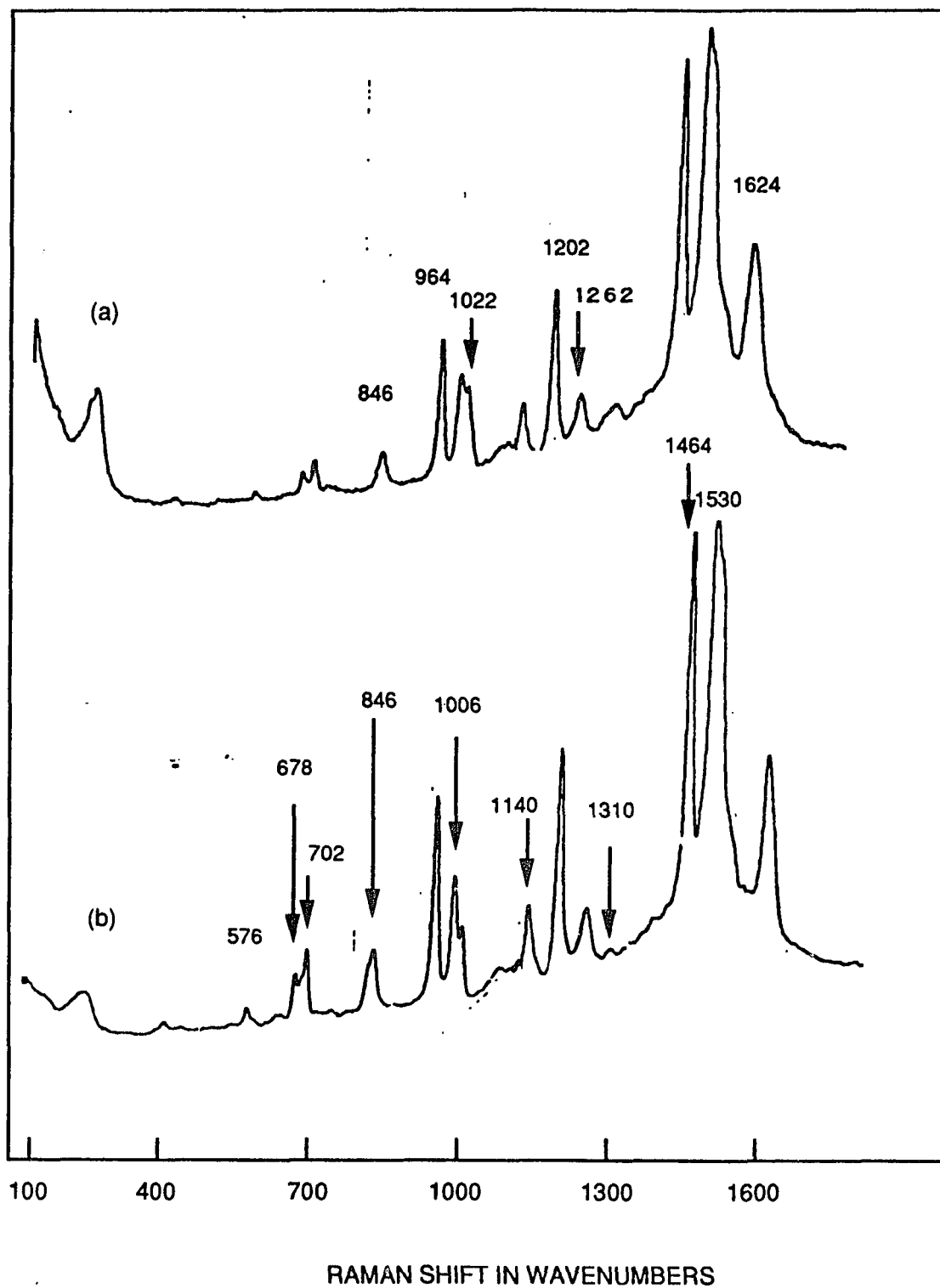


Fig.9 SERS spectra of NAD in 80 % methanol 20 % water solution , on a silver electrode with 488 nm laser excitation . (a) obtained by ex situ roughening and (b) by in situ roughening. Both spectra were recorded at -0.2V.

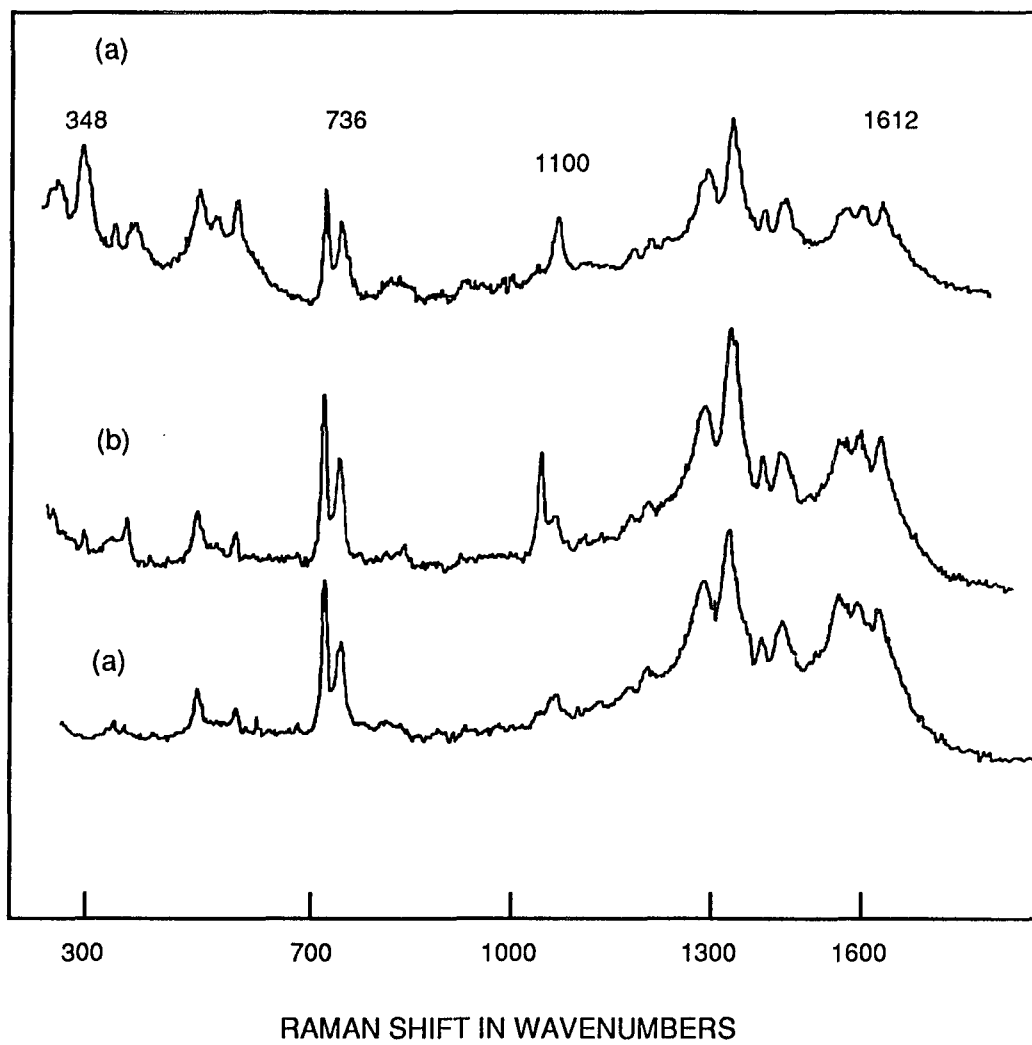


Fig.10 SERS of NAD on a Ag electrode at pH 7.4 with 488 nm laser excitation. (a) 2, 2 sec. pretreatment pulses (b) 4, 1 sec. pulses and (d)4, 2sec. pulses.

BAND	ASSIGNMENT *
736	ADENINE RING BREATHING
800	PHOSPHODIESTER P-O-P
852	RIBOSE
1090	PYROPHOSPHATE
1248	C8 - H
1338	N7 - C5
1344	ADENINE RING
1370	ADENINE C2 - H
1462	ADENINE
1500	C6 - NH ₂
1582	NICOTINAMIDE

* Ref. 20 and 21

ASSIGNMENT OF NAD VIBRATIONS IN WATER

Table 1

BAND	ASSIGNMENT
678	Adenine Ring
702	Sugar
846	P - O - P
964	Ribose
1006	Ribose
1022	Adenine
1140	Adenine ring (C2N3N1C2)
1202	Sugar
1264	Adenine Ring (C8H)
1310	Adenine Ring (NH2 rock)
1464	Adenine
1530	Adenine Ring
1624	Adenine Ring (NH2)

Table 2

Band assignments for NAD in a m ethanol/water solution.

Band frequencies are in wavenumbers

BIBLIOGRAPHY

Chapter 1

- 1) S. Shibata
Electrochim. Acta 17 395 (1972)
- 2) G. J. Slusser and N. Winograd
Surface Science 95 53 (1980)
- 3) W. G. Johnson and L. A. Heldt
J. Electrochem. Soc. 121 34 (1974)
- 4) H. Frotzheim
Topics in Current Physics Vol. 4 Pg. 205 Springer N.Y. 1977
- 5) F. Kimura ; J. Umemura and T. Takenaka
Langmuir 2 96 (1986)
- 6) R. P. Van Dyne
"Laser excitation of Raman Scattering from Adsorbed molecules
on Electrode surfaces" in Chemical and Biochemical Applications of Lasers.
Vol. 1v Edited by C. B. Moore Chapter 5
- 7) M. Fleischman ; P. J. Hendra and A. J. Mc Quillan
J. Chem. Soc. Chem. Comm. 80 (1973)
- 8) M. Fleischmann ; P. J. Hendra and A. J. Mc Quillan
Chem. Phys. Lett. 26 163 (1974)
- 9) D. L. Jeanmarie ; R. P. VanDuyne
J. Electroanal. Chem. 84 1 (1977)
- 10) M. G. Albrecht and J. A. Creighton
J. Am. Chem. Soc. 99 5215 (1977)
- 11) P Gao ; M. L. Peterson M. A. Tadayyoni and M. Weaver
Langmuir 1 173 (1985)
- 12) C. C. Busby and J. A. Creighton
J. Electroanal. Chem. 140 379 (1982)
- 14) P. N. Sanda ; J. M. Warlaumont ; J. E. Demuth ; J. C. Tsang ; K. Christman
and J. A. Bradley.
Phys. Rev. Lett. 45 1519 (1980)
- 15) G. M. Goncher ; C. A. Parsons and C. M. Harris
J. Phys. Chem. 88 1200 (1984)
- 16) B . Pettinger and A . Gerolymanton
Surface Science 156 859 (1984)

- 17) P. Gao and M. Weaver
J. Phys. Chem. 89 5040 (1985)
- 18) M. Moskovits and D. P. Dilella
Chem. Phys. Lett. 73(3) 500 (1980)
- 19) E. Burstein ; C. Y. Chen and S. Lanquist
Proc. US - USSR Symp. " Inelastic Light Scattering in Solids "
Editors: J. Birman ; H. Z. Cummins and K. K. Rebane
Pg. 475 Plenum Press N.Y. (1975)
- 20) S . Sun
PhD. Dissertation City University of N.Y.
- 21) M. Takahashi ; M. Fujita and M. Ito
Chem. Phys. Letters 109(2) (1984)
- 22) J. A. Creighton
Surface Science 124 209-219 (1983)
- 23) M. Moskovits
J. Chem. Phys. 77(9) 4404 (1982)
- 24) R. G. Greenler
J. Chem. Phys. 44 310 (1960)
- 25) R. G. Greenlear
J. Chem. Phys. 50 1963 (1969)
- 26) H. A. Pearce and N. Shepard
Surface Science 59 295 (1976)
- 27) M. Moskovits and J. S. Suh
J. Phys. Chem. 88 5526 (1984)
- 29) C. A. Murraray ; D. L. Allara ; H. F. Hebard and F. J. Padden
J. of Surface Sci. 119 449 (1982)
- 30) P. F. Liao ; J. G. Bergman ; D. S. Chemla ; A. Wokaun ; J. Melngailis; A. M. Havrylukad and N. P. Economou
Chem. Phys. Lett. 82 355 (1981)
- 31) H. Wetzel and H. Gerischer
Chem. Phys. Letts. 76 460 (1980)
- 32) J. R. Lombardi and R. L. Birke
'Surface Enhanced Raman Scattering" from
Spectroelectrochemistry: Theory and Practice Edt. by R. J. Gale

Plenium Publishing Company 1988

33) J. R. Lombardi, R. L. Birke, L. Sanchez, I. Bernard and S. Sun
Chem. Phys. Letts. 104(2,3) 240 1984

34) P. N. Sanda ; J. M. Warlaumont ; J. E. Demuth ; J. C. Tsang ;
K. Chritman and J. A. Bradley
Phys. Rev. Lett. 45 1519 (1980)

35) T. E. Furtak and S. H. Macombe
Chem. Phys. Lett. 95 328 (1983)

36) A. Smekal
Weiner Anz. Pg. 79 1927, Physik. Ber. 3 1104-1105

37) C. V. Raman and K. S. Krishnan
Nature 121 1 1928

38) A. T. Tu
Raman spectroscopy in biology: Principles and Applications
Wiley, N.Y. 1982

39) M. C. Tobin
Laser Raman Spectroscopy
Wiley Interscience N.Y. 1971

40) E. I. Rabinowitch
"Photosynthesis" Vol. 2 Part 2 Wiley (Interscience) NY 1956

41) R. K. Clayton
Annu. Rev. Biophys. Bioeng. 2 131 1973

42) T. Streckas, T. Spiro
Biophys. and Biochim. Acta 263 830 1972

43) H. Brunner, A. Mayer and H. Sussner
J. Mol. Biol. 70 153 1972

44) Van Duyne
J. Phys. (Paris) 38 C-5 239 (1977)

45) E. Kloglin ; J. M. Squaris ; P. Valenta and H. W. Nurnberg
Proc. 14 th Eur. Cong. on Molecular Spect. 3 7-9 Frankfrut

46) E. Kloglin ; J. M. Squaris ; P. Valenta and H. W. Nurnberg
Fresenius Z. Anal. Chem 317 698 (1984)

47) J. M. Sequaris ; E. Koglin and P. Valenta
Ber. Bunsenges. Phys. Chem 85 512 (1981)

- 48) H. H. Lewinsky
PhD dissertation Univ. of Frankfurt
- 49) H. Kisters
PhD dissertation Univ. of Koln
- 50) M. Kerker ; O. Siiman ; L. A. Brumm and D. S. Wang
Appl. Opt. 19 3253 (1980)
- 51) C. G. Blatchford ; D. Siiman and M. Kerker
J. Phys. Chem. 87 2503 (1983)
- 52) M. Kerker ; O. Siiman ; L. A. Brumm and D. S. Wang
J. Phys. Chem 87 1014 (1983)
- 53) M. Kerker ; O. Siiman and D. S. Wang
J. Phys. Chem. 88 3168 (1984)
- 54) E. Koglin
Fresenius Z. Anal. Chem. 317 698 (1984)
- 55) R. A. Copeland ; S. P. A. Fodder and T. S. Spiro
J. Am. Chem. Soc. 106 3872 (1984)
- 56) X. Xu ; R. L. Birke and J. R. Lomdardi
J. Am. Chem. Soc. 109 5645 (1987)
- 57) I. R. Nabiev ; R. G. Eifremov and G. D. Chumanov
Biol. Membranes V 2 1985
- 58) T. M. Cotton ; S. G. Schultz and R. P. Van Duyne
J. Am. Chem. Soc. 104 6528 (1982)
- 59) M. Itabashi ; K. Kato and K. Itoh
Chem. Phys. Letters . Vol. 97 NO. 6
- 60) R. Holze
Electrochimica Acta 33 No. 11 1619
- 61) J. J. McMahon ; S. Baer and C. A. Melendres
J. Phys. Chem. 90 1572 (1986)
- 62) L. Sanchez and T. G. Spiro
J. Phys. Chem. 89 763 (1985)
- 63) T. Koyama ; M. Yamaga ; M. Kim and K. Itoh
Inorg. Che . 24(25) 429 (1985)

- 64) P. Hilderbrant and M. Stockburger
J. Phys. Chem. 90 6017 (1986)
- 65) T. M. Cotton ; S.. Schultz and R . P . Van Duyne
J. Am. Chem. Soc. 102 7960 (1980)
- 66) K. Nikki, Y. Kimura, Y. Higuchi and N. Yasuoka
Langmuir 3 982 1987
- 67) T. M. Cotton ; R. Timkovich and M. S. Cook
FEBS Lett . 133 39 1981
- 68) M E. Lippitsch
Chem. Phys. Letts. 77 224 (1981)
- 69) T. M. Cotton and R. P. Van Dyne
FEBS Letts. 147 81 (1982)
- 70) R. A. Copeland ; S. P. A. Fodder and T. S. Spiro
J. Am. Chem. Soc. 106 3872 (1984)
- 71) Y. Shiratori ; M. Serita and K. Itoh
Chem. Phys. Letts. 595
- 72) A . Takenaka ; S. Takeuchi ; Y. Kobayashi and K. Itoh
Sur. Sci. 158 359
- 73) Y. Kobayashi and K. Itoh
J. Phys. Chem. 89 5174 (1985)
- 74) K. Shoji ; Y. Kobayashi and K. Itoh
Chem. Phys. Lett. 102(2,3) 1983
- 75) M. Gouterman
"The Porphyrins" Vol. 3 Part A Edited by D. Dolphin
Academic press N.Y.

Chapter 2

- 1) The Porphyrins. Edited by D. Dolphin Academic Press N.Y.
- 2) W. D. Hewson and L. D. Hager in "The porphyrins" Edited by D. Dolphin Vol.7 Academic Press N.Y. 1975
- 3)K. M. Kadish, C. Araullo, G. B. Maiy, D. Sazon, J. M. Barbe and R. Guillard
Inorg. Chem. 28 2528 (1989)

- 4) K. M. Kadish, D. Sazon, Y. M. Li, A. Saoiabi, M. Ferhart and R. Guillard
Inor. Chem. 27 1198 (1989)
- 5) M. Fleischman, P. J. Hendra and A. J. McQuillan
J. Chem. Soc. Chem. Comm. 80 1973
- 6) M. Takahashi, Y. Sakai, M. Fujita and M. Ito
Surface Sci. 176 351 (1986)
- 7) P. Gao and M. Weaver
J. Phys. Chem. 89 5040 (1985)
- 8) K. Hutchinson, A. J. McQuillan and R. E. Hester
Chem. Phys. Letts. 98 27 (1983)
- 9) A. M. Stacy and R. P. Van Duyne
Chem. Phys. Lett. 102(4) 365 1983
- 10) L. Sanchez and T. G. Spiro
J. Phys. Chem. 89 763 (1985)
- 11) X. Hong and C. Guo
submitted for publication
- 12) C. Guo and X. Hong
Unpublished results
- 13) S. Parshad
PhD Dissertation C.U.N.Y.
- 14) J. Xu, J. Lombardi and R. L. Birke
J. Am. Chem. Soc. 109 5645 (1987)
- 15) T. M. Cotton, S. G. Schultz and R. P. Van Dyne
J. Am. Chem. Soc. 104 6528 (1982)
- 16) M. Itabashi ; K Kato and K. Itoh
Chem. Phys. Lett . 97(6) 528 (1983)
- 17) J. M. Burke, J. R. Kincaid and T. G. Spiro
J. Am. Chem. Soc. 100 6077 (1978)
- 18) M. Itabashi ; K Kato and K. Itoh
Chem. Phys. Lett . 97(6) 528 (1983)
- 19) J. G. Lanese and G. S. Wilson
J. Electrochem. Soc. 119(8) 1039 (1972)

- 20) C . M . Kadish et al
Inorg. Chem. 22 686 (1988)
- 21) P . Gao and M . Weaver
J. Phys. Chem. 89 5040 (1985)
- 22) H . Shindo
J. Chem. Soc. Farad. Tran. 119 1039 (1972)
- 23) M. Gouterman in "The porphyrins" Edited by D. Dolphin Academic Press
- 24) M. Gouterman
Ann. N.Y. Acad. Sci. 206 70 (1973)
- 25) S. A Silvers and A. Tulinsky
J. Am. Chem. Soc. 86 927 (1964)
- 26) S . Silvers and A . Tulinsky
- 27) A . Wolberg
J. Mol. Struct. 21 61 (1974)
- 28) S . S . Eaton ; G . R . Eaton and R . H . Holm
J. Organomet. Chem. 39 179 1972
- 29) W. Fuchsman, Q. R. Smith and M. Stein
J. Am. Chem. Soc. 99:12 4190 (1977)
- 30) E . M . Gouterman
Ann. N.Y. Acad. Sci. 206 70 (1973)
- 31) M . Meot-Ner and A . D . Adler
J. Am. Chem. Soc. 94 4763 72
- 32) M . Meot-Ner and A . D . Adler
J. Am. Chem. Soc. 97 5107 (1975)
- 33) W . Schneider
Struct. Bonding. 23 123 (1975)
- 34) W . H . Fuchsman ; R . Smith and M . M . Stein
J. Am. Chem. Soc. 99:12 4190 (1977)
- 35) P. George
Chem. Rev. 75 85 (1975)
- 36) T. M. Cotton and M. Van Duyne
Chem. Phys. Lett. 106(6) 491 (1984)

37) T. Takahashi and S. Maeda
Chem. Phys. Lett. 24(4) 584 (1974)

Chapter 3

1) M. Fleischman, P. J. Hendra and A. J. Mc Quillian
Chem. Phys. Lett. 26 163 1973

2) "The Porphyrins." Edited by D. Dolphin. Academic Press NY

3) "Biochemistry" by Lubert Stryer W. H. Freeman and Co. NY 1988

4) "Iron Porphyrins" Part 11 A. B. Lever and H. B. Gray Editors Addison-Wesley.

5) M. Itabashi, K. Kato and K. Itoh
Chem. Phys. Letts. 97(6) 528

6) L. A. Sanchez and T. G. Spiro
J. Phys. Chem. 89 763 (1985)

7) T. Koyama and K. Itoh
J. Electroanal. Chem. 215 209 (1986)

8) J. J. McMahon, S. Baer and C. M. Melendres
J. Phys. Chem. 90 1572 (1986)

9) Guo
J. Chem. Phys. 30 1139 (1986)

14) C. M. Hosten, R. L. Birke and J. R. Lombardi
Submitted for publication

15) R. Holze
Electrochimica Acta 33(11) 1619

16) J. A. Bergeron, G. L. Gaine and W. D. Bellamy
J. Colloid and Interface Sci. 25 97 (1967)

17) R. H. Tredgold and A. J. Vickers
J. Phys. D Applied Physics 18 1139 (1985)

18) M. Itabashi, K. Kato and K. Itoh
Chem. Phys. Lett. 97 528 (1983)

19) T. M. Cotton, S. Schultz and R. VanDyne
J. Am. Chem. Soc. 104 6528 (1982)

Chapter 4

- 1) R. A. Bull, F. F. Fan and A. J. Bard
J. Electrochem. Soc. 129 1009 1982
- 2) A. J. Bard, H. S. White, H. D. Abruna
J. Electrochem. Soc. 103 1849 1981
- 3) M. Umana, P. Denisevich, D. Rolison, S. Nakahama
and R. Murraray.
Anal. Chem. 53 1170 1981
- 4) R. W. Murraray
Acc. Chem. Res. 13 135 1980
- 5) R. W. Murraray
Chemically Modified Electrodes in Electroanalytical Chemistry
- 6) G. J. Samuels and J. J. Meyer
J. Amer. Chem. Soc. 103 307 1981
- 7) J. B. Keer and L. L. Miller
J. Electroanal. Chem. 101 263 1979
- 8) A. Bettelheim, R. J. Chan and T. Kumana
J. Electroanal. Chem. 101 263 1979
- 9) K. A. Macro and T. G. Spiro
J. Electroanal. Chem. 163 223 1984
- 10) A. Bettelheim, B. A. White and R. W. Murray
J. Electroanal. Chem. 217 271 1987
- 11) D. Ozer, R. Harth, V. Mor and A. Bettelheim
J. Electroanal. Chem 266 109 1989
- 12) A. Bettelheim, D. Ozer, R. Harth and R. W. Murray
J. Electroanal. Chem. 246 139 1988
- 13) T. Kobayashi ; H. Yoneyama and H Tamura
J. Electroanal. Chem. 161 419 (1964)
- 14) T. Kobayashi ; H. Yoneyama and H Tamura

J. Electroanal. Chem. 177 419 (1974)

15) R. N. Adams
Electrochemistry at solid electrodes
Marcel Dekker, NY 1969 Pg.323

16) B. A. White and R. Murray
J. Electroanal. Chem. 189 345 (1985)

17) A. F. Diaz and J. A. Logan
J. Electroanal. Chem. 111 111 (1980)

18) R. Noufi ; A. J. Nozik ; J. White and L. F. Warren
J. Electrochem. Soc. 129 2261 (1982)

19) T. Kobayashi ; H. Yoneyama and H. Tamura
J. Electroanal. Chem. 161 419 1984

20) T. Ohasaka ; et al
J. Electroanal. Chem. 161 399 (1984)

21) D. M. Mohilner ; R. N. Adams and W. J. Argersinger Jr.
J. Am. Chem. Soc. 84 3618 (1962)

22) P. M. Mc Manus ; S. C. Yang and R. Cushman
J. Chem. Soc. Chem. Commun. 1556 1985

23) A. Bettleheim ; D. Ozer ; R. Harth ; and R. W. Murray
J. Electroanal. Chem. 266 93 (1989)

24) K. A. Macro, Y. Oliver Su, L. A. Miller and T. G. Spiro
Inorg. Chem. 26 2594 1987

25) A. F. Diaz and J. A. Logan
J. Electroanal. Chem. Interfacial Electrochem. 111 111 (1980)

26) T. Kobayashi ; H. Yoneyama and H. Tamara
J. Electroanal. Chem. Interfacial Electrochem. 161 419 (1984)

27) W. S. Huang ; B. D. Humphrey and A. G. Mac Diarmid
J. Chem. Soc. Faraday Trans.1 82 2385 (1986)

28) T. Ohsaka ; Y. Ohnuki ; N. Oyama ; G. Katagiri and J. Kamisako
J. Electroanal. Chem. Interfacial Electrochem. 161 399 (1984)

29) J. Bacon and R. N. Adams
J. Am. Chem. Soc. 90 6596 (1968)

- 30) J. Brendmuller ; H . Hacker and H. W. Schrottler
Chem. Ber. 99 765 (1966)
- 31) H. Hacker
Spectrochim. Acta. 21 1989 (1965)
- 32) C. D. Ellis ; L. D. Marger ; R. W. Murraray and T. J. Meyer
Inorg. Chem. 22 1283 (1983)
- 33) J. W. Robinson
"CRC handbook of Spectroscopy" ; J . Robinson Editor
Chemical Rubber Publishing Co . Cleveland Ohio 1974 Vol 11
- 34) I. Harada
Synthetic Metals 29 E303 (1989)
- 35) I. Harada
Synthetic Metals 16 189 (1986)
- 36)K. Brahama
Solid State Commun. 57(8) 673
- 37) J. Brandmuller and H. Hacker
Z. Physik. 184 14 (1965)
- 38) T. M. Cotton, S. Schultz and R. VanDuyne
J. Am. Chem. Soc. 104 6528 (1982)
- 39) G. S. Calabrese ; R. M. Buchanan and M. S. Wrighton
J. Am. Chem. Soc. 104 5786 (1982)
- 40) P. Martigny and F. C. Anson
J. Electroanal. Chem. 139 383 (1982)
- 41) S. Prashad
PhD Dissertation City University of New York

Chapter 5

- 1) A. L. Underwood and R. Burnett in Electroanalytical Chemistry
Edited by Bard Vol. 6 Pg. 1 1973
- 2) Y. Hatefi
Ann. Rev. Biochem. 54 1015 (1985)

- 3) S. C. Daubner and J. L. Schrishsher
Biochemistry 24 7059 (1985)
- 4) M. E. Jones
Ann. Rev. Biochem. 49 253 (1980)
- 5) L. Lee, R. E. Kelley and D. R. Evans
Proc. Nat. Acad. Sci. 82 6802 (1985)
- 6) D. G. Nicholls
Bioenergetics Academic Press 1982
- 7) M. Wilkstrom and M. Scrase
"Bioenergetics" Edited by L. Ernster Elsevier Publication 1984
- 8) H. Sand in "Biological Oxidations" T. P. Singer Editor
Interscience NY. 1968
- 9) G. Weber
Nature(London) 180 1409 (1957)
- 10) S. F. Velick
J. Biol. Chem. 233 1455 (1958)
- 11) O. Jardetzky and N. G. Wade Jardetzky
J. Biol. Chem. 241 85 1966
- 12) H. Sand in Biological Oxidations. T. P. Singer Editor NY 1968
- 13) G. Weber
Nature 180 1409 (1957)
- 14) S. F. Velick
J. Biol. Chem. 233 145 (1958)
- 15) M. Fleischman, P. J. Hendra and A. J. McQuillan
J. Chem. Soc. Chem. Commun. 80 1973
- 16) T. M. Cotton, S. Schultz and R. Van Duyne
J. Am. Chem. Soc. 104 6528 (1982)
- 17) M. Moskovits and J. S. Suh
J. Phys. Chem. 88 5526 (1984)
- 18) W. J. Plieth and K. J. Forster
J. Electroanal. Chem. 214 675 (1986)
- 19) J. A. Creighton

Surface Science 124 209 (1983)

20) I . Taniguchi ; K . Umekita and K . Yasukouchi
J. Electroanal. Chem. 202 315 (1986)

21) O . Siiman ; R . Rivellini and R . Patel
Inorg. Chem. 27 3940 (1988)

22) W . D . Bowman and T . G . Spiro
J. Raman Spect. 9 369 (1980)

23) M . G . Rossman ; A . Liljas ; C . I . Branden and L . J . Banaszak
The Enzymes Edt. by P . D . Boyer, Academia. NY (1975)

24) B. S. Reddy, W. Saenger, K. Muhlegger and W. Weiman
J. Am. Chem. Soc. 103 907 (1981)

25) K . G . Brown ; E . J . Kiser and W . L . Peticolas
Biopolymers 11 1855 (1972)

26) S . C . Erfurth ; E . J . Kiser and W . L . Peticolas
Proc. Natl. Acad. Sci. 69 938 (1972)

27) W . A . Catterral ; D . P . Hollis and C . F . Walter
Biochem. 8(10) 4032 (1969)

28) R . H . Sarma ; V . Ross ; and N . O . Kaplan
Biochem. 7(9) 3052 (1968)

29) C . Otto ; F . F . deMul ; A . Hiuizingo and J . Greve
J. Phys. Chem. 92(5) 1239 (1988)

30) E . Koglin ; H . Lewinsky and J . M . Sequasis
Surf. Sci. 158 370 (1985)

31) T . Watanbe et al
Surf. Sci. 158 341 (1985)

32) J . S . Shu and M . Moskovits
J. Am. Chem. Soc. 108 4711 (1986)

33) W . Saenger Principles of Nucleic Acid Structure
Springer- Verlag. NY. (1984)

34) T. W. Barrett
J. Raman Spectrosc. 9 130 1980

35) K . D . Beer ; W . Tanner and R . Garrell
J. Electroanal. Chem. 258 313 (1989)